(NASA-CR-165246) ON VARIABLE HYDROSTATIC TRANSMISSION FOR ROAD VEHICLES, POWERED BY SUPPLY OF FLUID AT CONSTANT PRESSURE (Volvo Flygmotor A.B., Trollhaettan) 122 p HC A06/MF A01 CSCL 13F G3/44

N81-25489

Unclas 26566

NASA Contractor Report 165246

ON VARIABLE HYDROSTATIC TRANSMISSION FOR ROAD VEHICLES, POWERED BY SUPPLY OF FLUID AT CONSTANT PRESSURE

Mart Mägi
Solvo AB
31 Hammarliden
S - 412 62 Gothenburg, Sweden

and

Are Freivald
Volvo Flygmotor AB
S - 461 01 Trollhätten, Sweden

and

Ingvar Andersson and Ulf Ericsson
Solvo AB
31 Hammarliden
S - 412 62 Gothenburg, Sweden

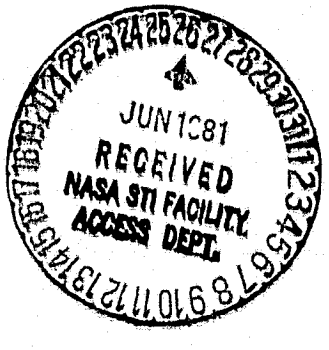

May 1981

Prepared for

NATIONAL AERONAUTICS AND SPACE ADMINISTRATION
Lewis Research Center
Under Contract NASW-3299

CONTENTS

		Page
	List of Illustrations	ii
	Preface	iii
	Acknowledgments	v
	Notation	vi
1.	Design Specifications	1
2.	Required Driving Force	3
3.	Characteristics of Variable Displacement Motors/Pumps	8
4.	Available Design Concepts	14
5.	Recommended Design Concepts	22
6.	Modeling of Hydrostatic Components	26
7.	Modeling of Geared Components	36
8.	Optimization Criteria	39
9.	Methods of Evaluation	42
10.	Numerical Results	44
11.	Concluding Remarks	50
	Appendix 1 : Configurations of Candidate Systems	52
	Appendix 2 : Test results V20-180 Machine	65
	Appendix 3 : Performance maps of optimized systems	79

LIST OF ILLUSTRATIONS

FIGURES:

1 Road load vs. cruising speed
2 Road load and available driving force when a manual 4-speed transmission is used
3 EPA Urban Driving Cycle
4 Driving cycle matrix F vs. v
5 Driving force requirements
6 Types of axial piston machines
7 Qualitative relationship η_{mech} vs. Δp
8 Qualitative relationship η_{vol} vs. ω
9 Qualitative relationship η_{tot} vs. ε
10 Scheme of two hydraulic motors in parallel
11 Relative power loss for a variable displacement machine
12 Relative losses in two-unit arrangements
13 Losses in a throttled system
14 Fundamental design concept of system A
15 Fundamental design concept of system B
16 F-11 series trends for weight and speed
17 Circuit diagram of the test setup
18 V-20 and V-30 series trends for weight
19 System characteristics matrix
20 Performance map - total efficiency (complete drive system)
21 Performance map - volumetric efficiency (hydrostatic unit)
22 Performance map - control data
23 Performance map - power loss
24 Performance map - input flow rate

TABLES:

1 Comparison of various design concepts
2 Loss coefficients for pump and motor operation
3 Loss and weight/size data on geared transmission
4 Computed main results for systems A and B

PREFACE

This work has been performed as part of the NASA LERC PROJECT under Contract NASW-3299. It has been carried out as a joint effort by Volvo Flygmotor AB, Trollhättan, and Tekniska Konsultbyrån SOLVO AB, Gothenburg, Sweden.

Volvo Flygmotor AB has served as the main contractor, performing the experimental part of the work and supporting the analytical part with its know-how and design experience.

The analysis has been carried out on a subcontract basis by Tekniska Konsultbyrån SOLVO AB, a group of consultants consisting of Members of the Staff of the Dept. of Mechanical Engineering, Chalmers University of Technology, Gothenburg, Sweden.

This report includes a consolidation of five separate reports on Tasks I through V,

TASK I:	Screening of Candidate Hydraulic Drive Systems
TASK II:	Testing of Hydraulic Motors and Pumps at Low RPM, Low Volume Conditions
TASK III:	System Performance Optimization with Constant Differential Hydraulic Pressure
TASK IV:	Quantitative Behavior and Losses of Volvo Flygmotor Motors/Pumps
TASK V:	Back Pressure Performance Evaluation at Constant Differential Pressure

SI units have been used throughout this report, although the primary project specification was given in imperial units.

The few references used are identified by notes on the pages where they appear.

The responsibilities of the four co-authors have been as follows:

Mr ARE FREIVALD, Volvo Flygmotor AB, has served as project coordinator.

Dr MART MÄGI, SOLVO AB, has served as scientific and technical director of the project and has written the final report

Dr INGVAR ANDERSSON, SOLVO AB, has been responsible for the lay-out of the computer program and has written all subroutines, except those on the modeling of components and the optimization

Dr ULF ERICSSON, SOLVO AB, has programmed the modeling of components, including the fitting of loss coefficient to experimental data.

September 1980

Mart Mägi
Gothenburg

Åre Freivald
Trollhättan

Ingvar Andersson
Gothenburg

Ulf Ericsson
Gothenburg

ACKNOWLEDGEMENTS

Without the extensive interest and the full financial support from NASA, the present work could not have been performed.

The authors also want to acknowledge the close cooperation with the Dept. of Mechanical Engineering (Machine Elements) Chalmers University of Technology, Gothenburg, Sweden, which made academic knowledge and know-how available to the project.

Mr Claes Elmén treated the optimization problem of this project in his M.Sc. thesis, thereby contributing considerably to the progress of this work.

Mrs. Gerd Eng has read the manuscript and has given valuable linguistic advice regarding the English language.

NOTATION

m	[kg]	=	vehicle weight (mass)
p	[N/m^2]	=	pressure
Δ p	[N/m^2]	=	differential pressure
q	[m^3/s]	=	flow rate
Δ q	[m^3/s]	=	flow loss, leakage
v	[m/s]	=	vehicle speed
A	[m^2]	=	piston area
C	[-]	=	loss coefficient, clutch
D	[m^3/rev]	=	displacement per revolution
D'	[m^3/rad]	=	displacement per radian
E	[Nm]	=	energy
F	[N]	=	force (driving)
L	[m]	=	length (of driving cycle)
P	[W]	=	power
Δ P	[W]	=	power loss
R	[-]	=	transmission ratio
R'	[1/m]	=	transmission ratio of final gear
T	[Nm]	=	torque
Δ T	[Nm]	=	torque loss
Vo	[m^3]	=	package volume
We	[kg]	=	package weight (mass)
α	[^{o}]	=	yoke or swash plate angle
ε	[-]	=	fraction of maximum displacement
η	[-]	=	efficiency
θ	[-]	=	size ratio
μ	[Ns/m^2]	=	absolute viscosity
ϱ	[kg/m^3]	=	density
ω	[rad/s]	=	angular velocity

Subscripts (selected)

vol	=	volumetric, see efficiency of speed transmission
mech	=	mechanical, see efficiency of speed transmission
tot	=	total, see efficiency of speed transmission power
var	=	variable, see displacement
fract	=	fractional, see displacement
max	=	see displacement and force
conn	=	connect, see ratio of connecting drive
low	=	low gear, see ratio of planetary drive
theor	=	theoretical, losses neglected
equ	=	equivalent, see pressure
back	=	see pressure

1. DESIGN SPECIFICATIONS

The scope of Contract NASW-3299, within the NASA LERC PROJECT, concerns the principal development, evaluation, and optimization of a power transmission system of a road vehicle, where the prime mover (such as a free-piston Stirling engine) produces hydraulic energy, available at constant pressure and with no short-term limitations on flow rate. The power transmission system is to be based upon the Volvo Flygmotor V-20 type variable displacement motor/pump as the principal unit.

According to the contract, the transmission system was to be designed and sized to meet the performance criteria specified below, at the same time minimizing:

- size
- weight
- complexity

and exhibiting optimum efficiency when cruising at constant speed within the range of 6.7 through 22.4 m/s (15 through 50 mph).

During the course of the work the efficiency criteria were re-formulated to the following, more precise, terms:

> the transmission system should exhibit, when optimized, the lowest possible energy consumption when completing an EPA Urban Driving Cycle.

The steady-state speed road load was to be based on the following prescribed expression:

$$P = 228.6 * v + 1.06 * v^2 + 0.5775 * v^3 \qquad (1)$$

where P = power on driving wheels in W
v = vehicle speed in m/s

The weight m of the vehicle was prescribed to be:

$$m = 1542 \text{ kg (3400 pounds)} \qquad (2)$$

The special performance criteria to be met were:

- The minimum distance to be covered in 10 s from a standing start is 134 m (440 feet)

- The maximum time to reach a speed of 26.8 m/s (60 mph) from a standing start is 15 s

No special gradability criteria were prescribed.

2. REQUIRED DRIVING FORCE

The most important quantity in the design and analysis of the propulsion systems of road vehicles is the total driving (or braking) force F acting on the periphery of the driving wheels.

The instantaneous value of F defines:

- either the cruising speed v (when F is in equilibrium with the road load and with the component of the vehicle weight, when grading)
- or the acceleration/deceleration (when F exceeds/falls below the road load)

The vehicle speed v is thus controlled by the driving force F, and it is appropriate to discuss the design criteria as well as the transmission performance in F vs. v diagrams (see Fig. 1). Note that such diagrams also contain information on the output power P (W), because

$$P = F * v \tag{3}$$

The F vs. v diagram will be used from here on in this report to discuss design criteria and transmission performance.

Cruising at steady-state speed requires the following driving force (cf. Eq. 1):

$$F = 228.6 + 1.06 * v + 0.5775 * v^2 \tag{4}$$

which may be interpreted as

- 1.5 % rolling resistance
- a frontal area of 3.2 m^2 at a 0.30 aerodynamic drag coefficient

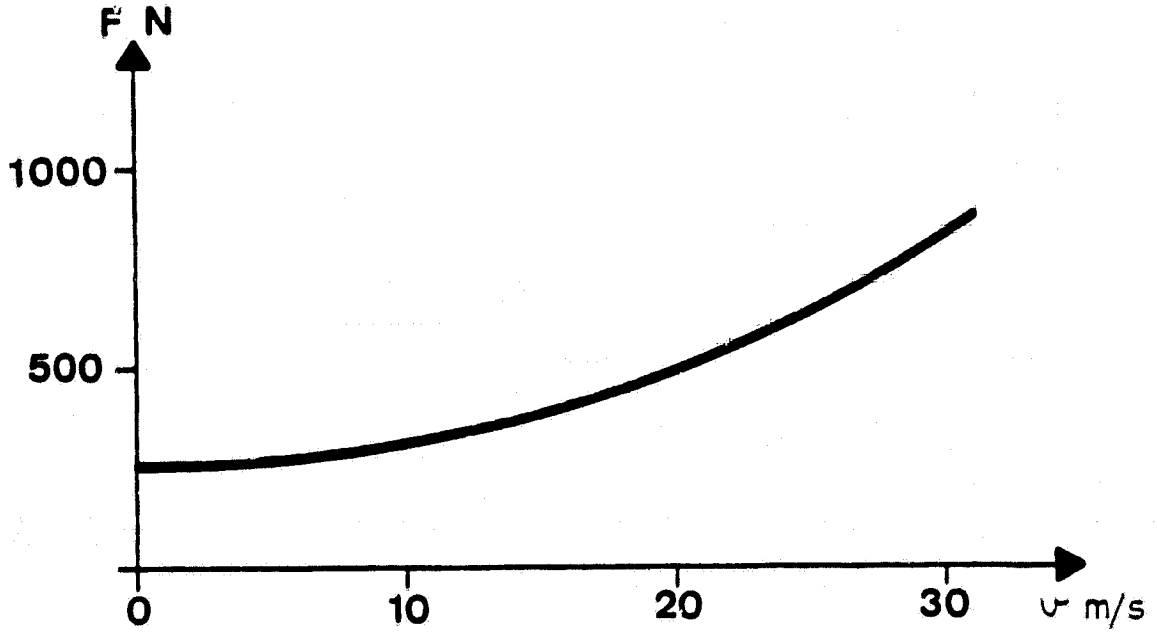

Fig. 1. Road load F vs. cruising speed v

The acceleration criteria may be met by various F vs. v configurations. Conventional automobiles with a manual four-speed transmission produce high driving forces in the low-speed regime (limited by wheel spin) and low driving forces in the high-speed regime (limited by engine power) as indicated in

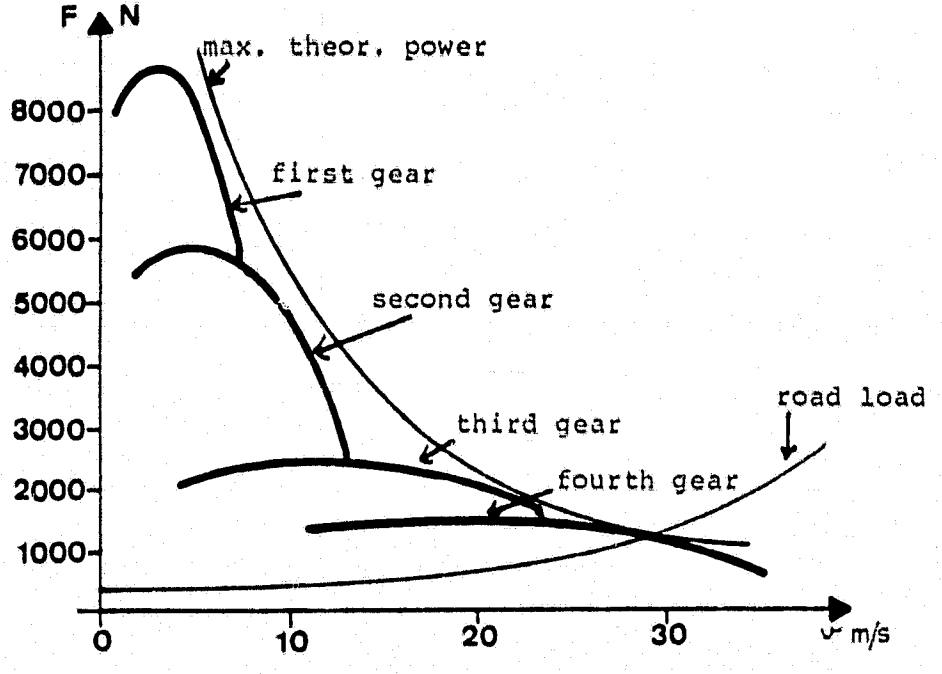

Fig. 2. Road load and available driving force when a manual four-speed transmission is used

In the present design situation it is possible to choose an alternative approach. The same constant maximum driving force may be utilized over the whole speed regime, as there are no short-term power-supply limitations. The maximum driving force is thereby reduced, resulting in reduced weight and size of the final drive.

If the rise time for the driving force and time lost when shifting gears are neglected, a net acceleration force may be calculated to meet the performance criteria:

- acceleration from standing start to 134 m in 10 s requires F_{acc}=4140 N, and the corresponding maximum driving force must also include the road load, thus F_{max}=4600 N (approx)
- acceleration from standing start to 26.8 m/s in 15 s requires F_{acc}=2760 N, and with the road load added, F_{max}=3250 N (approx)

Driving force requirements, established by the EPA Urban Driving Cycle, are calculated as follows:

The driving cycle is defined over a period of 1372 s, and the vehicle speed is specified for each second (cf. F 3).

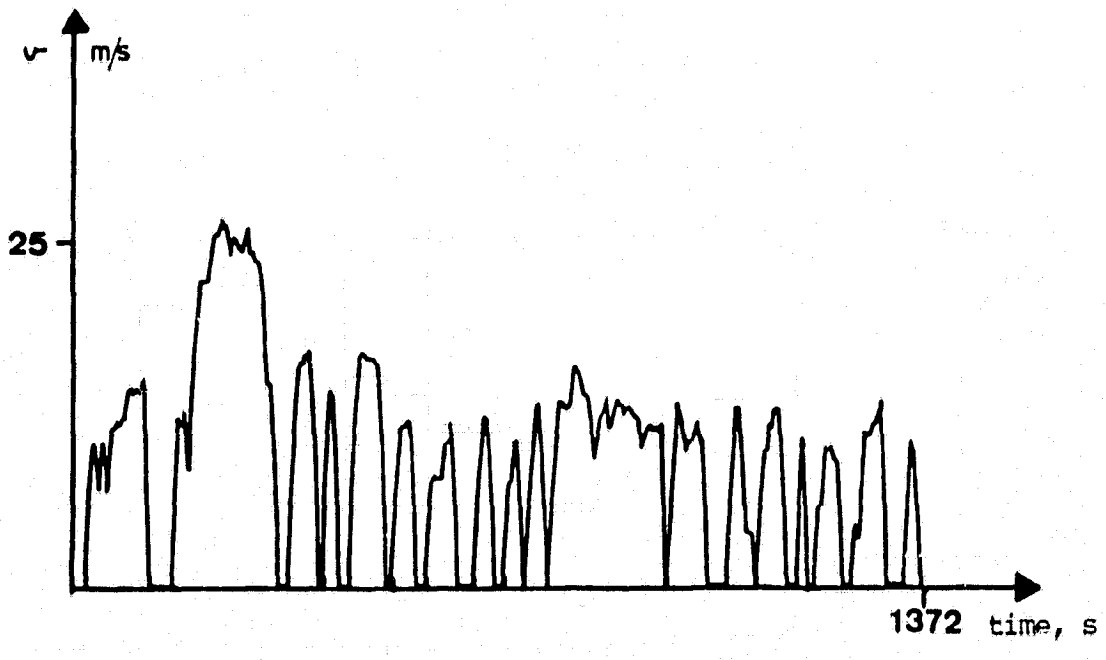

Fig. 3. EPA Urban Driving Cycle

Polynomials of the third power have consecutively been fitted to four adjacent, defined points on the EPA Cycle. Time derivatives of the polynomials yield vehicle accelerations.

Vehicle speed and acceleration have been calculated at time increments of 0.1 s over the driving cycle. The cycle length has been integrated to:

$$L = 11.99 \text{ km} \tag{5}$$

For each time increment the total driving (or braking) force has been calculated as the sum of the road load (from Eq.(4)) and the product of the vehicle mass and acceleration (deceleration). The resulting 13,720 values have been grouped in a driving cycle matrix (F4), where the increments are 0.5 m/s for speed and 50 N for force. About 5000 different combinations of F and υ appear, with peak F values at about 2600 N, and peak speeds at 25 m/s. Negative (i.e., braking) forces have been omitted from the matrix.

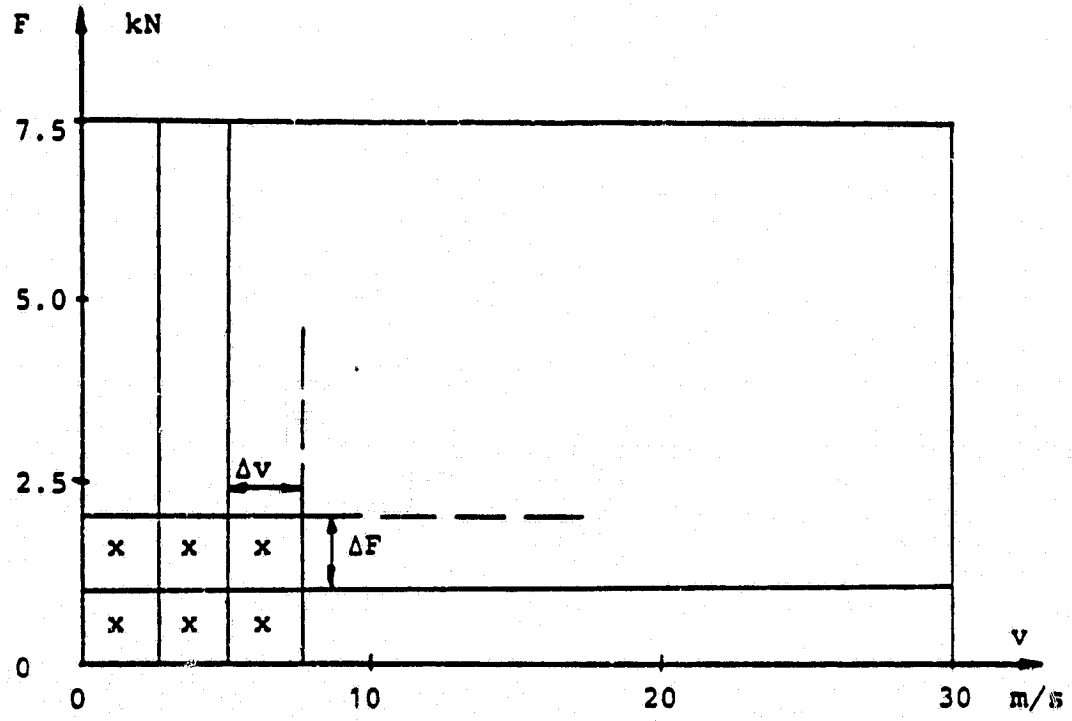

x = duration of requested combination of F and v
ΔF = force increment, Δv = speed increment

Fig. 4. Driving cycle matrix F vs. υ

Based upon the preceding discussions, the driving force requirements are summarized in F5.

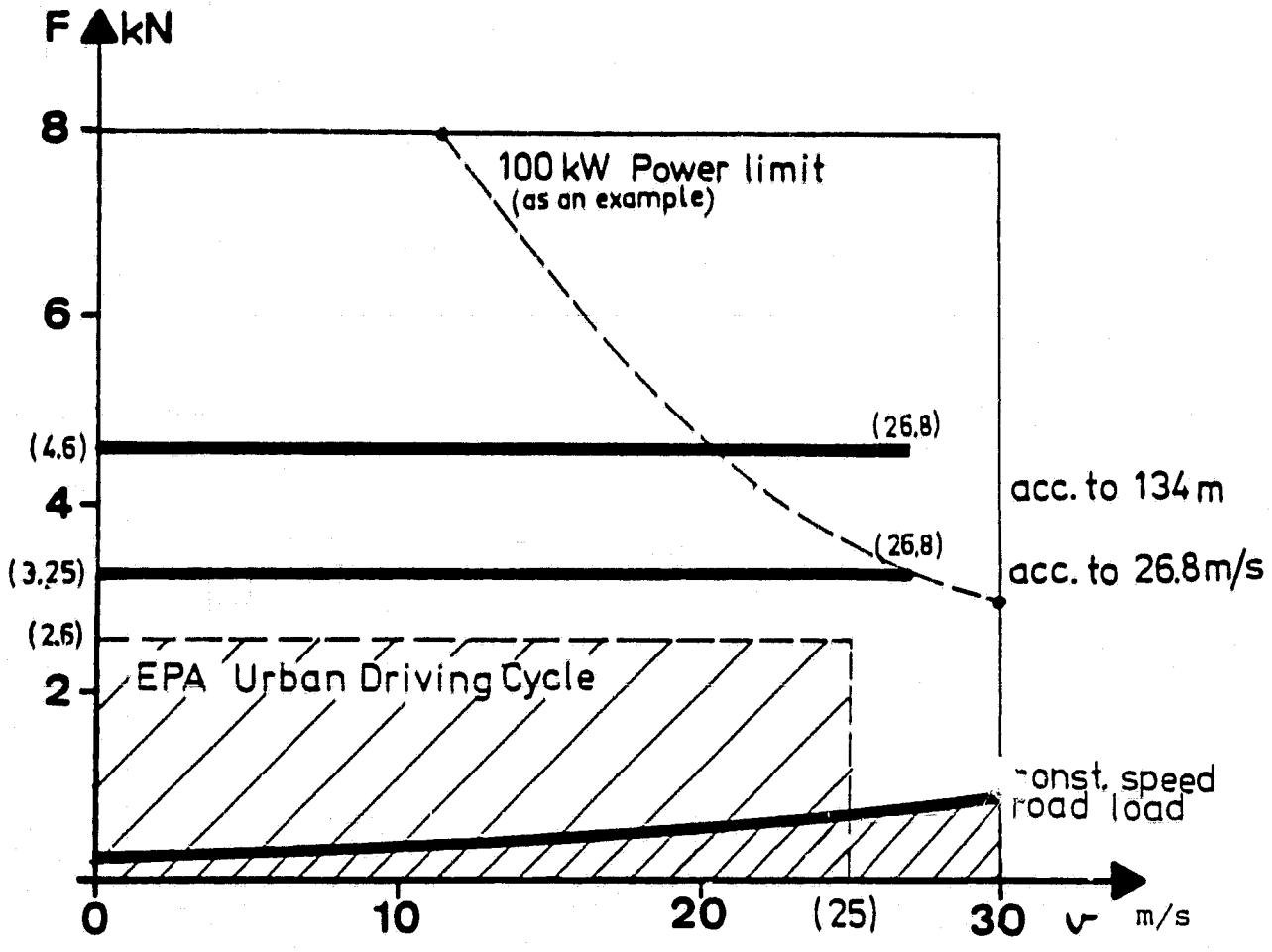

Fig. 5. Driving force requirements

3. CHARACTERISTICS OF VARIABLE DISPLACEMENT MOTORS/PUMPS

General background

Hydrostatic machinery is used either to convert mechanical power into hydrostatic power (pumps) or vice versa (motors).

Hydrostatic power is defined by:

Δp = hydrostatic differential pressure in N/m^2

q = flow rate in m^3/s

$P = \Delta p * q$ = power in W

The theoretical power transmission relationships are easily understood for the linear mode of operation, e.g., for actuators:

equilibrium yields

$$F = \Delta p * A \tag{6}$$

continuity yields

$$q = v * A \tag{7}$$

where A is the actuator area (m^2)

Similar relationships hold for transmissions operating in the rotational mode:

equilibrium yields

$$T = \Delta p * D' \tag{8}$$

continuity yields

$$q = \omega * D' \tag{9}$$

where T = torque in Nm

ω = rotational speed in rad/s

and D' = hydraulic displacement in m^3/rad

Instead of D', data sheets etc. from manufacturers often give the displacement in another unit, namely:

D = hydraulic displacement in vol/one rev.

The two displacements are interrelated by:

$$D = 2 * \pi * D' \tag{10}$$

The basic relationships, Eqs. (6) through (9), indicate that

load transmission: F or $T \leftrightarrows \Delta p$

and

speed transmission: σ or $\omega \leftrightarrows q$

do not mutually influence each other. The transmission ratio is for both cases D' in the rotational mode and A in the linear mode.

There are designs of hydrostatic machinery where a continuous change of the displacement is possible. Such units may thus be considered as Continuously Variable Transmissions, (CVT's).

In the case of variable displacement machines, for each machine exists a maximum displacement D'_{max}.

The displacement change could then be expressed by a non-dimensional quantity ε -displacement fraction - defined as follows:

$$D'_{fract} = \varepsilon * D'_{max} \tag{11}$$

$$|\varepsilon| \leq 1$$

In a formal analysis (where the machine design is adequate)

$$\varepsilon \gtrless 0 \tag{12}$$

could be used, whereby the transition from positive to negative ε corresponds to a transition from motor to pump operation or vice versa, provided that the hydraulic connection and the direction of Δp are unchanged. If not otherwise stated, $\varepsilon > 0$ means motor operation and $\varepsilon < 0$ means pump operation.

In real transmissions the power conversion is influenced by unavoidable losses. The theoretical, no loss reationships, Eqs. (8) and (9), are then modified to:

motor operation:

$$T = \eta_{mech} * D' * \Delta p \tag{13}$$

$$\omega = \eta_{vol} * q/D' \tag{14}$$

pump operation:

$$\Delta p = \eta_{mech} * T/D' \tag{15}$$

$$q = \eta_{vol} * D' * \omega \tag{16}$$

η_{mech} and η_{vol} denote mechanical and volumetric efficiencies, respectively. By definition the efficiencies are limited to the interval:

$$0 \leq (\eta_{mech} \text{ and } \eta_{vol}) < 1 \qquad (17)$$

Efficiency is normally defined for power transmission, whereby

$$P_{out} = \eta_{tot} * P_{in} \qquad (18)$$

Substitution for the hydraulic and mechanical power yields the same expression for η_{tot} at both motor and pump operation:

$$\eta_{tot} = \eta_{vol} * \eta_{mech} \qquad (19)$$

Note that η_{mech} and η_{vol} are not constants. In most cases, however, they could be described with reasonable accuracy as functions of load, speed, and fractional displacement, or

$$\eta = f(\Delta p, \omega, \varepsilon) \qquad (20)$$

Volvo Flygmotor motors/pumps

Volvo Flygmotor has produced and is marketing hydrostatic machines since 1970 . The products are all of the axial piston type, a design concept that makes continuous change of displacement possible.

The axial piston machines could be divided into two groups:

- the bent axis-type
- the in-line type (see F6):

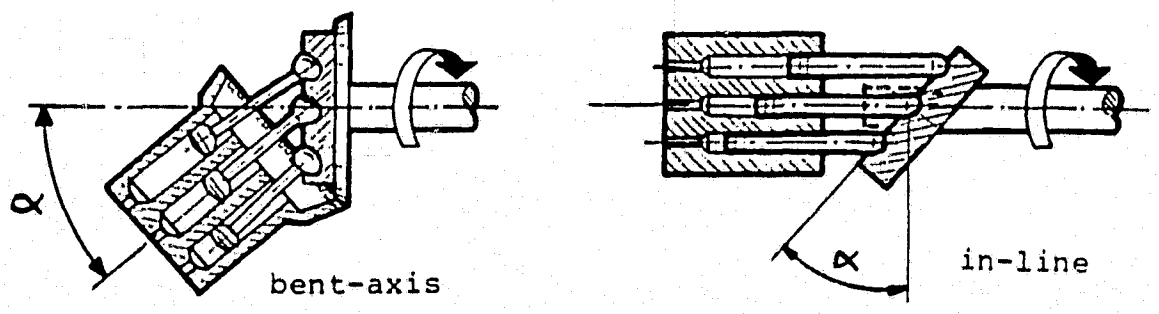

Fig. 6. Types of axial piston machines

The product introduced first was the fixed displacement F-11 series machine. The design concept is of the bent-axis type, which is made possible by the unique, patented spherical piston, reducing the piston losses to a minimum.

Before modifying the F-11 series to a variable displacement version, the V-30 in-line type of variable displacement machines was introduced. This design cannot take advantage of the spherical piston.

The third step of development was the V-20 bent-axis type variable displacement machine, which takes full advantage of the spherical piston, contributing to the high efficiency of such machines.

The displacement fraction ε is related to the yoke or swash plate angle α as follows:

in-line type:

$$\varepsilon = \tan \alpha / \tan \alpha_{max} \tag{21}$$

bent-axis type:

$$\varepsilon \simeq \sin \alpha / \sin \alpha_{max} \tag{22}$$

Some general characteristics of the efficiencies of Volvo Flygmotor pumps and motors are:

- At any reasonable fractional displacement ε and rotating speed ω the mechanical efficiency η_{mech} decreases to zero in the low-pressure regime, (cf. F 7). This is due to unavoidable parasitic friction.

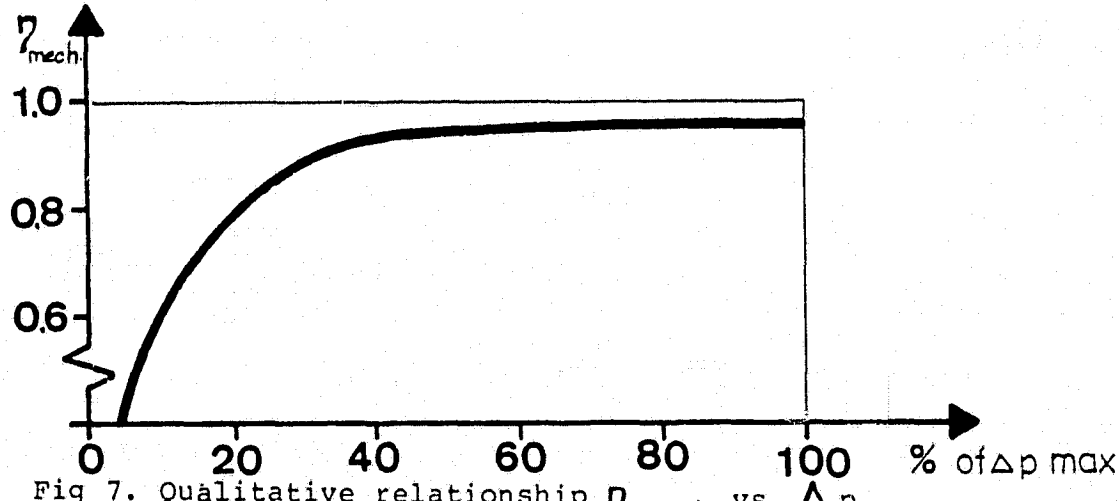

Fig 7. Qualitative relationship η_{mech} vs. Δp

- At any reasonable fractional displacement ε and differential pressure Δp, the volumetric efficiency η_{vol} decreases to zero in the low-speed regime (cf. F 8), due to unavoidable clearance leakage.

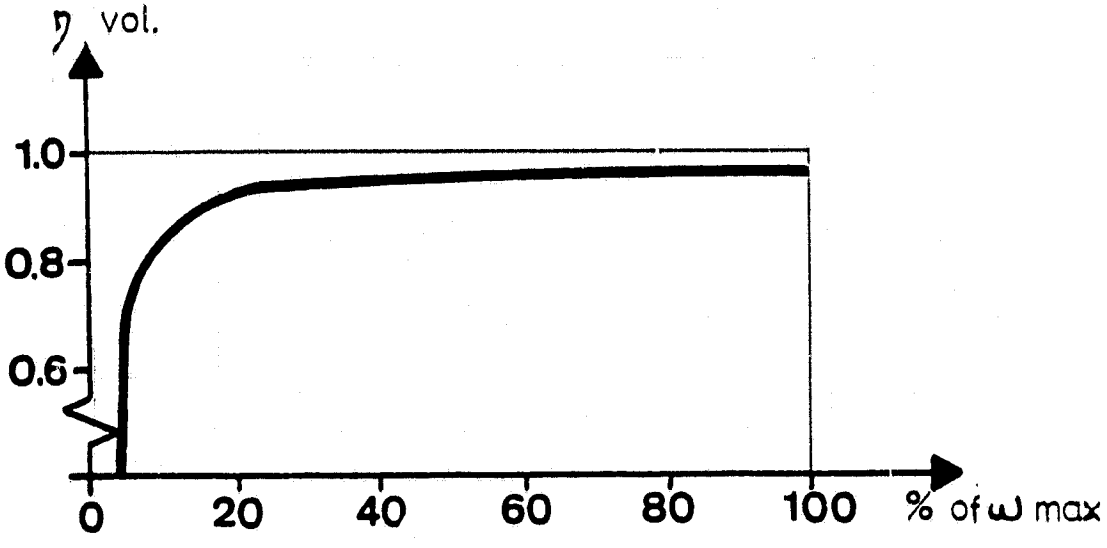

Fig. 8. Qualitative relationship η_{vol} vs. ω

- At any reasonable operating speed ω and differential pressure Δp, the total efficiency η_{tot} decreases to zero in the low displacement regime (cf. F 9). The reason is that some basic losses are fixed, while the transmitted useful power is decreasing.

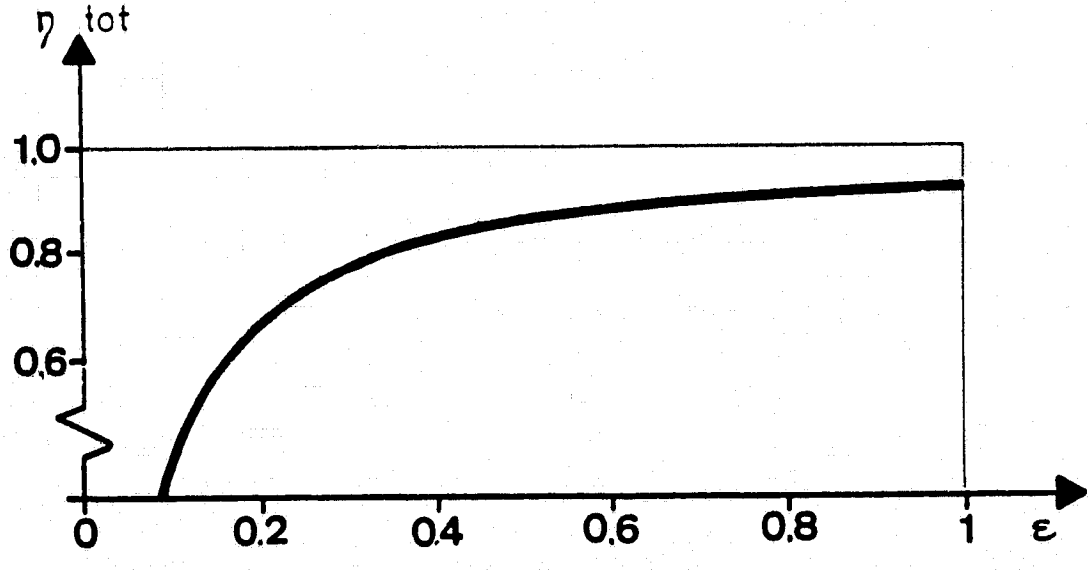

Fig. 9. Qualitative relationship η_{tot} vs. ε

From the diagrams in Figs. 7 through 9 can be concluded that operation within any of the low-value regimes, <10%, of the maximum speed, pressure, and displacement, causes considerable losses, η < 80%, and should thus be avoided, if possible.

A detailed discussion and quantification of the losses will be given in Chapter 6.

4. AVAILABLE DESIGN CONCEPTS

The design problem consists of converting a constant hydrostatic pressure into a variable driving force, covering the range of 0 through approximately 5000 N at any peripheral velocity of the driving wheels up to about 30 m/s.

The main control problem is control of the driving force, while vehicle speed is a dependent variable, controlled indirectly via the driving force. This concept may seem unusual in automotive applications. However, it is beneficial in the design of conventional automobile propulsion systems, as well, as advocated by A. Frank et al. *)

In terms of hardware, the problem could be solved in a straightforward manner by a variable-displacement hydrostatic unit connected to the pressurized fluid supply and delivering its torque to the driving wheels via a conventional final drive. Torque control is obtained by controlling the variable displacement.

This solution could be quantified (cf. Eqs. (11) and (13)) to:

$$T = \varepsilon * \eta_{mech} * D'_{max} * \Delta p \qquad (23)$$

where T is the input torque to the final drive, corresponding to any desired driving force F, which is controlled by a proper choice of ε.

The size of the hydrostatic motor is then:

$$D'_{max} = T_{max} / (\eta_{mech} * \Delta p) \qquad (24)$$

where T_{max} corresponds to a selected maximum driving force F_{max} (cf. F 5).

However, some alternative concepts also exist. The total displacement D'_{max} could be obtained:

- either as a sum of the displacements of two or more units (some of them having fixed displacements)

*) cf. e.g. paper presented at the ASME Power Transmission & Gearing Conference, San Fransisco, Aug. 1980, entitled "Principles and Definitions of Continuously Variable Transmissions with Emphasis on Automotive Applications".

- or by a "magnification" of a basic displacement obtained by connecting a, two- or more speed, reduction gear between the hydrostatic motor and the final gear

- or by a combination of the two abovementioned concepts.

Before listing a number of design concepts that might have a potential of high energy economy, low weight, etc, we will explain two subconcepts, namely, power recirculation and hydraulic polarity shift.

Power recirculation (PRC)

The interpretation of two hydrostatic motors working in parallel is obvious:

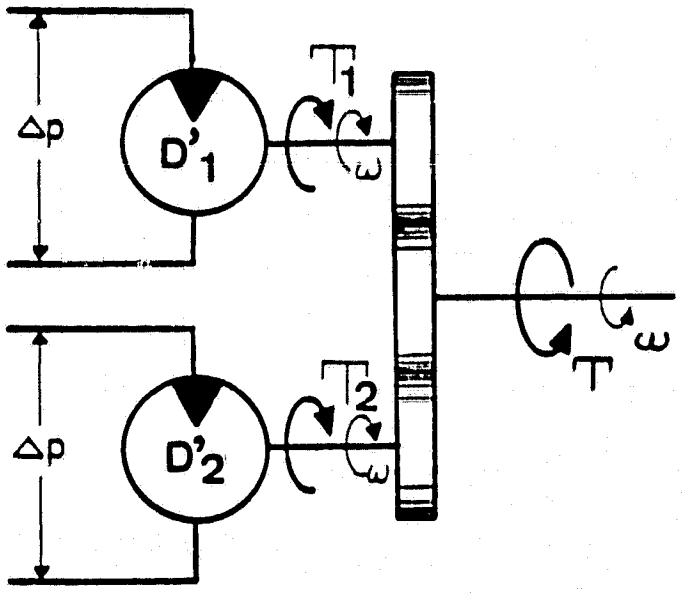

Fig. 10. Scheme of two hydrostatic motors in parallel

$$\left.\begin{aligned} T_1 &= \eta_{mech,1} * D_1' * \Delta p \\ T_2 &= \eta_{mech,2} * D_2' * \Delta p \end{aligned}\right\} \Rightarrow \text{assuming } \eta_{mech,1} \simeq \eta_{mech,2}$$

$$T = (D_1' + D_2') * \eta_{mech} * \Delta p \qquad (25)$$

The question may arise as to whether or not $(D_1' - D_2')$ has a physical interpretation in the context of equations like Eq. (25).

The answer is yes, and the interpretation is that one of the units is operating as a motor, e.g., D_1', and the other, D_2', as a pump. Physically this means that Unit 1 is picking up hydrostatic power from the reservoir and converts it into mechanical power. Thereby some power is lost (friction and leakage).

Part of the mechanical power passes to the output shaft without special losses.

The remaining mechanical power is recirculated to the hydrostatic reservoir via Unit 2, whereby some additional power is lost (friction and leakage).

Analytically the situation is described as follows:

$$\begin{aligned} T_1 &= \eta_{mech,1} * D_1' * \Delta p \\ T_2 &= D_2' * \Delta p / \eta_{mech,2} \\ T &= T_1 - T_2 \end{aligned} \tag{26}$$

$$\begin{aligned} q_1 &= \omega * D_1' / \eta_{vol,1} \\ q_2 &= \omega * D_2' * \eta_{vol,2} \end{aligned} \tag{27}$$

The net output power is

$$P_{out} = T * \omega = (\eta_{mech,2} * D_1' - D_2' / \eta_{mech,2}) \cdot \Delta p * \omega \tag{28}$$

and the net input power is

$$P_{in} = (q_1 - q_2) * \Delta p = (D_1' / \eta_{vol,1} - D_2' * \eta_{vol,2}) * \omega * \Delta p \tag{29}$$

which could be combined to a total net efficiency: (30)

$$\eta_{tot} = P_{out} / P_{in} = (\eta_{mech,1} - \theta / \eta_{mech,2}) / (1 / \eta_{vol,1} - \theta * \eta_{vol,2})$$

where $\theta = D_2'/D_1' < 1$

An evaluation of Eq. (30) shows that the total efficiency at PRC always is lower than the efficiency for one single unit transmitting the output power.

The PRC characteristics can be explained semi-quantitatively by a comparison of different solutions to the following basic problem:

A variable output torque is to be produced within the range $0 \leq T \leq T_{max}$, utilizing a given constant differential pressure Δp. For the sake of simplicity, the output speed ω will be considered constant.

a) A straightforward solution is to use a variable displacement motor, the displacement of which is calculated according to Eq. (24). The output torque is controlled by the fractional displacement ε.

b) A simple, but energy-wasting solution is to use a fixed displacement motor and to reduce continuously the input pressure Δp to zero by means of a variable throttle between the fluid reservoir and the motor.

c) One variable displacement unit and one fixed displacement unit are used, both with a displacement that is half of the displacement used in a) and b) above. Both units are active for all required torques, the fixed displacement unit operating as a motor the whole time, and the variable machine operating as a pump in the low-torque regime - leading to PRC - and as a motor in the high-torque regime.

d) One fixed and one variable displacement motor of the "half" size as in c) are used. In the low-torque regime the variable motor is used alone. In the transition to the high-torque regime, the fixed motor is connected to the fluid supply, at the same time as the displacement fraction ε for the variable motor is changed instantaneously from 1 to 0. Higher torques are then obtained by increasing the amount of ε.

The relative power loss for a variable displacement machine, $\Delta P/P_{max,out}$, is shown in Fig. 11, where the absolute power loss, ΔP, due to leakage and friction is related to the output power at the maximum displacement.

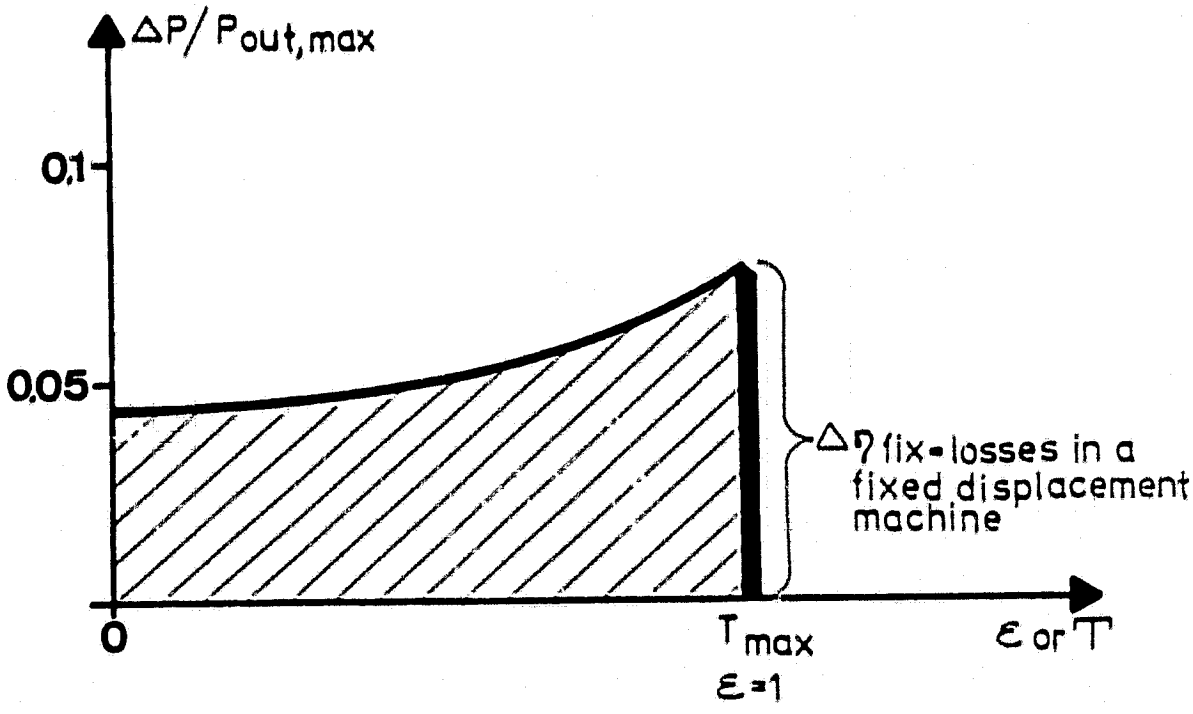

Fig. 11. Relative power loss for a variable displacement machine, pertaining to case a).

As will be shown later, the relative losses are almost independent of size. Thus, loss diagrams could be composed for the cases c) and d) (cf. F 12).

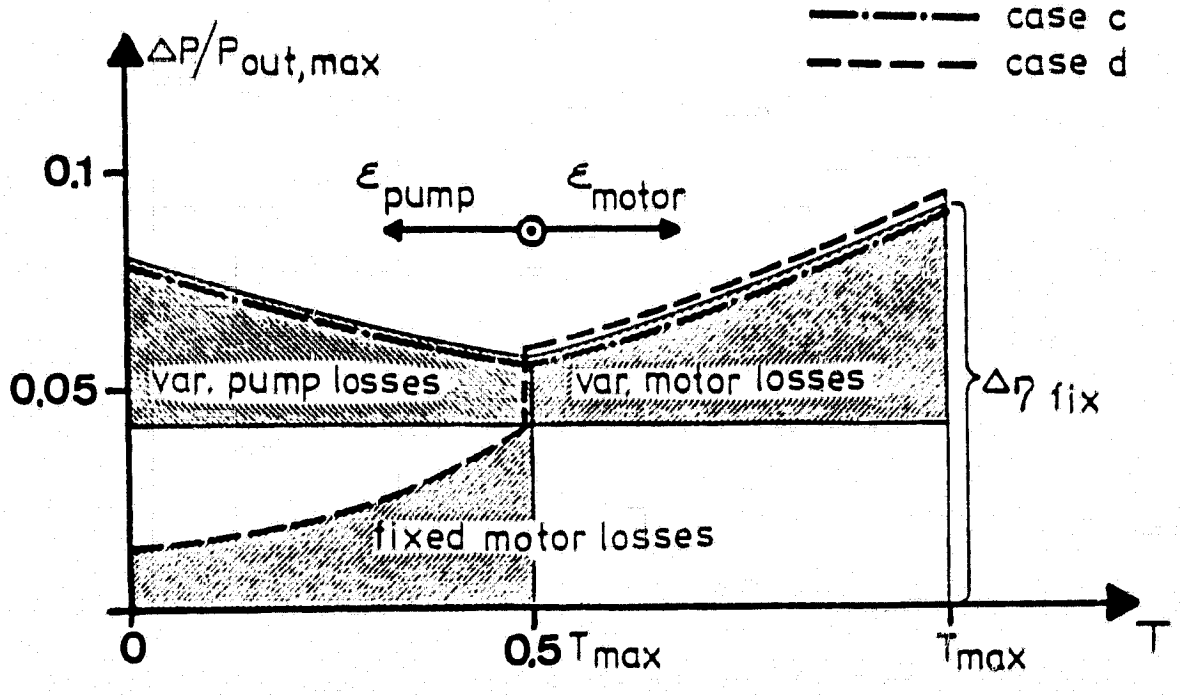

Fig. 12. Relative losses in two-unit arrangements.

At throttling, case b), the power input is constant at all output torques. Most of the power is therefore lost as internal friction in the fluid (cf. F 13).

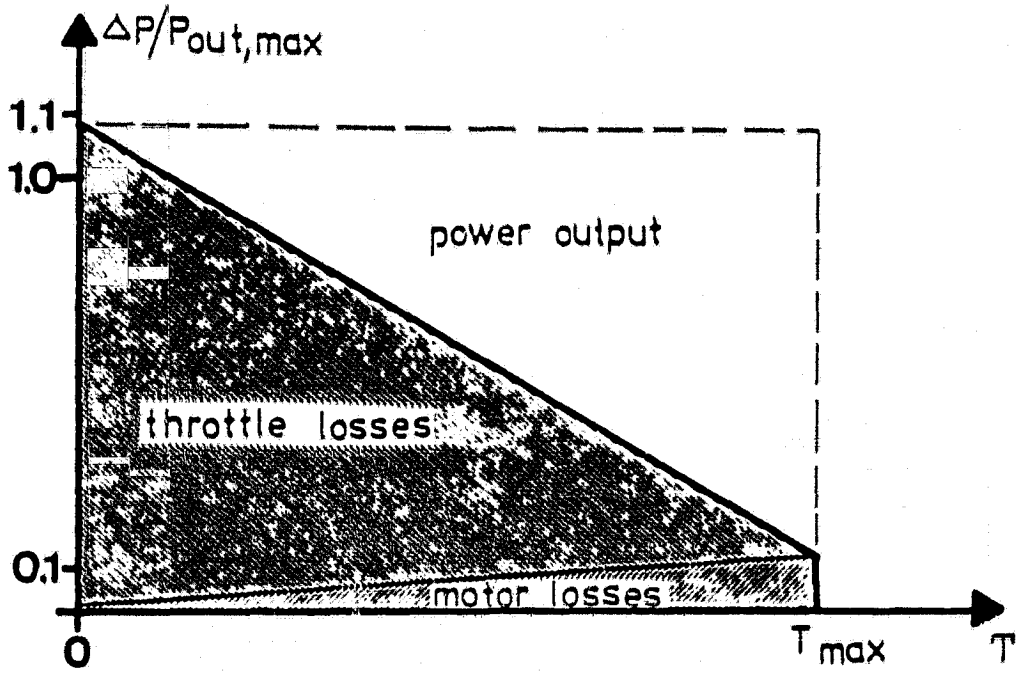

Fig. 13. Losses in a throttled system

The following conclusions can be made:

- losses are higher at PRC than in comparable systems with a straight power flow [case c) vs. cases a) and d)]
- losses are of the same order of magnitude for one large motor or several small motors in parallel [case a) vs. d)]
- losses are very high at torque control by throttling of fixed displacement motors [case b)]
- at very low torque output the mutual power loss is related for the cases a):c):d) as 2:4:1
- PRC is not justified by low-loss considerations; however, it offers a smooth shift between different modes of operation.

Hydraulic polarity shift (HPS)

The change of mode of operation from full displacement pump to full displacement motor may be obtained in one of two ways for the case with unchanged direction of rotation:

- by a continuous change of ε from one extreme (+1) via zero to the other extreme (-1), whereby the direction of flow, q, is changed continuously during the mechanical motion $\alpha \rightarrow 0 \rightarrow -\alpha$; the change may be completed in about 1 s
- by shifting - by valve operation - the hydraulic connections between the connecting ports and the high- and low-pressure reservoirs, respectively, whereby the rigid parts of the unit do not change their state of motion (thus no inertial forces), but the direction of flow is changed "instantaneously."

Design concepts considered

The following groups of design concepts have been considered.

1. One single motor
2. Two motors in parallel
3. One single motor with a two-speed transmission
4. Other compound systems of some merit

Groups 2 and 4 contain the following alternatives:

2a. Either one of two variable motors in operation
2b. Either one or both of two variable motors in operation
2c. One fixed and/or one variable motor in operation
2d. One fixed motor and/or one variable motor with PRC and HPS
2e. One fixed motor with HPS and/or one variable motor with PRC

4a. One single variable motor and a three-speed transmission
4b. One fixed and/or one variable motor with a two-speed transmission
4c. Two fixed motors and/or one variable motor
4d. Two fixed motors and/or one variable motor with PRC and HPS

All considered concepts have the potential of access to all driving forces $F \leq F_{max}$, hydraulic reverse gear, and recovery of braking energy.

In Appendix 1 are given the schemes of the main configurations of the different concepts and relevant control strategies, F vs. ε . It should be noted that the control strategies serve only as examples, using assumed (not optimized) displacements and gear ratios. As a common frame of reference the following is used:

$$\left.\begin{aligned} F_{max} &= 6000\ N \\ F_{urban} &\leq 2500\ N \quad \text{(light grey)} \\ F_{h\text{-}way} &\leq 600\ N \quad \text{(dark grey)} \end{aligned}\right\} \tag{31}$$

The F values in Eq. (31) are based upon Fig. 5, modified and adjusted according to experience and engineering intuition.

All the design concepts include other hardware in addition to that given in Appendix 1. Such components, e.g. a final transmission, flow control valves, hoses, micro-processor and other control components, are approximately of the same size, weight, and performance. Therefore, they have not been included in the sizing and optimization process.

5. RECOMMENDED DESIGN CONCEPTS

When evaluating the total merits of the candidate systems described in the preceding section, one should consider the following parameters:

- size of the variable motor/pump
- number of significant components
- number and character of gear shifts
- regime of ε used in urban/highway driving
- possible power recirculation (PRC) in urban/highway driving

The motor size is considered in terms of transmitted power, which presumes that both the maximum pressure and the maximum speed will be utilized in the optimized design. It is possible to meet any motor output speed by a proper choice of transmission ratios of the final and any intermediate mechanical transmission.

The character of the gear shifts - especially the time involved - varies among the systems described. The clutch operation and change of hydraulic polarity (HPS) are completed quickly; the change of displacement from one extreme to the other requires significantly longer time.

The fuel economy is influenced by the regime of ε that is most frequently used, as well as by possible power recirculation (PRC) under frequently used driving conditions.

It is assumed [cf. Eq. (31)] that urban driving requires up to about 40% and highway driving 10% of the maximum driving force. If low displacement ($\varepsilon < 0.20$) or PRC occur in these operating regimes ($F <$ 10% and 40% of F_{max}, respectively), a significant increase of losses will result.

Parameters of importance for the evaluation are listed in Table 1.

TABLE 1. Comparison of various design concepts

System type	1	2					3	4			
		a	b	c	d	e		a	b	c	d
Size of var.machine	1.0	0.8	0.67	0.5*	0.33	0.67	1.0	1.0*	0.5*	0.25	0.14
No. of var.machine	1	2	2	1	1	1	1	1	1	1	1
No. of fixed machine	0	0	0	1	1	1	0	0	1	2	2
No. of clutches	0	2	2	1	1	1	1	2	2	2	2
No. of gear meshes	0	1	1	1	1	1	2	2	2	2	2
No. of fast shifts	0	1	2	0	1	0	0	0	0	3	3
No. of slow shifts	0	0	0	1	0	2	1	2	3	0	0
PRC/urban	0	0	0	0	0	yes	0	0	0	0	yes
PRC/h-way	0	0	0	0	0	yes	0	0	0	0	no
Low ε/urban	yes	0	0	?	0	0	0	0	0	0	yes
Low ε/h-way	yes	0	0	yes	0	0	0	0	0	0	0
Magnitude of complexity	0	0	0	1	1	1	0	0	1	2	2

*) might be slightly reduced when a reduced driving force is accepted in the high speed regime of the vehicle.

A fully formalized selection of the most promising design concepts seems to be impossible. Some parameters are very difficult to quantify, such as complexity, riding comfort (jerks when gears are shifted), and reliability.

The first screening of candidate systems must to a great extent be done by engineering experience and intuition, which are difficult factors to incorporate into a computerized analysis of the systems.

A design concept with a high potential should meet the following criteria:

- only one variable displacement machine (heavy and expensive)
- smallest possible displacement for the variable machine (heavy and expensive)
- maximum two hydrostatic machines in all (i.e., the second one should be a fixed displacement machine) (complexity)
- low yoke angles (low ε) and PRC should be avoided as far as possible under normal driving conditions (high losses)
- the number of shifting points (discontinuous changes) should be minimized and the duration of the shifting procedure should be as short as possible (in order to make the ride comfortable).

None of the reviewed systems meets all the criteria mentioned above. Some systems are ruled out immediately, among them the single variable motor, which at normal driving conditions essentially has to operate in the low yoke angle regime.

The following two systems have been selected for further detailed analysis and optimization:

A: One variable displacement V-20 motor and a two-speed planetary gear train in series in front of the final gear (equivalent to Case 3 in Table 1) (cf. F 14).

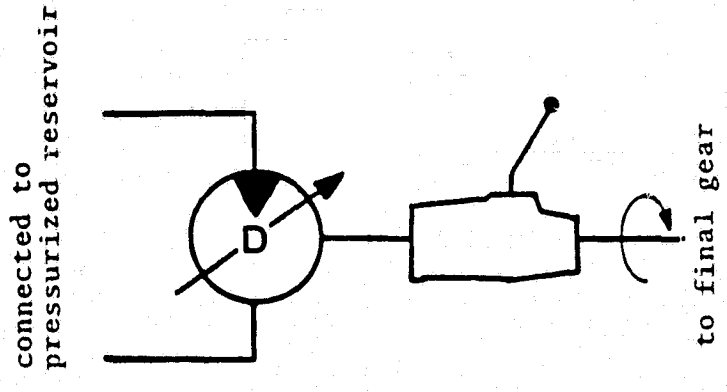

D= variable motor of type V-20

Fig. 14. Fundamental design concept of system A.

B: One variable displacement V-20 motor/pump in parallel with a disconnectable fixed displacement motor, both in front of the final gear (equivalent to Case 2d in Table 1) (cf. F 15). At low required driving force, the variable machine operates as a motor only. At an increased driving force (about 1/3 of F_{max}), the fixed motor is connected to the system and the variable machine is by HPS shifted to pump operation, whereby PRC conditions occur. At still higher driving force (2/3 of F_{max}), the V-20 machine changes to the motor operation mode.

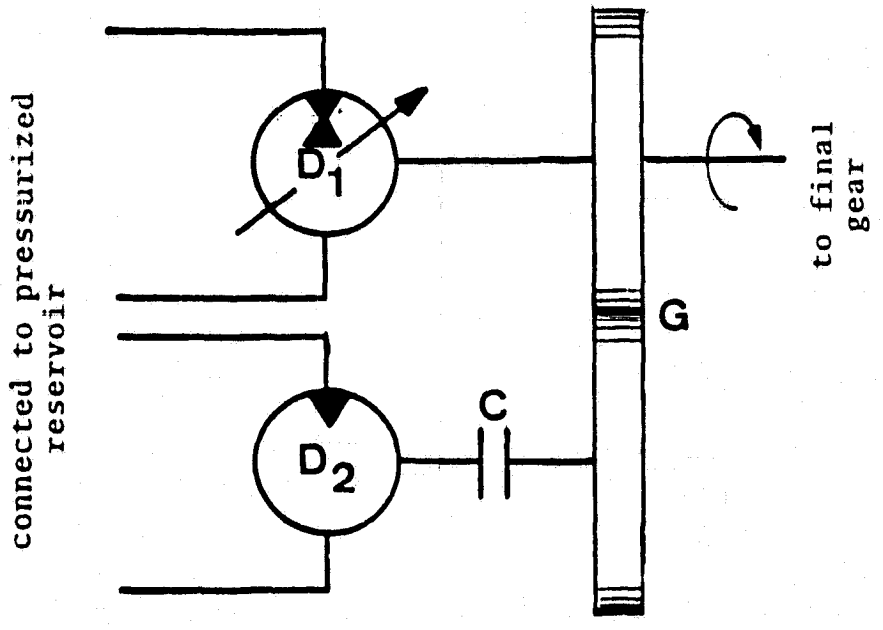

D_1 = variable motor/pump of type V-20
D_2 = fixed motor of type F-11
G = gearbox, constant ratio
C = clutch

Fig. 15. Fundamental design concept of system B.

N.B. System B may deliberately change towards system 2c in Table 1 if the optimization procedure is given full freedom. The displacements are then oversized, and the shift points are chosen in such a way that PRC is partly or fully avoided.

6. MODELING OF HYDROSTATIC COMPONENTS

General approach

Volvo Flygmotor has extensive experience with fixed displacement F-11 series pumps/motors. Performance data have been obtained for a variety of sizes.

The first type of variable displacement machines marketed by Volvo Flygmotor was the V-30 series of in-line machines. The design concept and thus also the performance, are to some extent different from those of the F-11 series of machines. Performance data is available from three different sizes of machines.

Later a variable displacement version of the F-11 series, named V-20, was developed. One basic size, D = 137 cm^3/rev, has been marketed since 1974. An updated version of the basic machine with the displacement D = 180 cm^3/rev has been developed quite recently and tested within this program.

All experience gained hitherto matches quite well the general theoretical description of losses in hydrostatic machinery which has been developed for the middle and full load operating regimes. There is a shortage of performance data on the low-load operating regime, and a special theory describing the losses needs to be developed as well. However, the middle and full-load theory covers the low-load regime with acceptable accuracy.

The state of the art of modeling losses in hydrostatic pumps/motors defines torque losses ΔT and leakage losses Δq as follows: *)

for motors:

$$T_{out} = T_{theor} - \Delta T = D' * \Delta p_{in} - \Delta T \qquad (32)$$

$$q_{in} = q_{theor} + \Delta q = D' * \Delta p_{in} + \Delta q \qquad (33)$$

for pumps:

$$T_{in} = T_{theor} + \Delta T = D' * \Delta p_{out} + \Delta T \qquad (34)$$

$$q_{out} = q_{theor} - \Delta q = D' * \Delta p_{in} - \Delta q \qquad (35)$$

*) Johansson, Ingvar & Larsson, Gunnar: Analysis of the efficiency of a hydraulic axial piston machine, M.Sc. thesis (in Swedish), Chalmers Univ. of Technology, Dept. of Mechanical Engineering (Machine Elements), 1967.

ΔT and Δq are assumed to consist of a number of partial losses, each of which is related to some identified physical phenomenon and thus proportional to some externally measurable parameter.

The various loss sources are:

- Parasitic torque loss (PTL)
  ΔT = const. (for a given machine) (36)

- Dry friction (DF)
  $\Delta T \sim p_{equ}$ (37)

- Viscous friction (VF)
  $\Delta_1 \sim \mu * \omega$ (38)

- Turbulent flow resistance (TFR)
  $\Delta T \sim \varrho * \omega^2$ (39)

- Viscous clearance leakage (VCL)
  $\Delta q \sim p_{equ}/\mu$ (40)

- Compressibility (C)
  $\Delta q \sim \Delta p * \omega$ (41)

As can be seen from Eqs. (36) through (41), the losses are proportional to some of the parameters load (Δp or p_{equ}), speed (ω), density (ϱ), and viscosity (μ).

The load parameter appears as Δp (=differential pressure) and p_{equ}. The equivalent pressure, p_{equ}, is introduced to take care of the back pressure, p_{back}, where adequate.

In most applications p_{back} is negligible; then $p_{equ} \simeq \Delta p$.

If, however, p_{back} is not negligible, it contributes to dry friction and viscous clearance leakage losses. Furthermore, Δp is active only over one half of a revolution, but p_{back} is active over the full revolution. Therefore, the "double" influence of p_{back} is taken into account as follows:

$$p_{equ} = \Delta p + 2*p_{back} \tag{42}$$

The experimental experience of the F-11 type of machines indicates that the relative losses are independent of the size of machines over a broad range of displacements. This fact could be used in a general type of loss expressions:

$$\Delta T = D'*(C_{PLT}+C_{DF}*p_{equ}+C_{VF}*\mu*\omega+C_{TFR}*\varsigma*\omega^2) \tag{43}$$

$$\Delta q = D'*(C_{VCL}*p_{equ}/\mu+C_c*\Delta p*\omega) \tag{44}$$

The loss expressions could be converted into efficiency expressions as follows:

<u>for motors:</u>

$$\eta_{vol} = "q_{out}"/q_{in} = q_{theor}/(q_{theor}+\Delta q) = 1/(1+\Delta q/(D'*\omega)) \tag{45}$$

$$\eta_{mech} = T_{out}/"T_{in}" = (T_{theor}-\Delta T)/T_{theor} = 1-\Delta T/(D'*\Delta p) \tag{46}$$

<u>for pumps:</u>

$$\eta_{vol} = q_{out}/"q_{in}" = (q_{theor}-\Delta q)/q_{theor} = 1+\Delta q/(D'*\omega) \tag{47}$$

$$\eta_{mech} = "T_{out}"/T_{in} = T_{theor}/(T_{theor}+\Delta T) = 1/(1+\Delta T/(D'*\Delta p)) \tag{48}$$

If the above expressions are used at low load and speed conditions, the best fit of the coefficients C_{PLT}, C_{VLC}, etc. to experimental data yields numerically different values of the coefficients at motor and pump operation respectively. Thus, the limit values of ΔT and Δq will not be equal for the pump and motor case when Δp and ω approach zero.

This discrepancy is, however, of lesser practical importance. It could probably - if necessary - be overcome by developing the state-of-the-art of the loss theory through splitting the load losses into ΔT and $\Delta(\Delta p)$ and the speed losses into Δq and $\Delta\omega$

F-11 machines

The following loss models developed by Volvo Flygmotor prior to the present project have been used:

pump:

$$\Delta T = D' * (1.42 * 10^{5} + 5.592 * 10^{-3} * p_{equ}) \quad (49)$$

$$\Delta q = D' * (1.78 * 10^{-8} * p_{equ} + 8.74 * 10^{-10} * \omega * \Delta p) \quad (50)$$

motor:

$$\Delta T = D' * (3.30 * 10^{5} + 8.96 * 10^{-3} * p_{equ}) \quad (51)$$

$$\Delta q = D' * (3.92 * 10^{-8} * p_{equ} + 3.50 * 10^{-10} * \omega * \Delta p) \quad (52)$$

The above coefficients are obtained for a fluid with ρ = 860 kg/m^3 and μ = 0.026 Ns/m^2. The coefficients may be modified to apply to other viscosities, as indicated in Eq. (44).

The estimation of weight, volume, and maximum speed is based upon trend curves for F-11 machines. (cf. F 16).

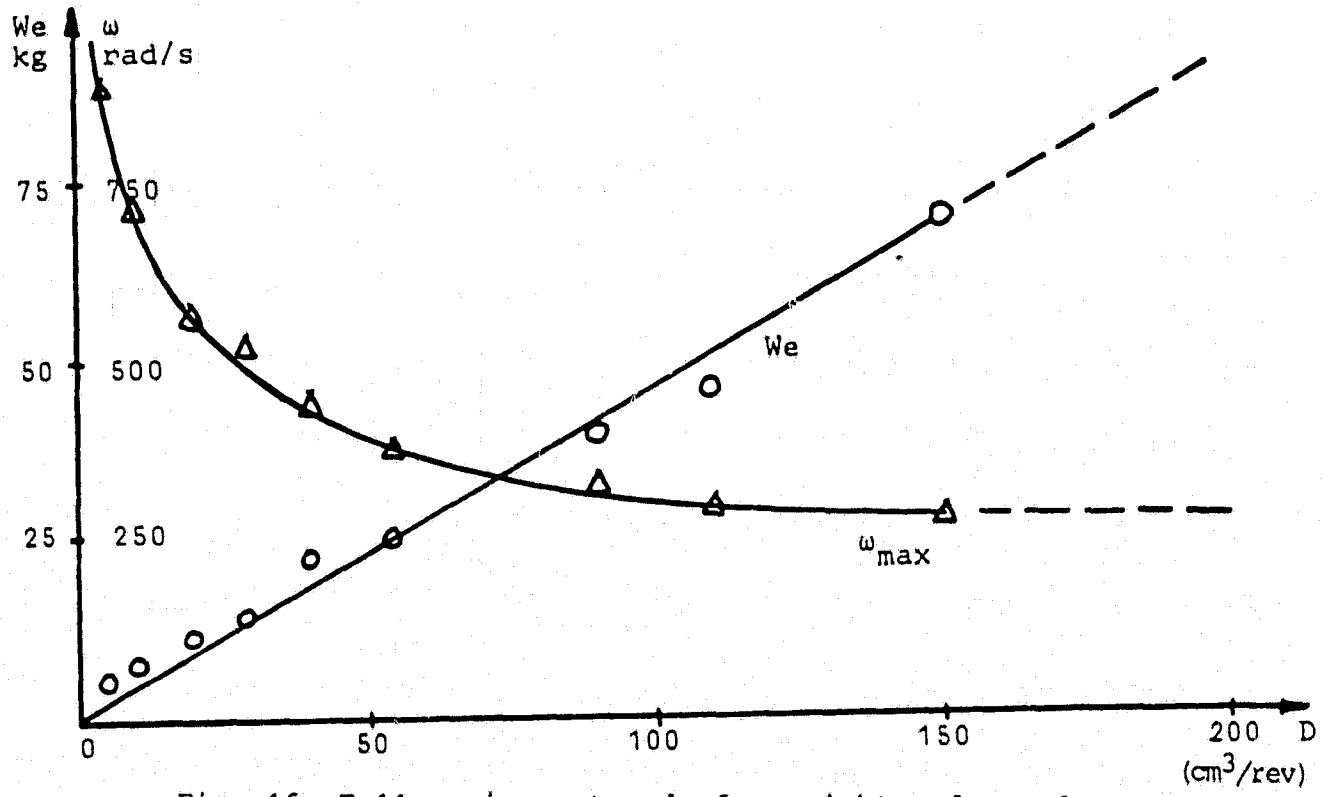

Fig. 16. F-11 series - trends for weight and speed

The data points in Fig. 16 represent a mixture of points from basic and updated designs. An almost linear relationship still exists between the weight We and the displacement, expressed as

$$We = D * 0.47 * 10^{6} \quad (kg) \tag{53}$$

The package volume is difficult to define uniquely. However, the density of an enveloping cube is approximately 2750 kg/m^3; thus, the volume Vo can be written,

$$Vo = D * 0.17 * 10^{3} \quad (m^3) \tag{54}$$

The maximum speed is modeled as

$$\omega_{max} = 4.0 * 10^{-3}/D + 240 \quad (1/s) \tag{55}$$

V-20 machines, experiments

The modeling of losses in the variable-displacement V-20 series of machines is based on a series of performance tests with special emphasis on operation at low yoke angles (low ε) and low speeds (ω) as well as at elevated back pressure.

A back-to-back testing technique (PRC) has been used. A circuit diagram of the performance test setup is shown in Fig. 17. The quantities measured were: (items 1 through 5 refer to meter positions, cf. F 17.

1. Torque,	10 through 100 Nm	± 2% through ± 1% *)
	100 through 1000 Nm	± 1% through ± 0.5%
2. Pressure,	2.5 through 10 MPa	± 3% through ± 1%
	10 through 40 MPa	± 1% through ± 0.25%
3. Flow,	0.17 through 7.6 * 10^{-3} m^3/s	± 0.5%
4. Speed,	(any)	± 0.5%
5. Temperature,	(any)	± 1^{o}C

*) the given measuring accuracy is assumed to change linearly over the given measuring regime.

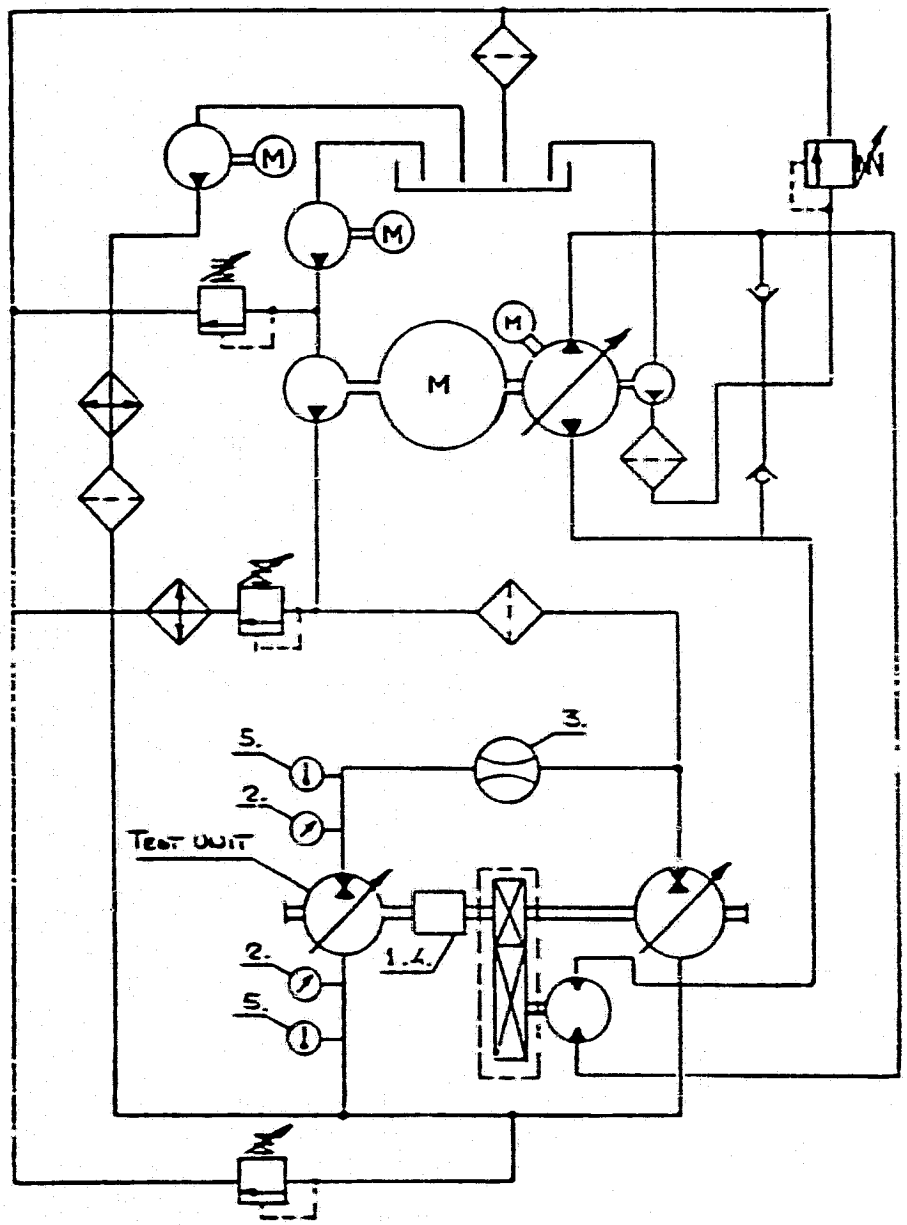

Fig. 17. Circuit diagram of the performance test setup.

TABLE 2. Legend to Fig. 17.

M	Electric Motor
	Oneway Pump with Fixed Displacement
	Pump/Motor with Variable Displacement
	Twoway Variable Displacement Pump
	Twoway Motor with Fixed Displacement
	Volume Flow Meter
	Thermometer
	Pressure Gauge
	Adjustable Max.Pressure Limiter
	Cooler
	Filter or Strainer
	Non-Return Valve

Measurements have been carried out for the following matrix of parameters:

pump operation

Δp: 0, 5, 15, 25, and 35 MPa
$n (\rightarrow \omega)$: 500, 1500, 2000, 2500, and 3000 rpm
$\alpha (\rightarrow \varepsilon)$: 40, 25, 15, 10, 6, and 3°

motor operation

Δp: 0, 5, 15, 25, and 35 MPa
$n (\rightarrow \omega)$: 100, 200, 500, 1500, 2000, 2500, and 3000 rpm
$\alpha (\rightarrow \varepsilon)$: 40, 25, 15, 10, 6, 4, and 3°

All tests above were run at p_{back} = 1 MPa, ρ = 860 kg/m^3 and μ = 0.026 Ns/m^2
(Shell Tellus 46 oil at 50°C)

Special tests were performed with elevated temperature and increased back pressure, respectively, for the following reduced matrix of paramters:

Δp: 5, 15, 25 (and 35) MPa
$n (\rightarrow \omega)$: 500 and 2500 rpm
$\alpha (\rightarrow \varepsilon)$: 25 and 10°

back pressure 10 MPa at t = 50°C, and
temperature 70°C at p_{back} = 1 MPa

Results of the tests, expressed as efficiencies, are given in Appendix 2.

V-20 machines, mathematical model

The mathematical model has been developed in the following way: Experimental data has been transformed to the form:

ΔT and Δq
as a function of
ε, ω, Δp (and p_{back})

For each ε, data has been plotted in various ways in order to refine and identify each of the losses given in Eqs. (36) through (41). The coefficients C_{PTL}, C_{VCL}, etc. were thus obtained as functions of ε.

The influence of the variable displacement ε was then taken into account purely numerically, by fitting a third order polynomical of ε to C_{PTL}, C_{VCL}, etc. Some of the polynomial terms vanished.

The remaining terms give the following loss expressions:

$$\Delta T = D'_{max} * [(C_1 + C_2 * \varepsilon) + (C_3 * \varepsilon + C_4 * \varepsilon^2 + C_5 * \varepsilon^3) * \omega^2 +$$

$$+ (C_6 + C_7 * \varepsilon) * \omega + (C_8 + C_9 * \varepsilon + C_{10} * \varepsilon^2 + C_{11} * \varepsilon^3) * p_{equ}] \quad (56)$$

$$\Delta q = D'_{max} * [C_{12} * p_{equ} + (C_{13} + C_{14} * \varepsilon + C_{15} * \varepsilon^2 + C_{16} * \varepsilon^3) *$$

$$* \omega * \Delta p] \quad (57)$$

Separate sets of C_1 through C_{16} for pump operation, C^p, and motor operation, C^m, are listed in Table 2. The fractional displacement ε is in both cases positive.

TABLE 2. Loss coefficients for pump and motor operation.

Type of loss	Subscript (Index)	C^p	C^m
Parasitic torque	1	$2.12 * 10^5$	$1.23 * 10^5$
	2	$-0.706 * 10^5$	$-0.706 * 10^5$
Turbulent flow resistance	3	1.66	-6.20
	4	6.00	23.63
	5	3.84	-10.51
Viscous friction	6	$1.10 * 10^3$	$1.24 * 10^3$
	7	$1.10 * 10^3$	$1.59 * 10^3$
Dry friction	8	$9.53 * 10^{-3}$	$8.21 * 10^{-3}$
	9	$3.53 * 10^{-3}$	$-2.72 * 10^{-3}$
	10	0	$80.16 * 10^{-3}$
	11	0	$-49.28 * 10^{-3}$
Viscous leakage	12	$6.00 * 10^{-8}$	$6.00 * 10^{-8}$
Compressibility	13	$4.62 * 10^{-10}$	$4.33 * 10^{-10}$
	14	$0.95 * 10^{-10}$	$3.77 * 10^{-10}$
	15	$13.41 * 10^{-10}$	$-4.70 * 10^{-10}$
	16	$-12.27 * 10^{-10}$	0

The coefficients in Table 2 are calculated for a fluid with ρ = 860 kg/m^3 and μ = 0.026 Ns/m^2.
They may be modified to apply to other densities and viscosities as indicated in Eqs. (43) and (44).

The accuracy of the numerical loss model is in most cases within the limits of experimental errors embedded in the data used. At full load there may be errors of $\pm$ 1% in both η_{vol} and η_{mech}. As the absolute errors are of the same order of magnitude, the relative errors increase with decreasing load, making the η predictions uncertain in the low-power regime (< 10% of maximum power).

The modeling of weight, size, and maximum speed is of necessity based upon a limited and inhomogeneous number of data for variable displacement machines. Only three units exist of the V-30 series and 2 units of the V-20 series. In each series one unit is of an updated design, the others of the basic design. Existing data are plotted in F 18.

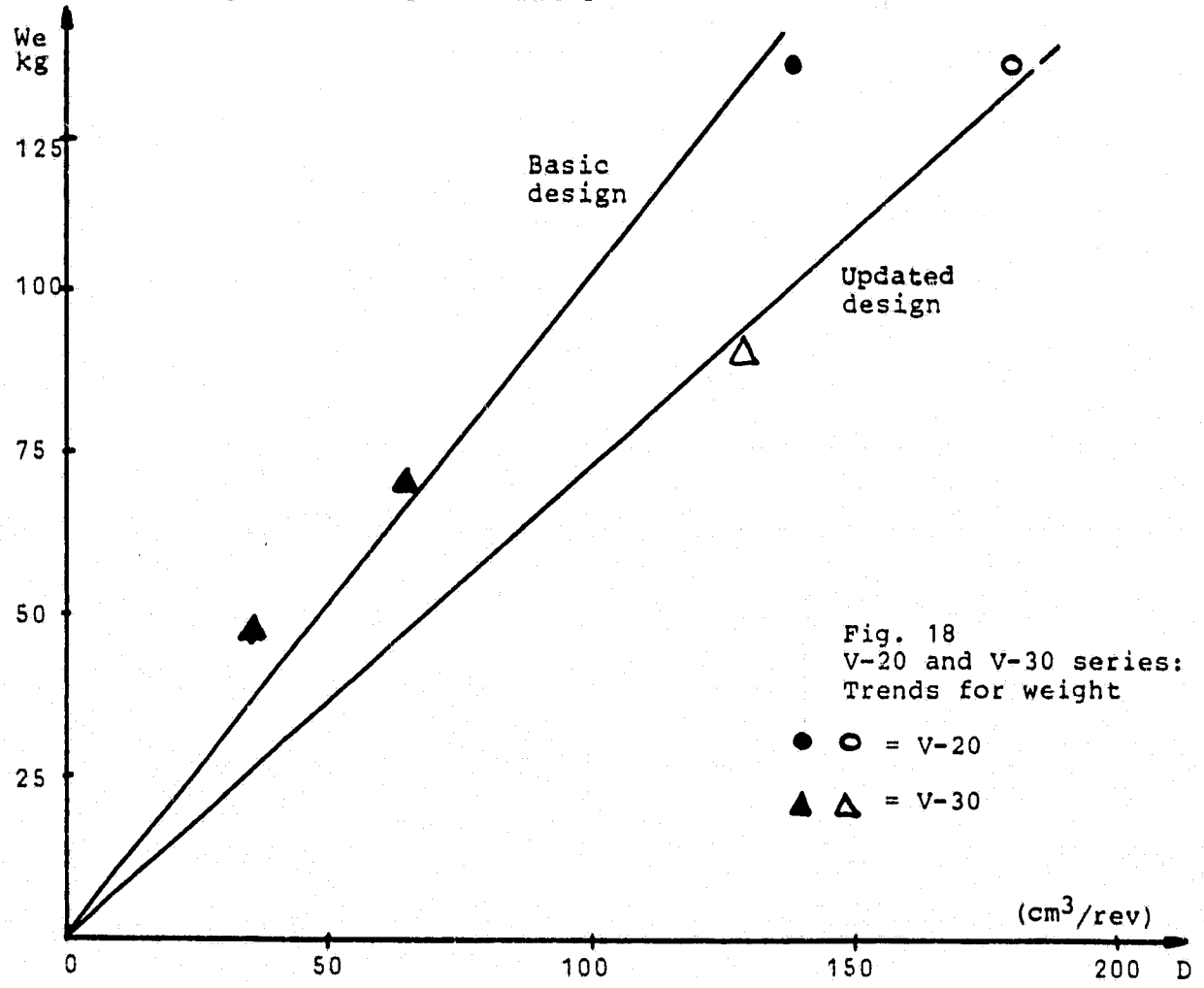

Fig. 18
V-20 and V-30 series:
Trends for weight

If the well-documented trends for the F-11 series machines are used (cf. Fig. 16 and Eqs. (53) and (55)), the models for V-20 series machines could be based upon these trends and the data for the V-20-180 updated machine only, yielding

$$We = D*0.75*10^{6} \quad (kg) \tag{58}$$

$$Vo = D*0.45*10^{3} \quad (m^3) \tag{59}$$

$$\omega_{max} = 4.0*10^{-3}/D+300 \quad (1/s) \tag{60}$$

7. MODELING OF GEARED COMPONENTS

The following significant geared components are parts of the transmission systems A and B and contribute to the power loss:

- fixed-ratio gear transmission
- two-speed planetary gear train
- final gear of the conventional type
- (clutch)

Other components, such as valves, hoses, fluid reservoirs, filters, coolers, and control equipment, are assumed not to influence the transmission characteristics appreciably. Also their weight and volume might be expected to be the same for various system configurations. Therefore, they are not modeled and not incorporated in the numerical evaluation and optimization procedure.

When modeling power losses for mechanically geared transmissions, one must consider the following types of losses. *)

Torque losses

ΔT = const.: idling/parasitic loss

$\Delta T \sim T$: load proportional/gear mesh loss

Speed losses

$\Delta\omega \equiv 0$: no losses/positive action.

The significant geared components are modeled numerically as follows:

Fixed-ratio gear transmission

The transmission ratio, denoted R_{conn}, gives the theoretical speed and torque conversion relationships

$$\omega_{out} = \omega_{in}/R_{conn} \tag{61}$$

$$T_{out,\ theor} = T_{in} * R_{conn} \tag{62}$$

*) Mägi, M: On the Efficiencies of Mechanical Co-Planer Shaft Power Transmissions, Diss. Chalmers Univ. of Technology, Gothenburg, Sweden, 1974.

Due to idling and gear-mesh losses, the real torque output is modified to

$$T_{out} = (T_{in} - \Delta T) * R_{conn} * \eta_{mech} \quad (63)$$

Numerical loss coefficient values are given in Table 3.

The weight and volume are assumed to be constant because the maximum transmitted power is constant (cf. Table 3).

N.B. When the transmission is disconnected from the fixed displacement machine, the load-dependent gear-mesh losses disappear, but the idling losses are still affecting the output torque (cf. the position of the clutch in Fig. 15).

Two-speed planetary gear train

At direct gear the transmission ratio is unity; the speed reduction gear has the ratio R_{low}, giving the theoretical speed and torque conversion relationships for the low gear:

$$\omega_{out} = \omega_{in} / R_{low} \quad (64)$$

$$T_{out,theor} = T_{in} * R_{low} \quad (65)$$

Due to idling and gear mesh losses, the real torque output is modified to

$$T_{out} = (T_{in} - \Delta T) * R_{low} * \eta_{mech} \quad (66)$$

For the direct gear the real output torque is

$$T_{out} = T_{in} - \Delta T \quad (67)$$

Numerical data on losses and weight/size coefficients are given in Table 3.

Final gear of the conventional type

This transmission consists of a hypoid gear and a differential gear in series, converting the rotational mode of motion into a linear mode of motion at the periphery of the driving wheels. The transmission ratio R' defines the theoretical speed and torque relationships. R' is given as the amount of rotation of the universal shaft (in radians) per traveled distance (in meters),

$$v = \omega_{in}/R' \tag{68}$$

$$F_{theor} = T_{in} * R' \tag{69}$$

Due to idling and gear mesh losses, the real torque output is modified to

$$F = (T_{in} - \Delta T) * R' * \eta_{mech} \tag{70}$$

Numerical data on losses and weight/size coefficients are given in Table 3.

TABLE 3. Loss and weight/size data on geared transmissions.

Component	ΔT *)	η_{mech} *)	We (kg) **)	Vo (m^3) **)
Fixed-ratio geared transm.	$0.03*T_{max}$	0.97	7	0.005
Two-speed planetary gear	$0.05*T_{max}$	0.96	$7+0.003*T_{max}$	0.004
Final gear	$0.05*T_{max}$	0.96	-	-
Clutch	-	-	3	0.003

*) Data extracted from: Reichenbächer, H: Gestaltung von Fahrzeuggetriebe, Springer-Verlag, 1955.

**) Data based upon Volvo Car Co. rules of thumb; data contain minimum casing.

8. OPTIMIZATION CRITERIA

The contract originally prescribed the highest possible efficiency at steady-state driving in the speed range of 6.7 through 22.4 m/s and the lowest possible volume, weight, and complexity as optimization criteria of the system.

Highest possible mean value of the total efficiency over some steady-state speed regime seems to be an oversimplified approach to the problem, since the total fuel economy is one of the main problem areas for road vehicles. The total fuel economy is, however, strongly linked to the type of driving, i.e., to some driving cycle.

In the present analysis the fuel economy in a wide sense is taken as a basis for the optimization of the systems A and B recommended for further analysis (cf. p. 24).

The direct fuel economy is based upon the EPA Urban Driving Cycle. Indirectly, the package weight increases the rolling resistance and the inertial load and thus the fuel economy. Similarly, the package volume increases the front area of the vehicle and thus the increased drag losses also increase the fuel consumption.

The complexity of the system (and the cost related thereto), the reliability, and the driving comfort and other non-quantitative values have been considered in the preceding investigation of candidate systems.

The EPA Urban Driving Cycle has been analyzed in detail. The results are summarized in the Driving Cycle Matrix (cf. F 4).

Another similar matrix may be computed, containing information on system performance as a function of F and v. If the system configuration, component size, and loss models as well as the control situation are known, it is possible to calculate the performance characteristics (efficiencies, flows, torques, etc) for each output condition defined by F and v.

Should two or more control positions (gear in operation and displacement utilized) permit the same output, the control mode having the lowest power loss is chosen. The results are summarized as system characteristics matrices (F 19).

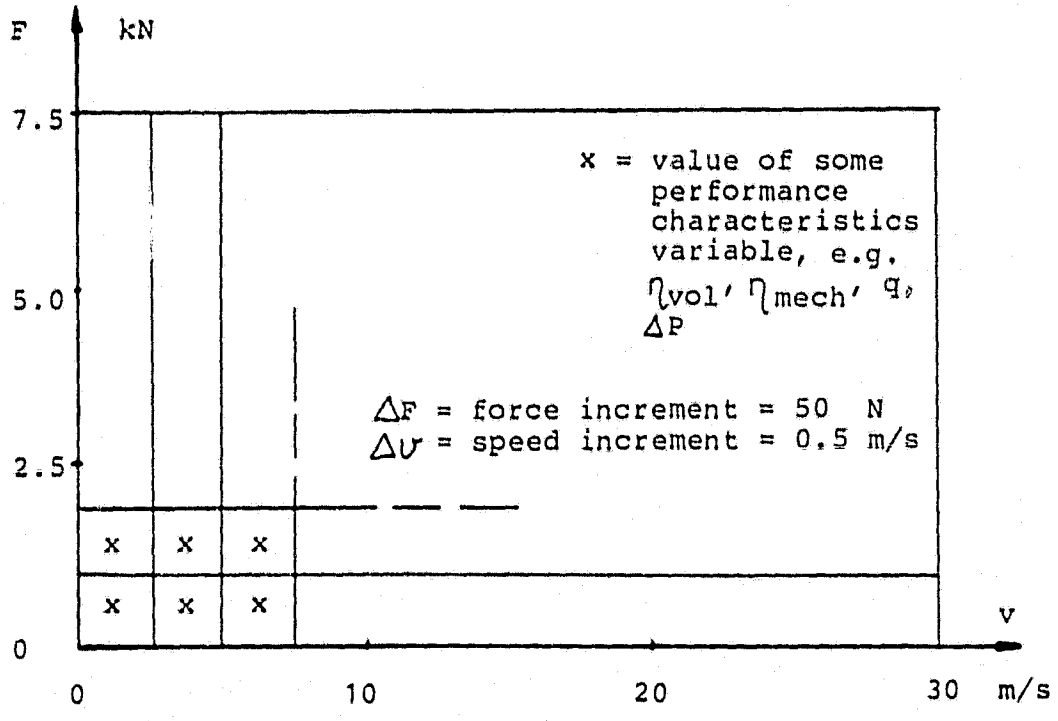

Fig. 19. System characteristics matrix

The total energy consumed during some specific driving cycle is obtained simply by multiplying the driving cycle matrix and the power input matrix, which is one of the system characteristics matrices.

This kind of energy consumption analysis could be repeated for any system with arbitrarily chosen sizes of components. In addition, for each system analyzed one must check if the system meets the acceleration requirements and if the configuration is capable of continuously producing any combination of force and speed in the operating range of the vehicle.

The results obtained are combined to a value function, the basic term of which is the calculated energy consumption, whereto are added terms for weight and volume, converted to increase of energy consumption as described earlier.

To the value function must also be added, for formal reasons, "penalty terms" for the cases where the acceleration and force continuity requirements are not fulfilled. These terms must, however, become zero when the value function is minimized, which means that at optimum conditions the acceleration requirements and driving force continuity are fulfilled.

9. METHODS OF EVALUATION

Numerical calculations have been carried out on an IBM computer, using the FORTRAN IV programming language.

The total computer program consists of a number of independent subroutines. The main subroutine blocks

- analyze the driving cycle and compile the matrix of the length of the driving time at various combinations of F and v (the driving cycle matrix)
- calculate the power consumed by each modeled component, provided that the operating conditions are known
- calculate the volume and weight of each modeled component
- check the acceleration and driving force continuity requirements
- find the operating conditions for a given set of components (maximum displacements and gear ratios) and boundary conditions (differential and back pressure, output force, and speed). This subroutine produces the data for the following system characteristics matrices: power loss, input flow, volumetric and total efficiencies, and control data (high/low gear and yoke angle).
  In order to eliminate time-consuming iteration, the computation is based on a function-mapping technique, whereby F and v are mapped as dependent variables, being functions of input pressures and flow as well as of control data. Interpolation then gives flow and control data as functions of F and v
- find the optimized set of components characterized by the minimum point of the value function as defined in the preceding section. The direct search method, developed by Nealder & Mead, using the simplex concept for non-linear problems, has been used to avoid just trial and error techniques for the optimization *)
- prepare output data (interpolate data for drawing of performance maps, etc).

---

*) Elmén, Claes: Optimization of Hydraulic Transmission of Vehicle, M.Sc. thesis (in Swedish), Chalmers Univ. of Technology, Dept. of Mechanical Engineering (Machine Elements), 1980.

The computation is governed by a control program, calling on the various subroutines. Each computation requests the specification to the control program of input pressures (differential and back) and an assumed set of values of parameters to be optimized. The optimization algorithm guarantees only the detection of local minima; therefore various starting sets of parameter values must be tried to find the global minimum of the value function.

Found global minima are all very flat. Therefore, the optimization is not very distinct.

The results of each computation are obtained as definite values of the total energy loss and characteristics of optimized components: displacement/gear ratio, weight, and volume. In addition, system characteristics matrices are obtained as discrete data with increments in accordance with Fig. 4, and as computer-drawn constant-value graphs.

10. NUMERICAL RESULTS

The computer program package developed in accordance with the description in the preceding sections has been used to analyze and optimize the hydrostatic drive systems A and B, as defined in Figs. 14 and 15.

Both systems have been evaluated for 5 different differential pressures: 6.895, 13.79, 20.68, 27.58, and 34.47 MPa (1000, 2000, 3000, 4000, and 5000 psi) and a negligible back pressure.

In addition, System A has been evaluated for 3 different back pressures: 3.447, 6.895, and 13.79 MPa (500, 1000, and 2000 psi) at a differential pressure of 20.68 MPa (3000 psi).

Optimized parameters are

for System A:

D_{var} = displacement of the variable motor

R_{low} = transmission ratio of the lower gear of the two-speed planetary gear train

R' = transmission ratio of the final gear (in radians of revolution per traveled distance)

for System B:

D_{var} = displacement of the variable machine

D_{fix} = displacement of the fixed motor

R_{conn} = transmission ratio of the connecting gear

R' = transmission ratio of the final gear (in radians of revolution per traveled distance)

Calculated quantitites for each set of optimized parameters are:

E_{loss} = energy loss during completion of the EPA Urban Driving Cycle

We = package weight

Vo = package volume

The theoretical amount of energy required to complete the EPA Urban Driving Cycle is the same for all cases evaluated:

$$E_{theor} = 6.70 * 10^{6} \text{ Nm} \quad (71)$$

The above-mentioned optimized and evaluated data is given in Table 4.

In addition to the limited amount of summarized information given in Table 4, a large amount of detailed data has been calculated for each of the 13 cases evaluated.

For each case, data of the following performance characteristics matrices has been evaluated:

- total efficiency
- volumetric efficiency
- control data (ε and high/low gear)
- power loss
- input flow rate

Each matrix contains about 5500 non-zero combinations of speed and force with a speed increment of 0.5 m/s and a force increment of 50 N. This number of data has been used to prepare the performance maps given in Appendix 3. The results obtained are illustrated by the reduced size performance maps depicted in Figs. 20 through 24 , computed for System A at a 20.68 MPa differential pressure and negligible back pressure.

The computed performance data points are also stored as data files on computer recording tape. The stored amount of data has been reduced by deleting every second row and column of the original performance characteristics matrices.

TABLE 4. Principal computed results for systems A and B

(The weight We and volume Vo include the following components: the variable machine and the train or the fixed machine, the connecting drive and the clutch, alternatively)

System	Δp MPa	p_{back} MPa	D_{var} 10^{-6} m^3	D_{fix} 10^{-6} m^3	R_{low} –	R_{conn} –	R' 1/m	E_{loss} 10^6 Nm	We kg	Vo 10^{-3} m^3
A	34.47	negl.	96,0	–	2.98	–	3.22	4.96	95.2	47.2
	26.58	"	112	–	2.91	–	3.56	4.68	106	54.3
	20.68	"	142	–	2.99	–	3.67	4.48	127	67.0
	13.79	"	255	–	2.72	–	3.37	4.42	215	119
	6.895	"	473	–	3.35	–	3.05	4.51	377	217
	20.68	"	142	–	2.99	–	3.67	4.48	127	67.0
	"	3.447	141	–	2.98	–	3.71	4.88	130	70.7
	"	6.895	141	–	2.99	–	3.68	5.31	130	70.5
	"	13.79	141	–	2.99	–	3.69	6.35	130	70.5
B	34.47	negl.	96.0	64.9	–	2.46	3.59	5.64	113	62.2
	26.58	"	124	78.0	–	2.61	3.53	5.43	140	77.0
	20.68	"	155	114	–	1.67	4.43	5.06	179	97.0
	13.79	"	211	154	–	1.89	4.62	4.97	241	129
	6.89	"	393	314	–	1.58	5.30	5.20	452	238

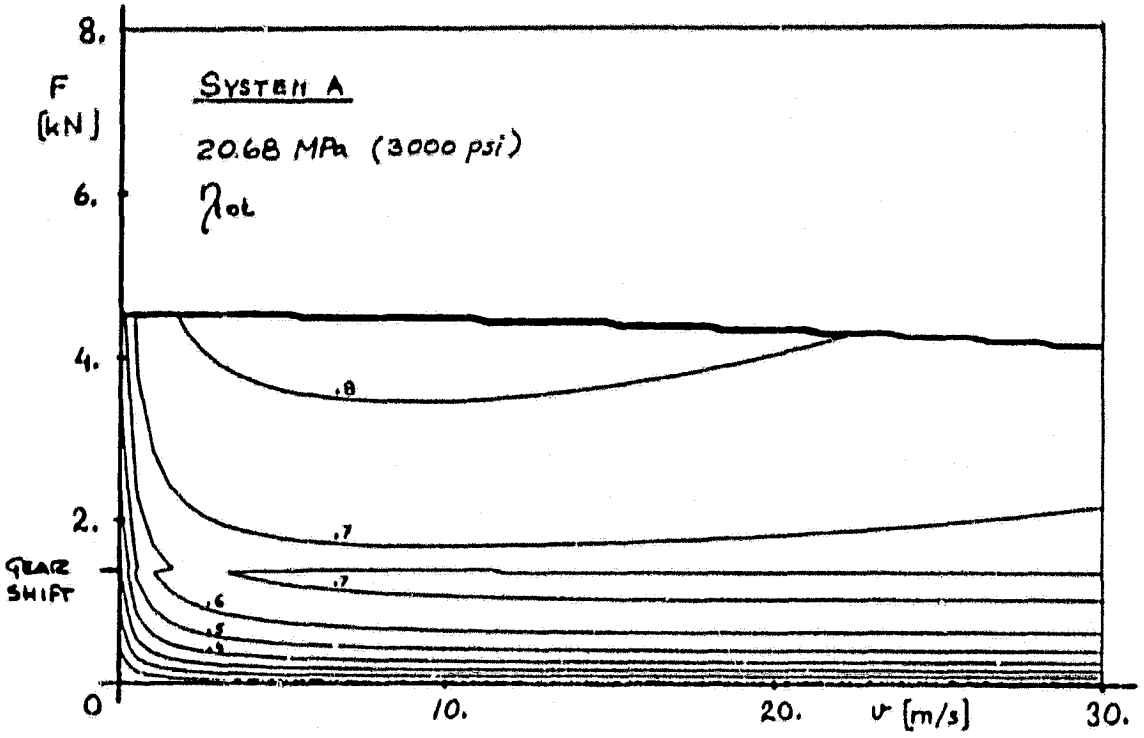

Fig. 20. Performance map - total efficiency (complete drive system)

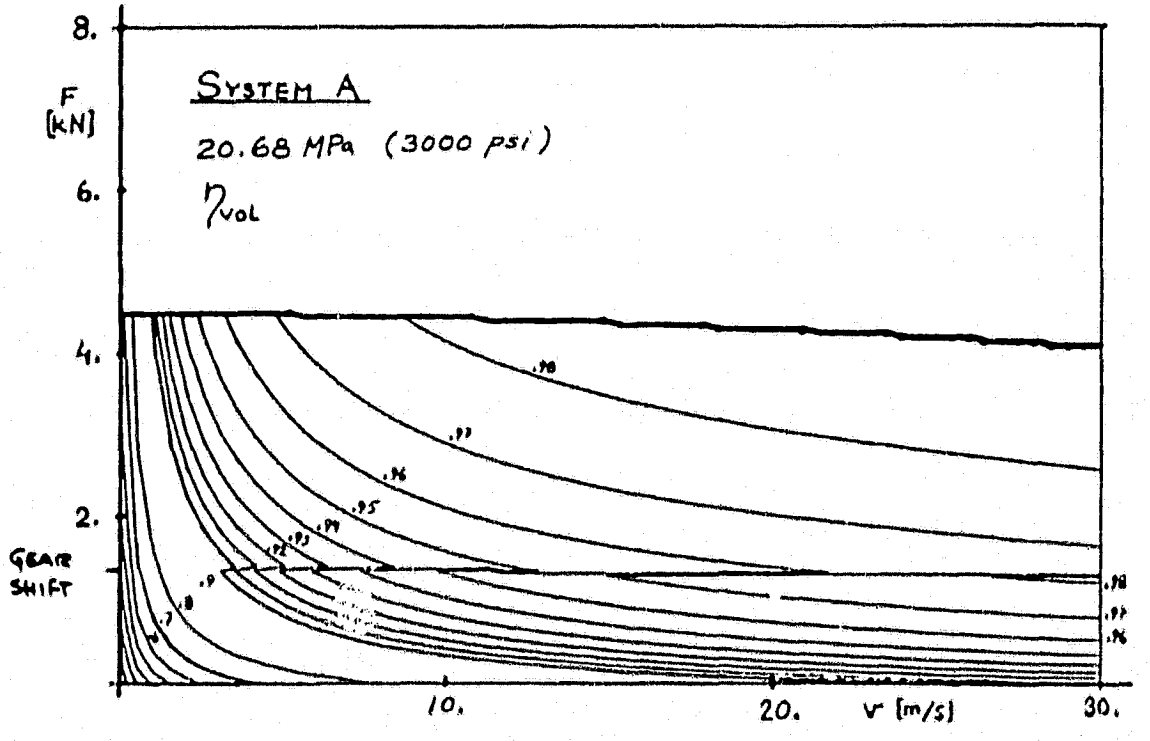

Fig. 21. Performance map - volumetric efficiency (hydrostatic unit)

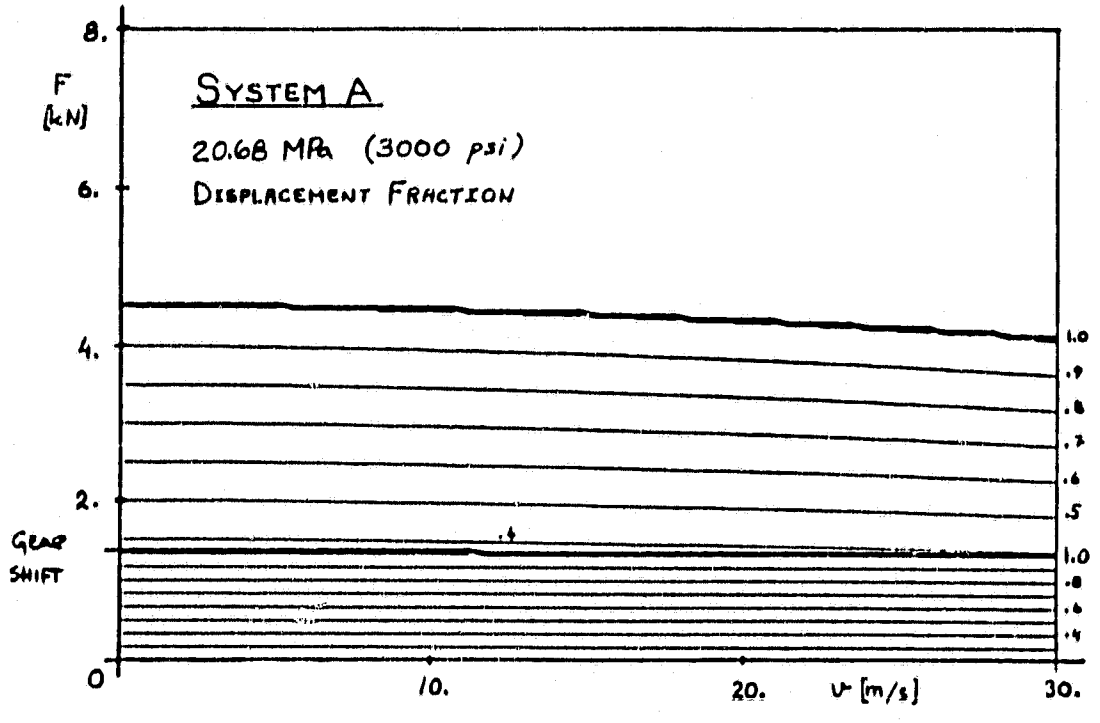

Fig. 22. Performance map - control data

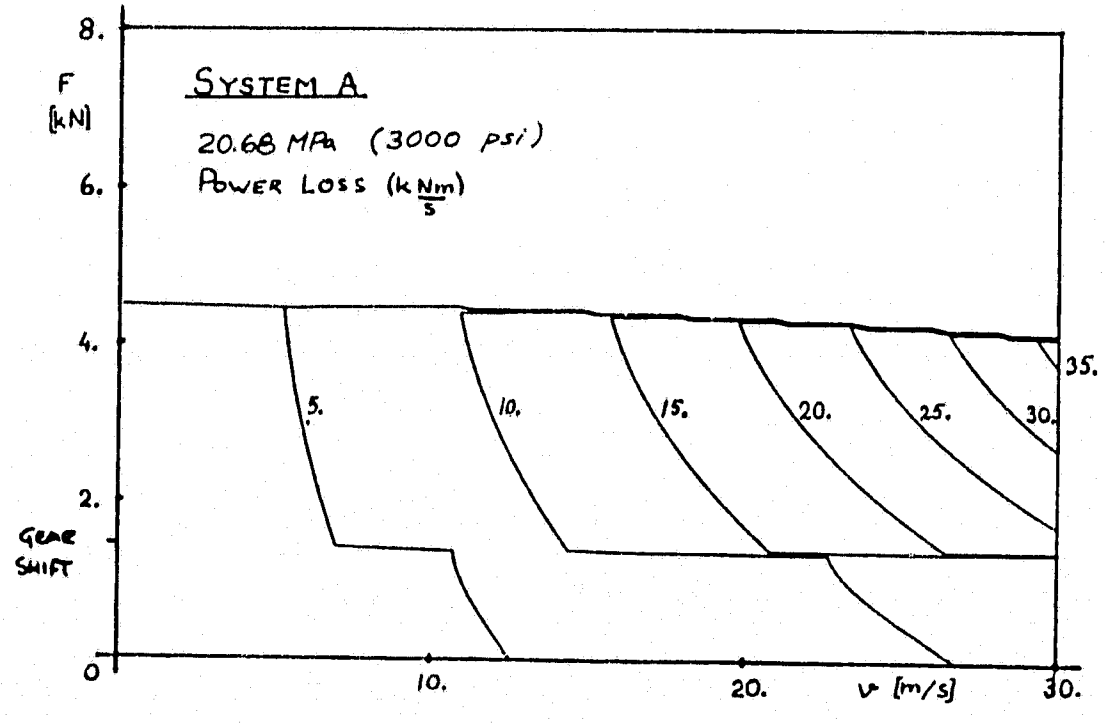

Fig. 23. Performance map - power loss

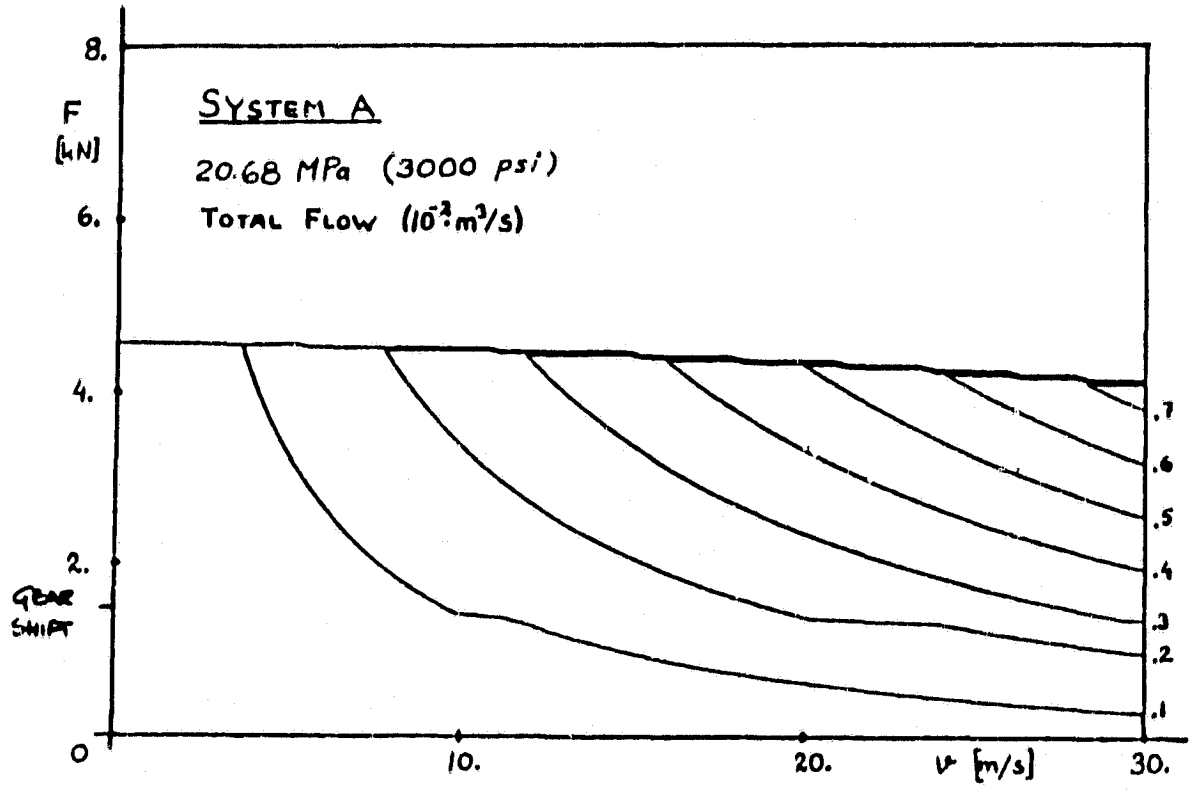

Fig. 24. Performance map - input flow rate

11. CONCLUDING REMARKS

Limitations in Theory Used

1. The theoretical model assumes perfect external control of torque, and no time losses are considered when applying the initial torque and when shifting the gears.

2. The influence of secondary units, e.g., valves, filters, and hoses, is not considered when calculating losses and evaluating package weight and volume. (The influence is assumed to be the same for all cases studied).

Component Models

3. The model of the VFA V20-180 machine predicts - in the loaded regime - loss values that are very close to the only set of available experimental results, but are somewhat lower (i.e. higher efficiency) than the values from the accumulated experience from V20-135 machines. The state-of-the-art of loss modeling does not permit an excellent loss prediction in the low-load regime of hydraulic machinery.

4. The model of the F-11 machines seems to overestimate the efficiency by maximum 2% in the high-load regime.

5. The loss models of the mechanical components are deliverately designed to be somewhat conservative. The real efficiencies of these components might be improved by a few percent.

6. The modeling of weight and volume of mechanical geared components depends very much on the assumptions made. Therefore, given data are to be considered more as an educated guess than definite values.

Obtained Results

7. All calculated optima are rather indistinct, i.e. neighbouring parameter values give almost the same performance characteristics.

8. The total losses are almost independent of pressures used; however, the weights and volumes of the systems increase drastically at decreasing differential pressure.

9. Calculated energy losses may be converted to milage figures for the EPA Driving Cycle. Assuming a 30% engine efficiency and a 95% efficiency of an additional hydrostatic pump connected to the engine, the best cases investigated will have a fuel (gasoline) consumption of less than 10 liters per 100 kilometer (23.7 mpg).

10. Obtained control strategies deviate somewhat from initial assumptions resulting in slightly "oversized" hydraulic components. This is especially true for system B, were power recirculation (PRC) tends to be suppressed.

Appendix 1: Configurations of Candidate Systems

DESCRIPTION OF CANDIDATE SYSTEMS

In the following description of candidate systems only the main components have been listed, as e.g. the hydrostatic motors, and necessary clutches and gears. Hydraulic valves and the (microprocessor-based) control system, as well as the final transmission have been excluded. As we do not manufacture hydraulic valves to be used outside our units the background for predicting the development on those parts is limited to some extent.

$D_{1,2...}$ indicate maximum (or constant) displacement of the hydrostatic machines, ε indicates the fraction of the max displacement used.

F indicates the driving force

P_1/P_2 indicate the hydrostatic supply and back pressure

$C_{1,2\ ...}$ indicate clutches

$G_{1,2\ ...}$ indicate single-step gear transmissions

1. Single motor

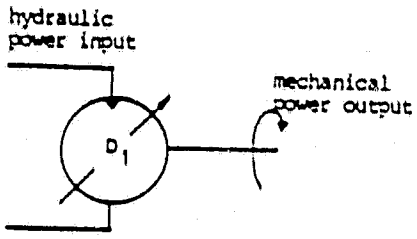

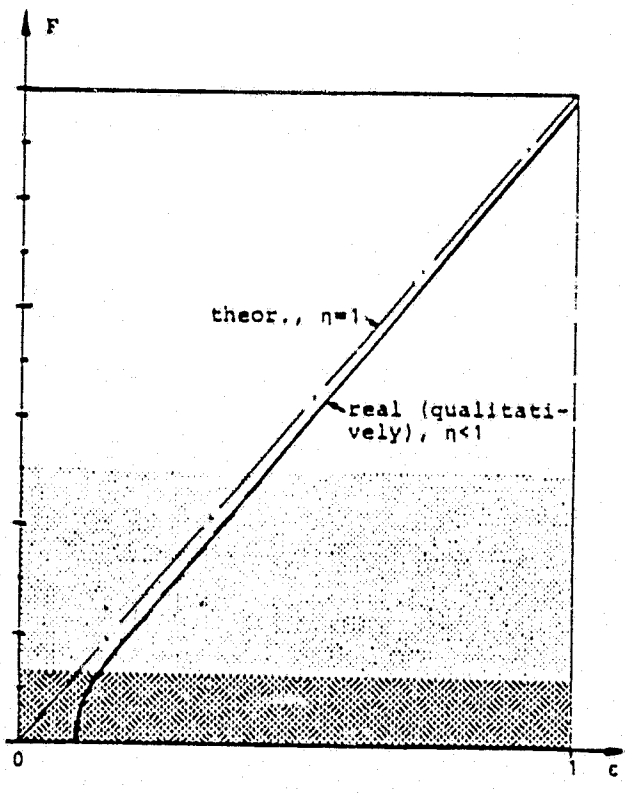

2. Two Motors, Clutched in Parallel to an Ordinary Shaft.

2a Two variable motors

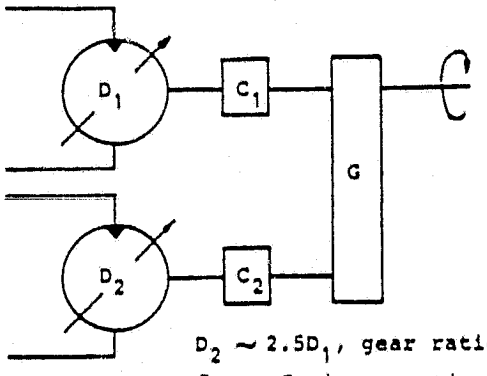

$D_2 \sim 2.5D_1$, gear ratio 1
C_1 or C_2 in operation

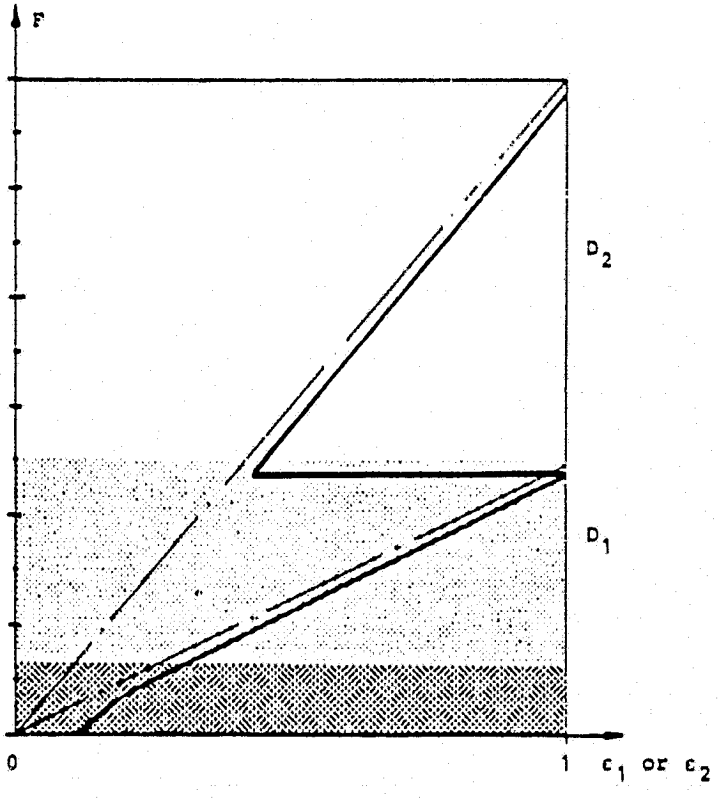

2b Two variable motors as in 2a

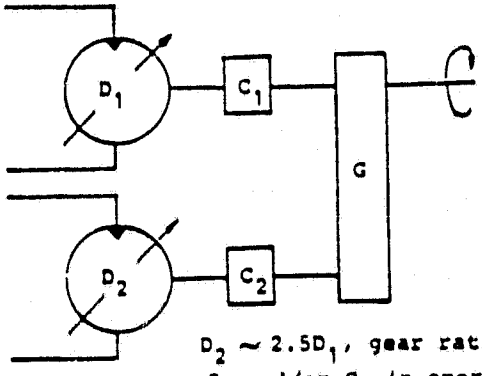

$D_2 \sim 2.5D_1$, gear ratio 1
C_1 and/or C_2 in operation

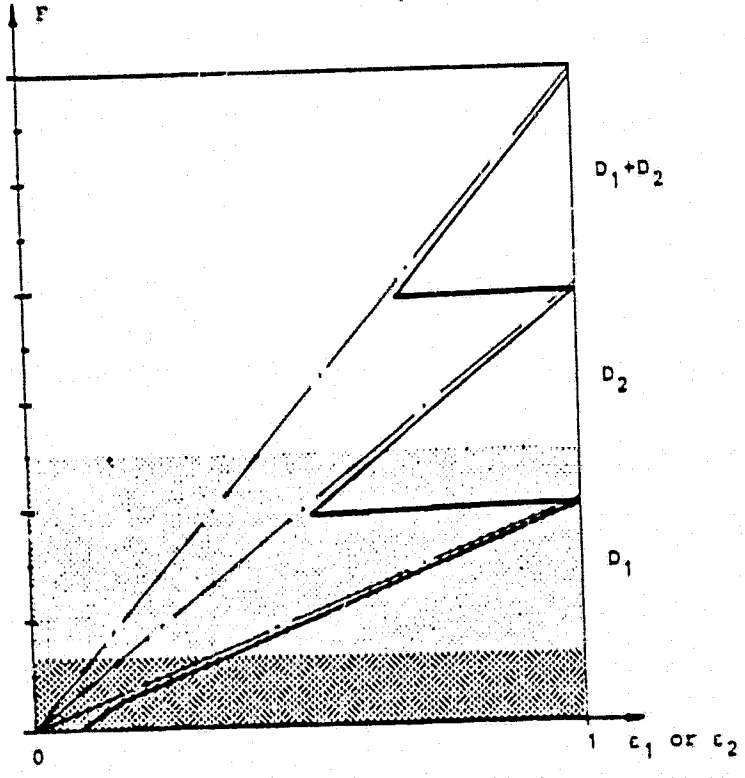

2c One variable and one fixed motor

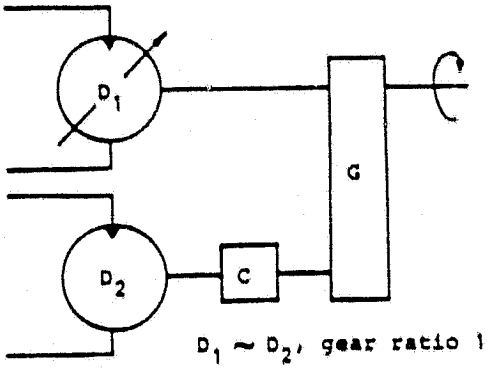

$D_1 \sim D_2$, gear ratio 1

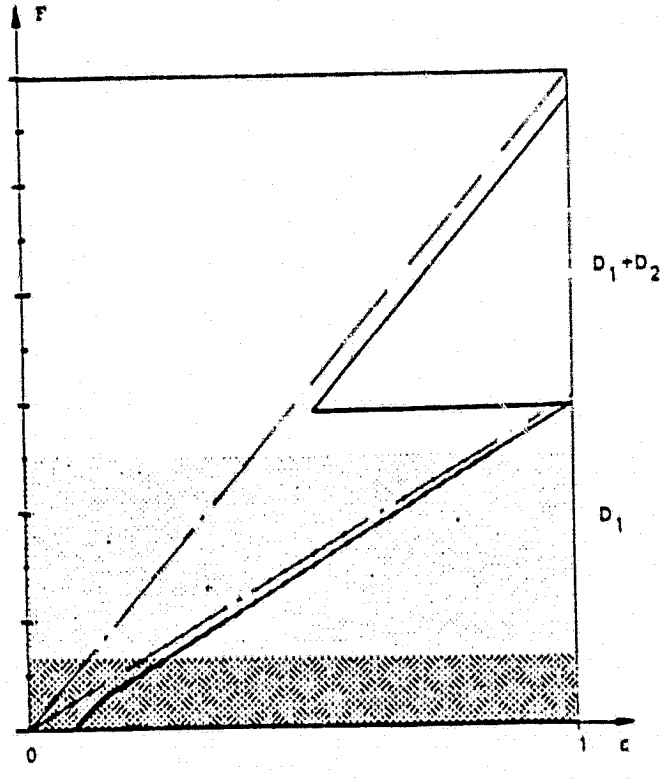

2d One variable and one fixed motor as 2c

In addition to the above configuration we use the "hydraulic polarity shift" for the D_1 unit in the higher force region where it partly operates as pump implying power circulation.

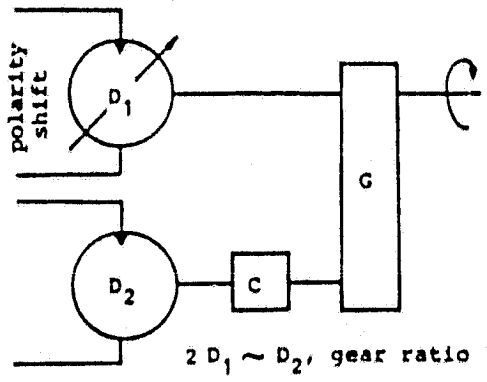

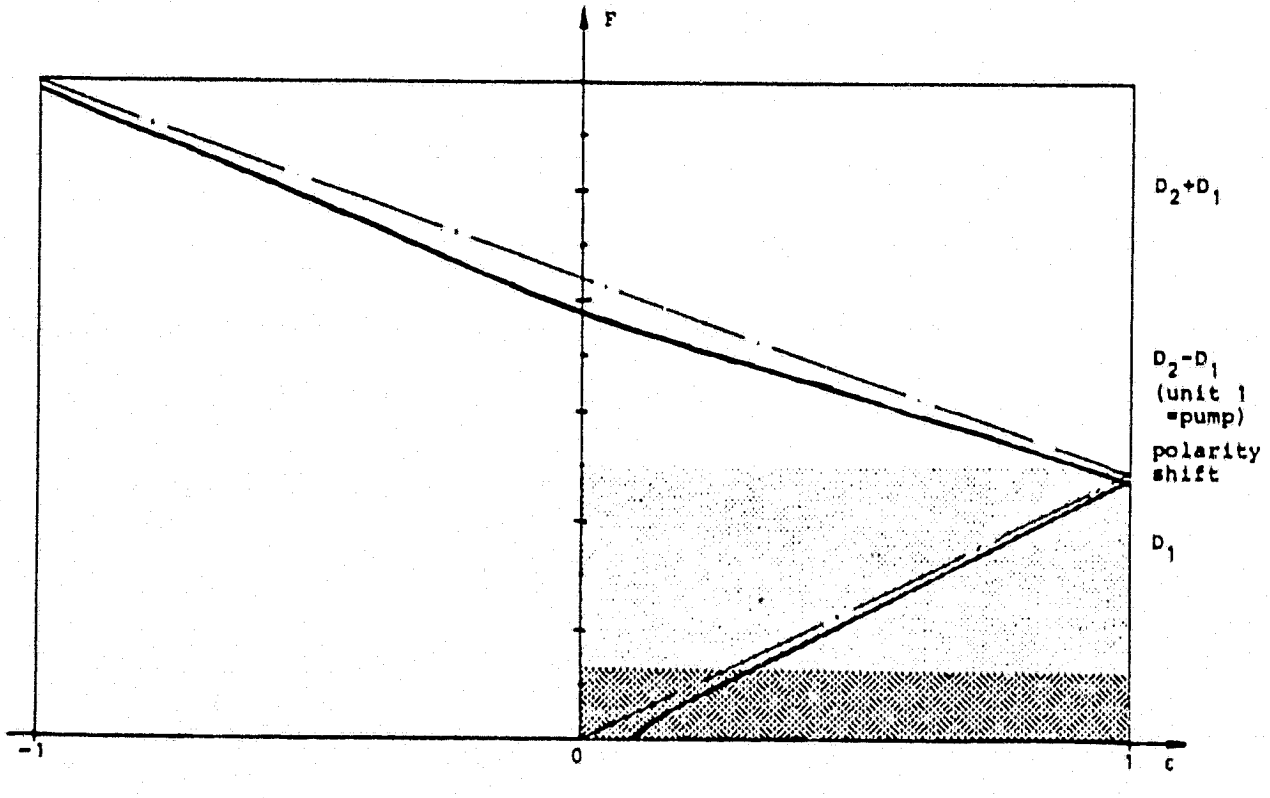

2e One variable and one fixed motor as 2c

Addition of "slow" hydraulic polarity swift for unit D_2.

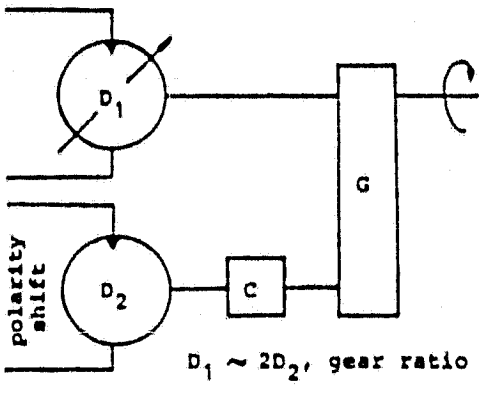

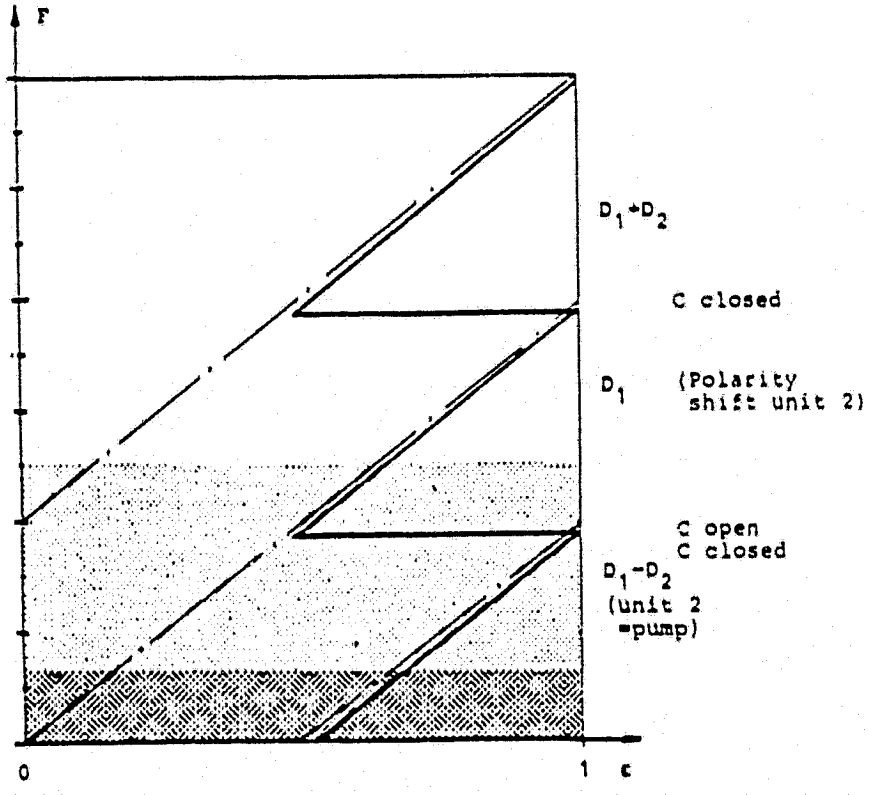

3. One Single Motor With a Two Speed Transmission

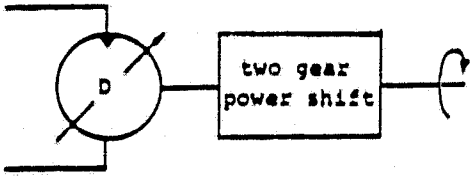

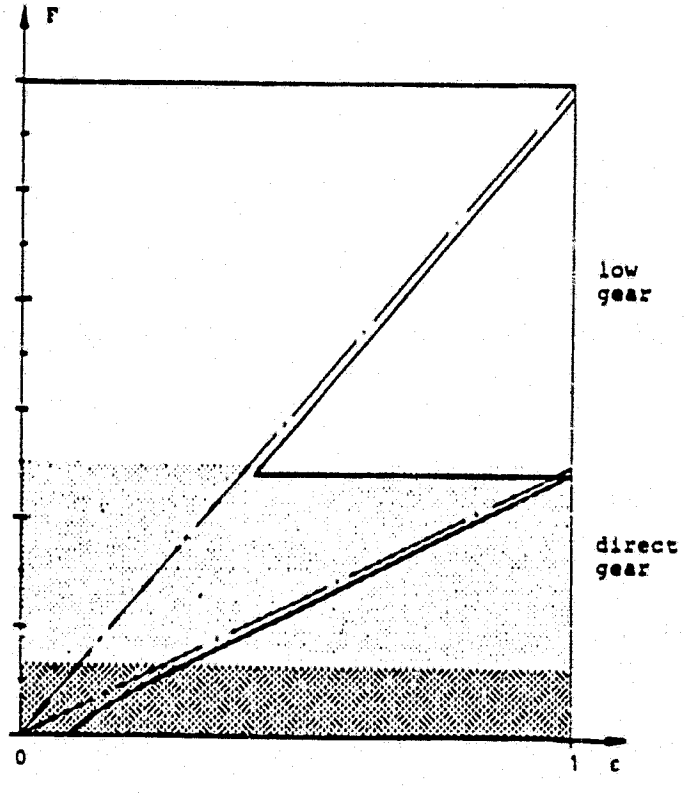

4. Other Systems of Some Merit.

4a One single motor with a three speed transmission

Possible gear ratios low 1:4
medium 1:2

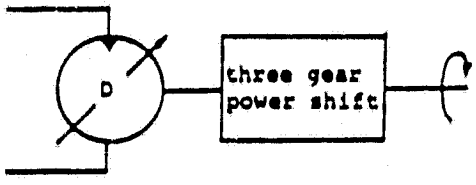

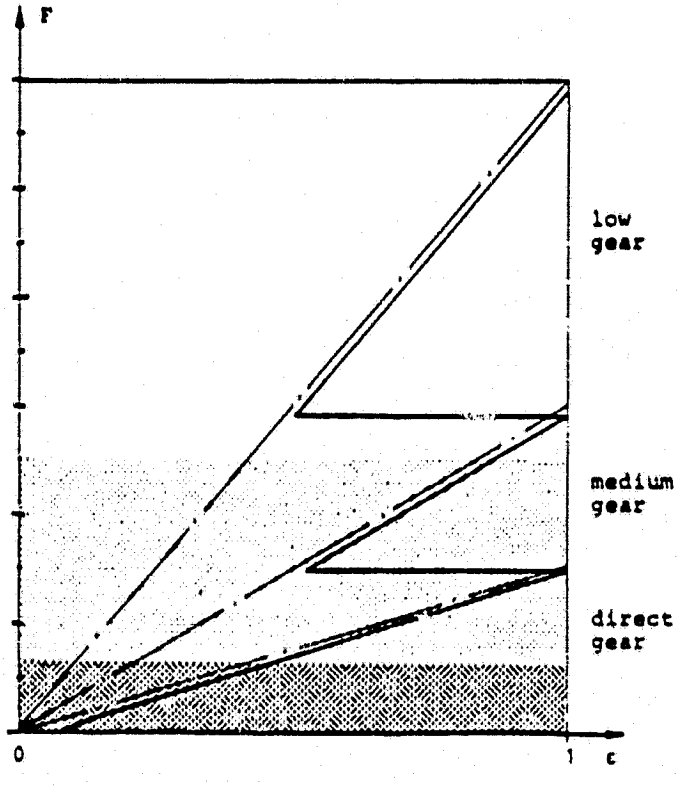

4b Two motors with a two speed transmission

Many choices of gear ratios are possible.

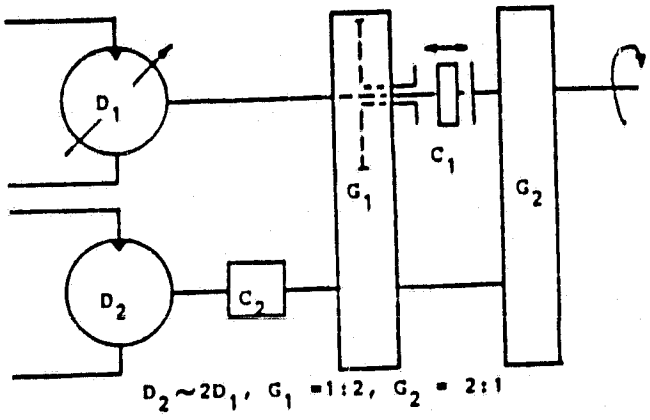

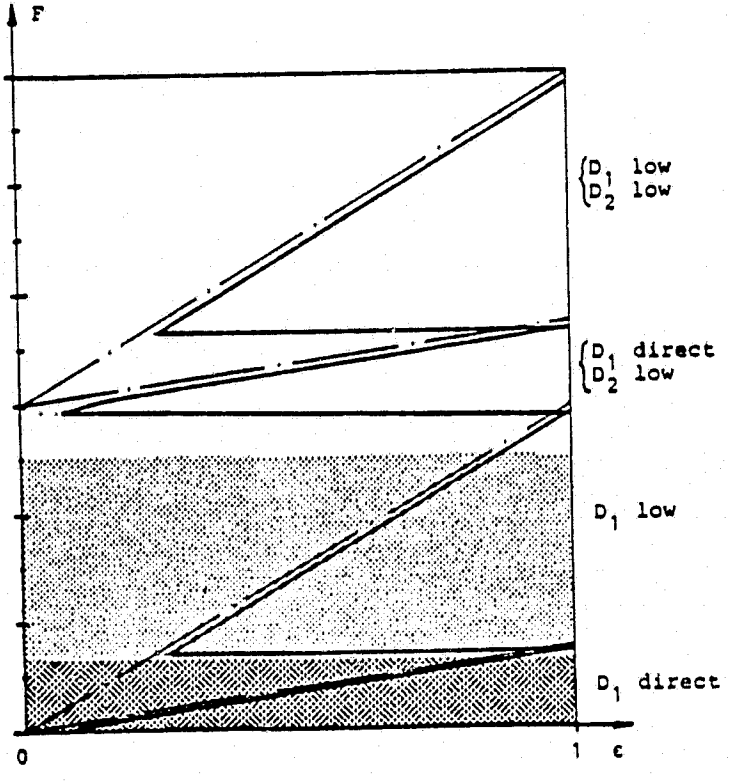

4c Three motors clutched in parallel without power circulation

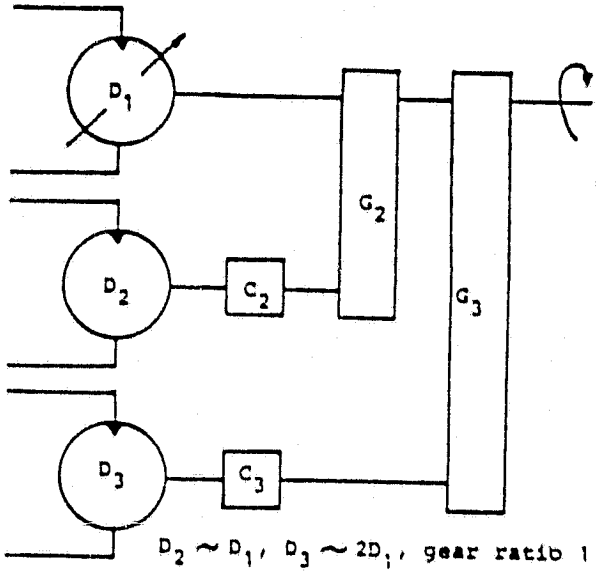

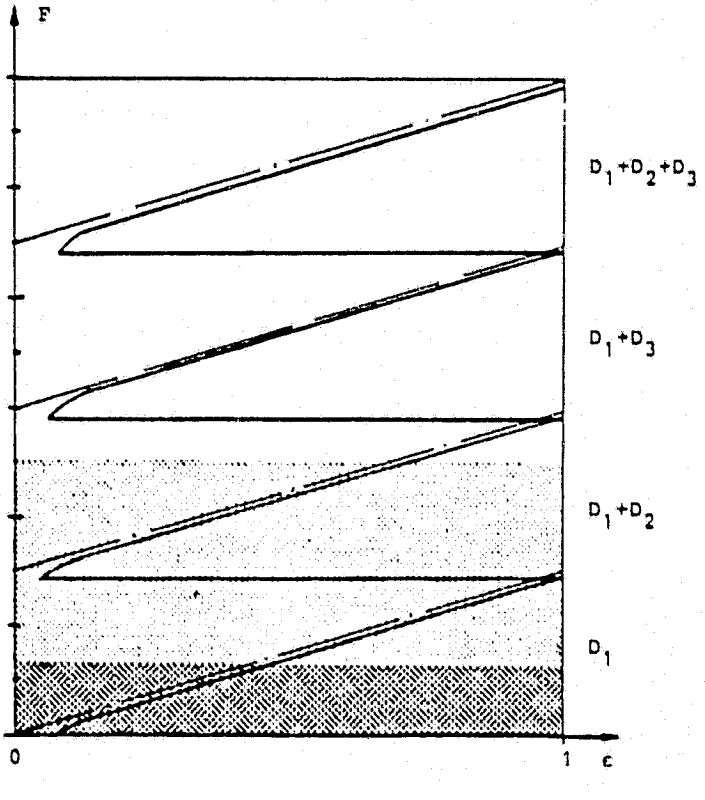

4d Three motors clutched in parallel with power circulation in the variable unit.

Arrangement same as 4c but with addition of possibility to change hydraulic polarity for unit D.

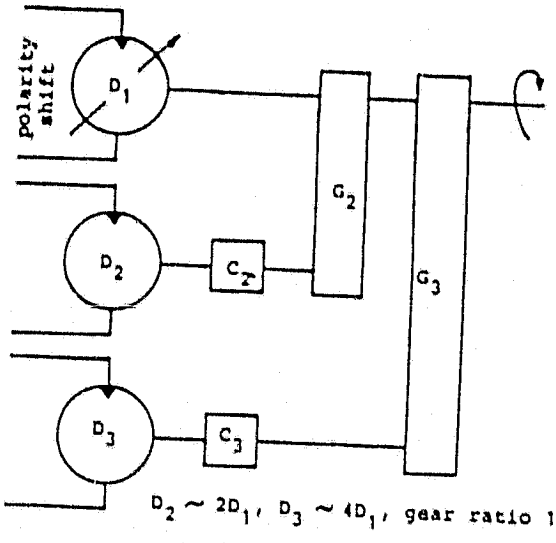

$D_2 \sim 2D_1$, $D_3 \sim 4D_1$, gear ratio 1

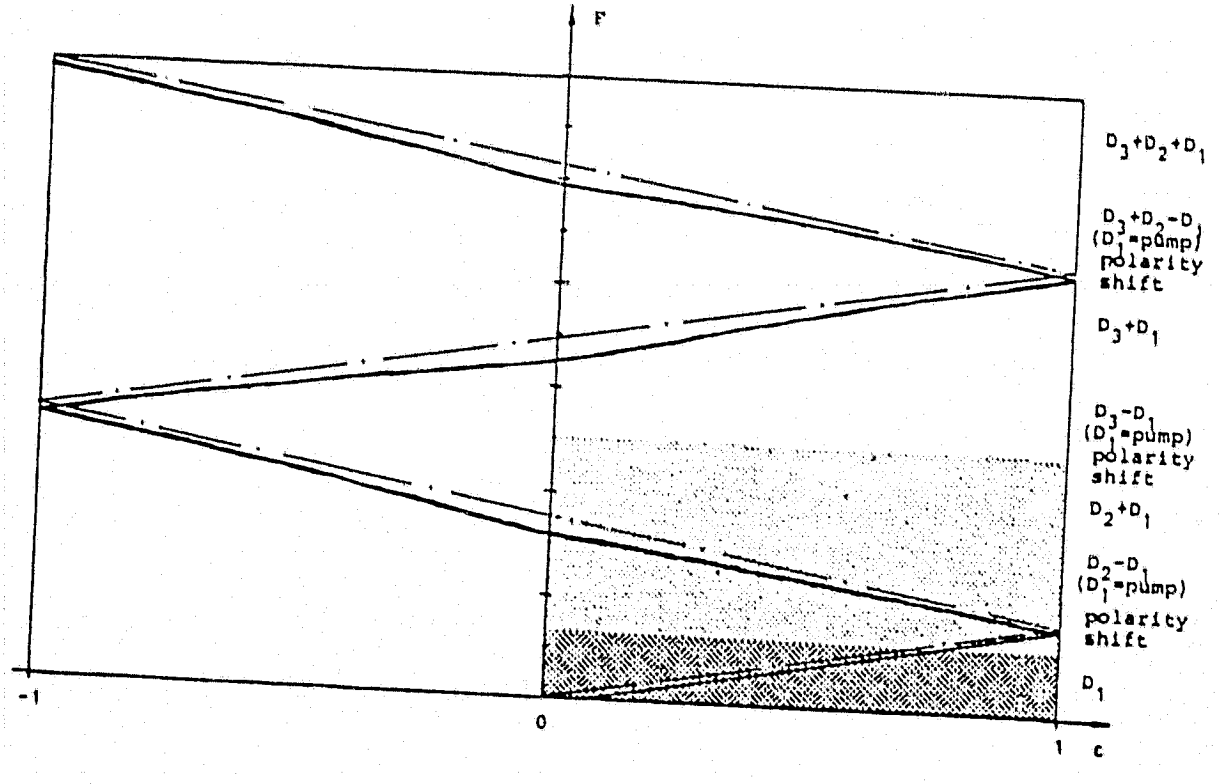

Appendix 2: Test results V20-180 Machine

V20-180 MACHINE

OPERATING AS A PUMP

EFFICIENCY V20A-180
AS PUMP. OIL SHELL TELLUS 46. TEMP 50°C FEED PRESSURE 10 BAR

DIFF. PRESSURE	α = 40° SPEED RPM D= 178,07 cm³/ Rev.				
Δ p bar	500.	1500	2000	2500	3000
Vol. eff.	0,998	0.999			
0 Mech. eff.	0,000	0,000			
Tot. eff.	0,000	0,000			
	0,988	0,995	0,996	0,995	0,995x
50	0,920	0,854	0,824	0,785	0,738
	0,909	0,850	0,821	0,781	0,734
	0,974	0,986	0,988	0,986	0,985x
150	0,969	0,945	0,932	0,919	0,894
	0,944	0,932	0,921	0,906	0,880
	0,956	0,975	0,978	0,977	0,976x
250	0,982	0,968	0,956	0,947	0,936
	0,939	0,944	0,935	0,925	0,914
	0,933	0,961	0,966	0,967	0,971x
350	0,977	0,976	0,972	0,964	0,949
	0,911	0,938	0,940	0,933	0,921
	α = 25°			D = 116,68 cm³/ Rev.	
	0,997	0,993	0,991	0,988	
0	0,000	0,000	0,000	0,000	
	0,000	0,000	0,000	0,000	
	0,981	0,993	0,990	0,982	0,989
50	0,912	0,836	0,807	0,774	0,725
	0,895	0,831	0,800	0,760	0,717
	0,972	0,974	0,974	0,972	0,977
150	0,947	0,935	0,929	0,913	0,893
	0,921	0,910	0,904	0,888	0,872
	0,942	0,962	0,966	0,968	0,964
250	0,960	0,956	0,951	0,942	0,936
	0,904	0,920	0,919	0,911	0,902
	0,902	0,943	0,950	0,953	0,951
350	0,956	0,960	0,959	0,957	0,953
	0,863	0,906	0,911	0,912	0,907

x - Test data fell beyond the calibrated range of the flowmeter. The number shown was calculated using extrapolation.

DIFF. PRESSURE	α = 15° SPEED RPM				D = 71,35 cm³/Rev.
Δ p bar	500	1500	2000	2500	3000
Vol. eff.	0,994	0,999	0,996		
0 Mech.eff.	0,000	0,000	0,000		
Tot.eff.	0,000	0,000	0,000		
	0.969	0,987	0,984	0,985	0,983
50	0,848	0,778	0,757	0,738	0,693
	0,822	0,768	0,746	0,726	0,681
	0,938	0,966	0,968	0,968	0,965
150	0,931	0,902	0,897	0,878	0,869
	0,873	0,871	0,868	0,851	0,639
	0,898	0,942	0,946	0,948	0,946
250	0,947	0,937	0,928	0,925	0,922
	0,850	0,883	0,878	0,877	0,873
		0,914	0,920	0,924	0,924
350		0,946	0,942	0,938	0,943
		0,865	0,867	0,866	0,872

	α = 10°				D = 48,43 cm³/Rev.
	0,992	0,999	0,998	0,997	0,994
0	0,000	0,000	0,000	0,000	0,000
	0,000	0,000	0,000	0,000	0,000
	0,954	0,983	0,984	0,983	0,981
50	0,803	0,727	0,701	0,665	0,643
	0,766	0,715	0,689	0,653	0,630
	0,910	0,956	0,958	0,959	0,956
150	0,904	0,870	0,857	0,838	0,850
	0,822	0,832	0,821	0,804	0,813
	0,869	0,921	0,925	0,929	0,930
250	0,922	0,909	0,905	0,897	0,888
	0,801	0,837	0,837	0,833	0,826
		0,877	0,886	0,893	0,893
350		0,924	0,924	0,921	0,918
		0,810	0,819	0,823	0,820

DIFF.PRESSURE	α = 6° SPEED RPM				D = 29,40 cm³/Rev.
Δ p bar	500	1500	2000	2500	3000
Vol. eff.	0,993	0,999	0,999	0,999	0,999
0 Mech. eff.	0,000	0,000	0,000	0,000	0,000
Tot. eff.	0,000	0,000	0,000	0,000	0,000
	0,931	0,972	0,975	0,978	0,977
50	0,709	0,632	0,585	0,557	0,532
	0,660	0,614	0,570	0,545	0,519
	0,864	0,928	0,931	0,937	0,939
150	0,856	0,816	0,789	0,771	0,755
	0,739	0,757	0,734	0,732	0,709
		0,872	0,881	0,891	0,895
250		0,873	0,854	0,848	0,842
		0,761	0,752	0,755	0,753
		0,811	0,828	0,840	0,847
350		0,895	0,886	0,879	0,869
		0,726	0,734	0,738	0,736
	α = 3°				D = 14,55 cm³/ Rev.
		0,999	0,999	0,999	0,999
0		0,000	0,000	0,000	0,000
		0,000	0,000	0,000	0,000
		0,943	0,954	0,957	0,956
50		0,464	0,430	0,400	0,374
		0,437	0,410	0,383	0,358
		0,854	0,867	0,878	0,883
150		0,696	0,669	0,633	0,621
		0,594	0,580	0,556	0,549
		0,749	0,767	0,796	0,800
250		0,784	0,763	0,744	0,725
		0,587	0,585	0,592	0,580
		0,621	0,658	0,679	0,697
350		0,823	0,806	0,796	0,787
		0,511	0,530	0,540	0,549

V20-180 MACHINE

OPERATING AS A MOTOR

EFFICIENCY V20A-180
AS MOTOR. OIL SHELL TELLUS 46. TEMP 50°C BACK PRESSURE 10 BAR

DIFF. PRESSURE	α = 40°	SPEED RPM			D = 177,46 cm³/ Rev.		
Δp bar	500	1500	2000	2500	3000	100	200
Vol. eff.	0,999	0,999	0,998	0,998	0,999x	0,995	0,996
0 Mech. eff.	0,000	0,000	0,000	0,000	0,000	0,000	0,000
Tot. eff.	0,000	0,000	0,000	0,000	0,000	0,000	0,000
	0,992	0,995	0,995	0,996	0,996x	0,952	0,976
50	0,934	0,849	0,793	0,729	0,651	0,948	0,970
	0,926	0,845	0,789	0,726	0,649	0,903	0,946
	0,981	0,990	0,990	0,991	0,992x		0,955
150	0,977	0,953	0,925	0,906	0,882		0,984
	0,958	0,943	0,916	0,898	0,875		0,939
	0,967	0,982	0,984	0,985	0,986x		
250	0,981	0,964	0,950	0,936	0,923		
	0,948	0,947	0,935	0,922	0,910		
	0,947	0,974	0,978	0,980	0,982x		
350	0,982	0,974	0,962	0,949	0,938		
	0,930	0,949	0,940	0,929	0,921		
	α = 25°				D = 114,48 cm³/ Rev.		
	0,994	0,999	0,993	0,991	0,996	0,999	0,987
0	0,000	0,000	0,000	0,000	0,000	0,000	0,000
	0,000	0,000	0,000	0,000	0,000	0,000	0,000
	0,982	0,996	0,988	0,987	0,993	0,940	0,956
50	0,944	0,845	0,801	0,735	0,659	0,911	0,944
	0,927	0,841	0,792	0,726	0,654	0,856	0,902
	0,968	0,986	0,981	0,980	0,986		0,924
150	0,970	0,940	0,933	0,911	0,882		0,970
	0,939	0,928	0,915	0,893	0,870		0,896
	0,952	0,972	0,970	0,971	0,978		
250	0,968	0,959	0,953	0,942	0,922		
	0,922	0,932	0,925	0,914	0,901		
	0,928	0,956	0,959	0,960	0,963		
350	0,967	0,970	0,963	0,956	0,945		
	0,898	0,927	0,923	0,918	0,910		

x - Test data fell beyond the calibrated range of the flowmeter. The number shown was calculated using extrapolation.

DIFF. PRESSURE	α = 15° SPEED RPM D = 70,54 cm³/ Rev.						
Δ p bar	500	1500	2000	2500	3000	100	200
Vol.eff.	0,991	0,999	0,995	0,991	0,987	0,999[x]	0,982
0 Mech. eff.	0,000	0,000	0,000	0,000	0,000	0,000	0,000
Tot. eff.	0,000	0,000	0,000	0,000	0,000	0,000	0,000
	0,969	0,991	0,988	0,984	0,980	0,897[x]	0,930
50	0,890	0,784	0,730	0,677	0,623	0,855	0,908
	0,863	0,771	0,721	0,666	0,611	0,767	0,845
	0,943	0,976	0,974	0,971	0,968		0,883
150	0,950,	0,920	0,902	0,890	0,873		0,950
	0,895	0,898	0,879	0,865	0,845		0,839
	0,916	0,955	0,957	0,956	0,954		
250	0,955	0,937	0,933	0,926	0,915		
	0,875	0,895	0,893	0,885	0,873		
	0,875	0,928	0,935	0,938	0,936		
350	0,954	0,954	0,948	0,945	0,936		
	0,838	0,885	0,886	0,886	0,877		

	α = 10° D = 47,13 cm³/ Rev.						
	0,991	0,999	0,989	0,990	0,989	0,999[x]	0,999[x]
0	0,000	0,000	0,000	0,000	0,000	0,000	0,000
	0,000	0,000	0,000	0,000	0,000	0,000	0,000
	0,956	0,984	0,976	0,977	0,977	0,817[x]	0,918[x]
50	0,853	0,693	0,640	0,560	0,507	0,827	0,880
	0,816	0,682	0,625	0,547	0,495	0,675	0,807
	0,917	0,961	0,955	0,958	0,957		0,843[x]
150	0,942	0,889	0,871	0,853	0,827		0,942
	0,864	0,854	0,832	0,817	0,791		0,794
	0,871	0,933	0,931	0,935	0,935		
250	0,949	0,912	0,907	0,901	0,891		
	0,827	0,851	0,844	0,843	0,833		
	0,800	0,895	0,904	0,909	0,910		
350	0,944	0,939	0,932	0,926	0,915		
	0,755	0,841	0,842	0,842	0,833		

x - Test data fell beyond the calibrated range of the flowmeter. The number shown was calculated using extrapolation.

DIFF. PRESSURE	$\alpha = 6^\circ$ SPEED RPM				D = 28,97 cm^3/ Rev.	
Δp bar	500	1500	2000	2500	3000	200
Vol. eff.	0,988	0,999	0,996	0,990	0,985	0,999[x]
0 Mech. eff.	0,000	0,000	0,000	0,000	0,000	0,000
Tot. eff.	0,000	0,000	0,000	0,000	0,000	0,000
	0,932	0,976	0,974	0,971	0,968	0,859[x]
50	0,738	0,521	0,434	0,347	0,260	0,781
	0,688	0,508	0,423	0,337	0,252	0,671
	0,862	0,938	0,939	0,937	0,936	0,754[x]
150	0,897	0,810	0,795	0,752	0,738	0,897
	0,773	0,759	0,747	0,705	0,690	0,676
	0,706	0,894	0,900	0,902	0,898	
250	0,920	0,868	0,859	0,850	0,842	
	0,649	0,776	0,773	0,767	0,756	
		0,843	0,851	0,859	0,858	
350		0,907	0,901	0,892	0,890	
		0,765	0,767	0,767	0,763	
	$\alpha = 4^\circ$				D = 19,73 cm^3/ Rev.	
	0,989[x]	0,997	0,998	0,999	0,998	0,999[x]
0	0,000	0,000	0,000	0,000	0,000	0,000
	0,000	0,000	0,000	0,000	0,000	0,000
	0,902[x]	0,958	0,965	0,973	0,967	0,694[x]
50	0,637	0,318	0,191	0,064	0,000	0,764
	0,575	0,305	0,184	0,062	0,000	0,531
	0,707[x]	0,903	0,914	0,924	0,919	0,534[x]
150	0,849	0,743	0,701	0,658	0,616	0,870
	0,601	0,671	0,640	0,608	0,566	0,465
		0,844	0,860	0,871	0,866	
250		0,828	0,803	0,777	0,752	
		0,699	0,690	0,677	0,651	
		0,779	0,803	0,813	0,805	
350		0,864	0,846	0,828	0,832	
		0,673	0,680	0,673	0,670	

x - Test data fell beyond the calibrated range of the flowmeter. The number shown was calculated using extrapolation.

DIFF. PRESSURE	$\alpha = 3^\circ$ SPEED RPM D = 14,74 cm^3/ Rev.				
Δ p bar	500	1500	2000	2500	3000
Vol. eff.	0,999	0,998	0,999	0,999	0,999
0 Mech. eff.	0.000	0,000	0,000	0,000	0,000
Tot. eff.	0,000	0,000	0,000	0,000	0,000
	0.879	0,947	0,958	0,961	0,956
50	0,511	0,085	0,000	0,000	0,000
	0,449	0,081	0,000	0,000	0,000
		0,879	0,890	0,900	0,894
150		0,652	0,596	0,539	0,462
		0,574	0,530	0,485	0,431
		0,810	0,821	0,835	0,833
250		0,766	0,732	0,715	0,664
		0,620	0,601	0,597	0,553
		0,733	0,748	0,768	0,770
350		0,827	0,802	0,778	0,754
		0,606	0,600	0,597	0,580

EFFECT OF ELEVATED TEMPERATURE ON V20-180 MACHINE OPERATING AS A MOTOR

MOTOR
TEMP. 70°C VISCOSITY 16 cSt BACK PRESSURE 10 BAR

DIFF. PRESSURE		α = 25°		= 10°	
Δ p bar		500	2500	500	2500
	Vol. eff.	0,985	0,994	0,979	0,989
50	Mech. eff.	0,933	0,744	0,868	0,605
	Tot. eff.	0,919	0,740	0,850	0,599
		0,963	0,985	0,925	0,965
150		0,959	0,907	0,939	0,860
		0,924	0,894	0,868	0,829
		0,935	0,973	0,836	0,934
250		0,962	0,938	0,937	0,900
		0,900	0,913	0,784	0,841
		0,902	0,960		0,902
350		0,958	0,951		0,921
		0,864	0,913		0,831

EFFECT OF HIGH BACK PRESSURE ON V20-180 MACHINE OPERATING AS A MOTOR

MOTOR
TEMP 50°C VISCOSITY 30 cSt BACK PRESSURE 100 BAR

DIFF. PRESSURE	α = 25°		= 10°	
Δ p bar	500	2500	500	2500
	Vol. eff.	0,973	0,993	0,949	0,987
50	Mech. eff	0,901	0,717	0,763	0,500
	Tot. eff.	0,877	0,712	0,724	0,493
		0,954	0,985	0,898	0,964
150		0,934	0,887	0,877	0,798
		0,891	0,873	0,787	0,770
		0,935	0,974	0,853	0,941
250		0,940	0,893	0,895	0,868
		0,879	0,869	0,764	0,818

Appendix 3: PERFORMANCE MAPS OF OPTIMIZED SYSTEMS

SYSTEMS A AND B
Pressures 34.47, 27.58, 20.68, 13.79 and 6.895 MPa
(5000, 4000, 3000, 2000 and 1000 psi)

SYSTEM A
Differential pressure 20.68 MPa (3000 psi)
Backpressures 3.447, 6.895, 13.79 MPa
(500, 1000, 2000 psi)

VARIABLES
Total efficiency
Volymetric efficiency
Displacement fraction
Power loss
Total flow

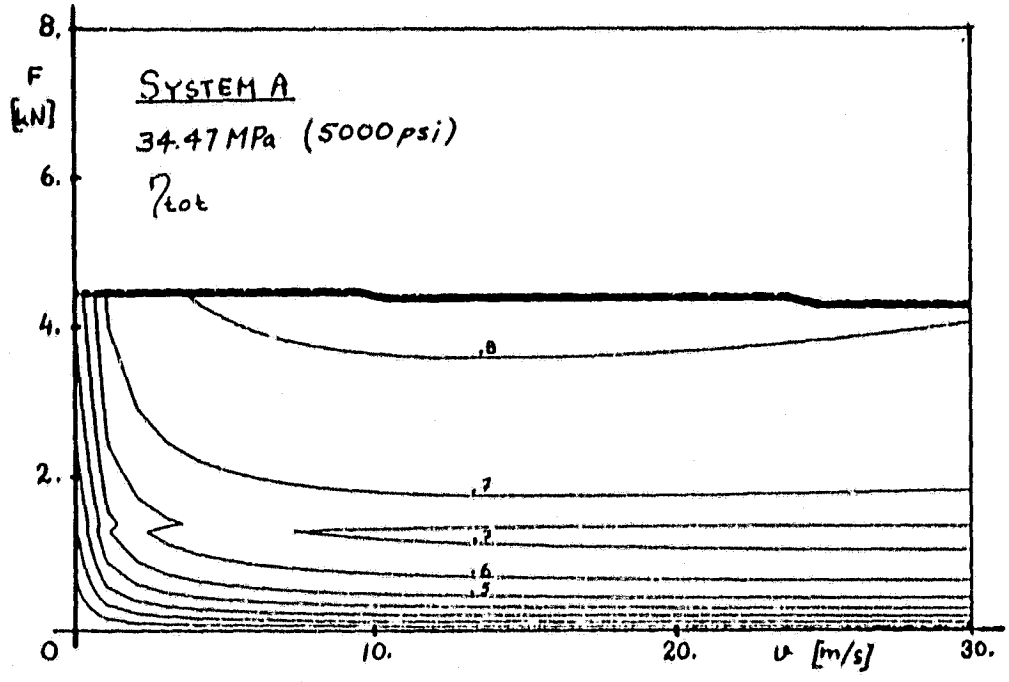
8.
F
[kN]
6.
4.
2.
0
SYSTEM A
34.47 MPa (5000 psi)
η_{tot}
.8
.7
.2
.6
.5
10.
20.
v [m/s]
30.

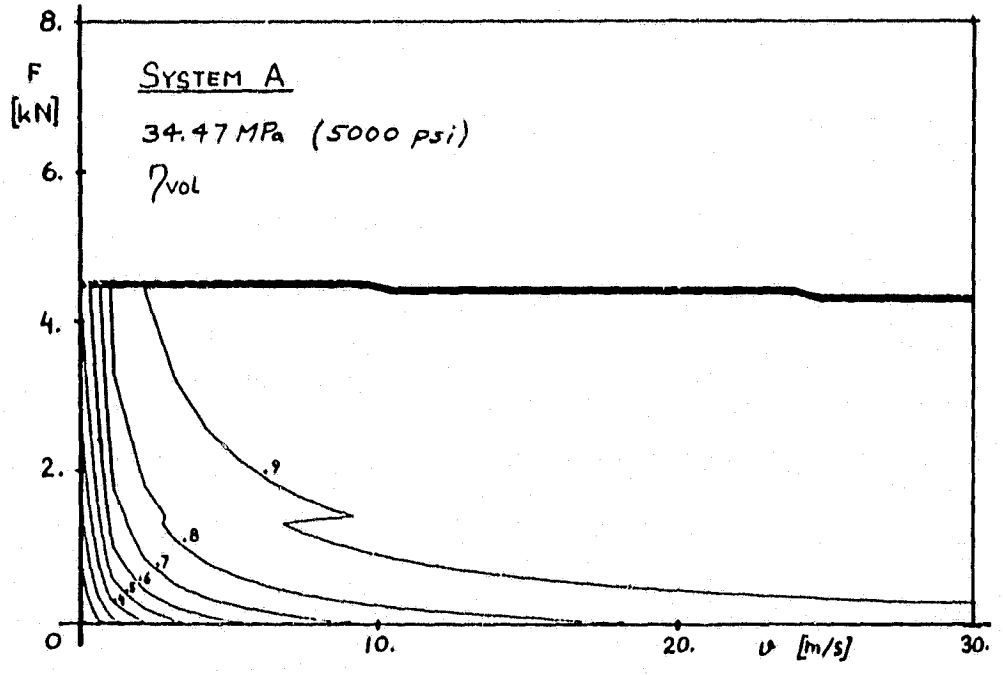
8.
F
[kN]
6.
4.
2.
0
SYSTEM A
34.47 MPa (5000 psi)
η_{vol}
.9
.8
.7
.6
.5
10.
20.
v [m/s]
30.

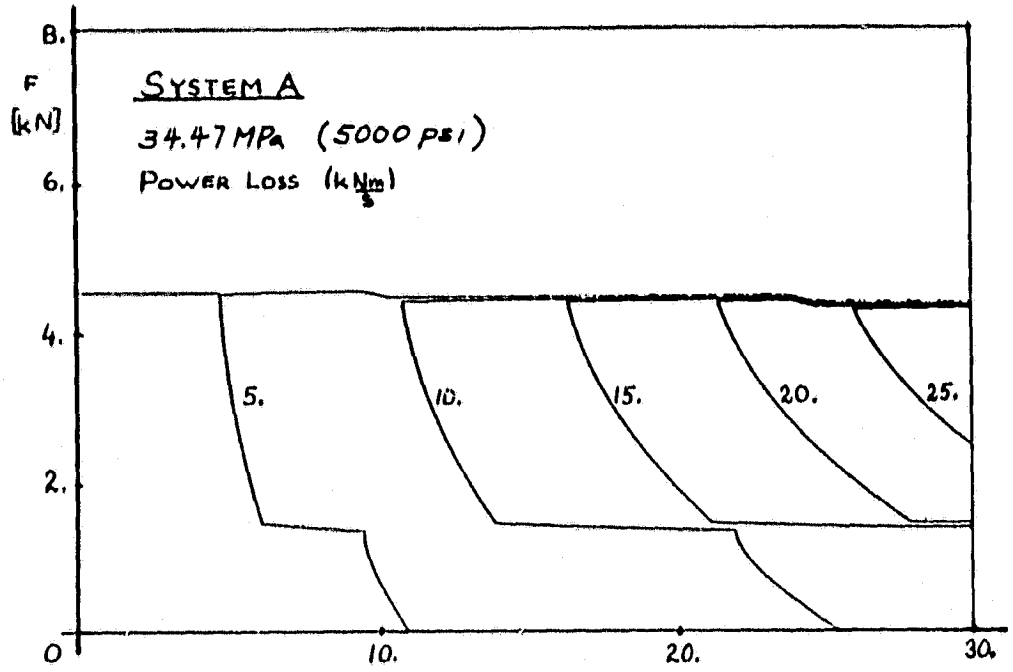
8.
F
[kN]
6.
4.
2.
0
SYSTEM A
34.47 MPa (5000 psi)
POWER LOSS (kNm/s)
5.
10.
15.
20.
25.
10.
20.
30.

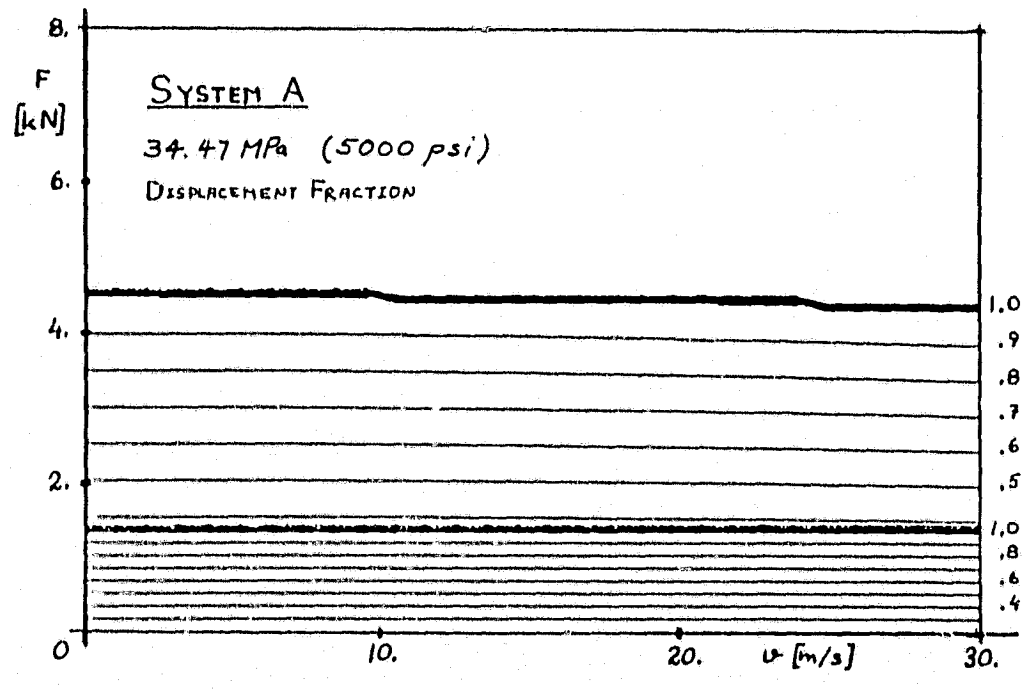
8.
F
[kN]
6.
4.
2.
0
SYSTEM A
34.47 MPa (5000 psi)
DISPLACEMENT FRACTION
1.0
.9
.8
.7
.6
.5
1.0
.8
.6
.4
10.
20.
v [m/s]
30.

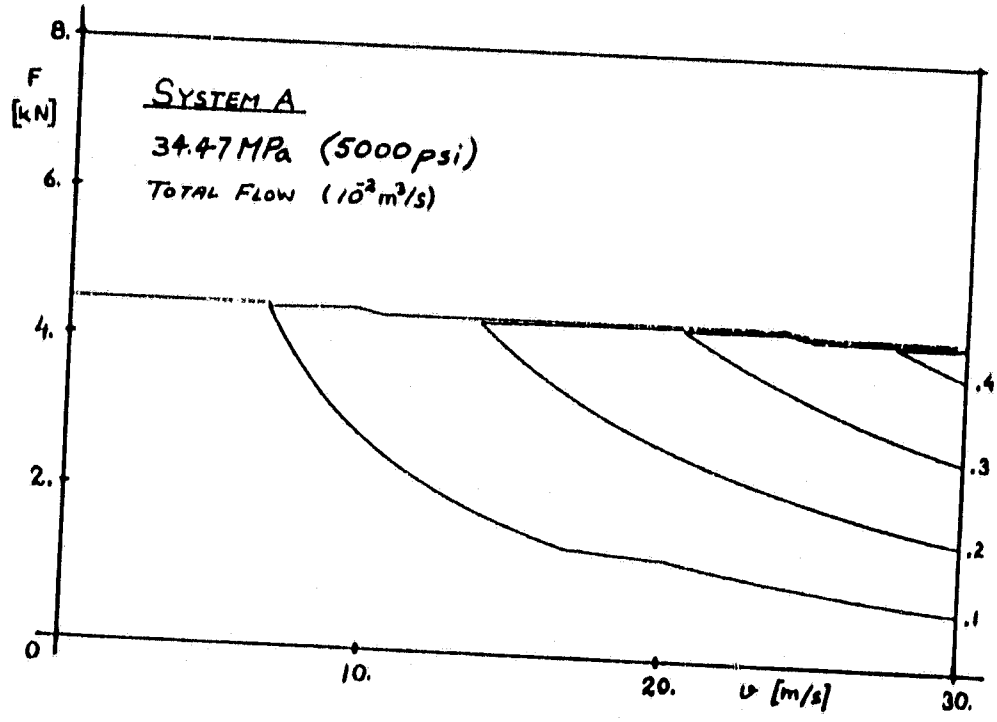
8.
F
[kN]
6.
4.
2.
0
SYSTEM A
34.47 MPa (5000 psi)
TOTAL FLOW (10^{-2} m³/s)
.4
.3
.2
.1
10.
20.
v [m/s]
30.

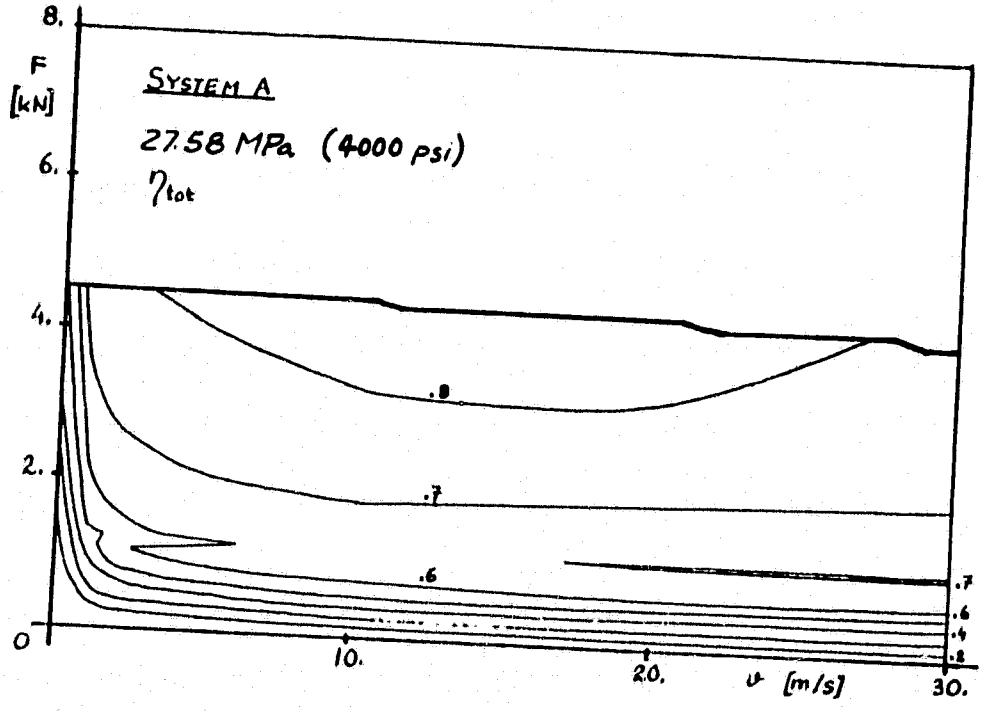
8.
F
[kN]
6.
4.
2.
0
SYSTEM A
27.58 MPa (4000 psi)
η_{tot}
.8
.7
.6
.7
.6
.4
.2
10.
20.
v [m/s]
30.

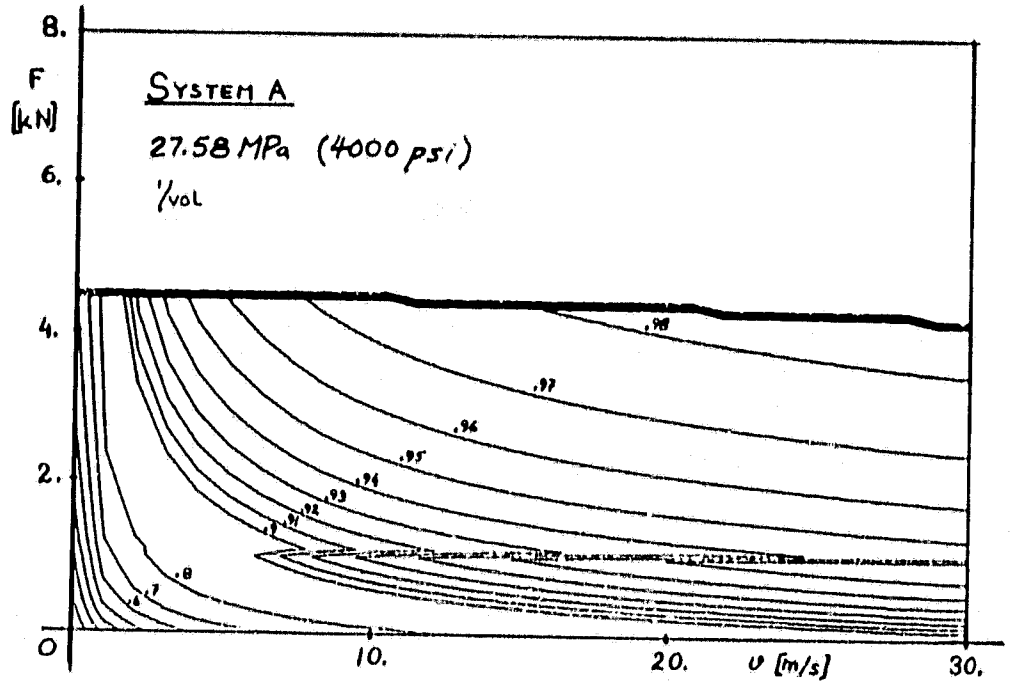
8.
F
[kN]
6.
4.
2.
0
SYSTEM A
27.58 MPa (4000 psi)
1/vol
.98
.97
.96
.95
.94
.93
.92
.91
.9
.8
.7
.6
10.
20.
v [m/s]
30.

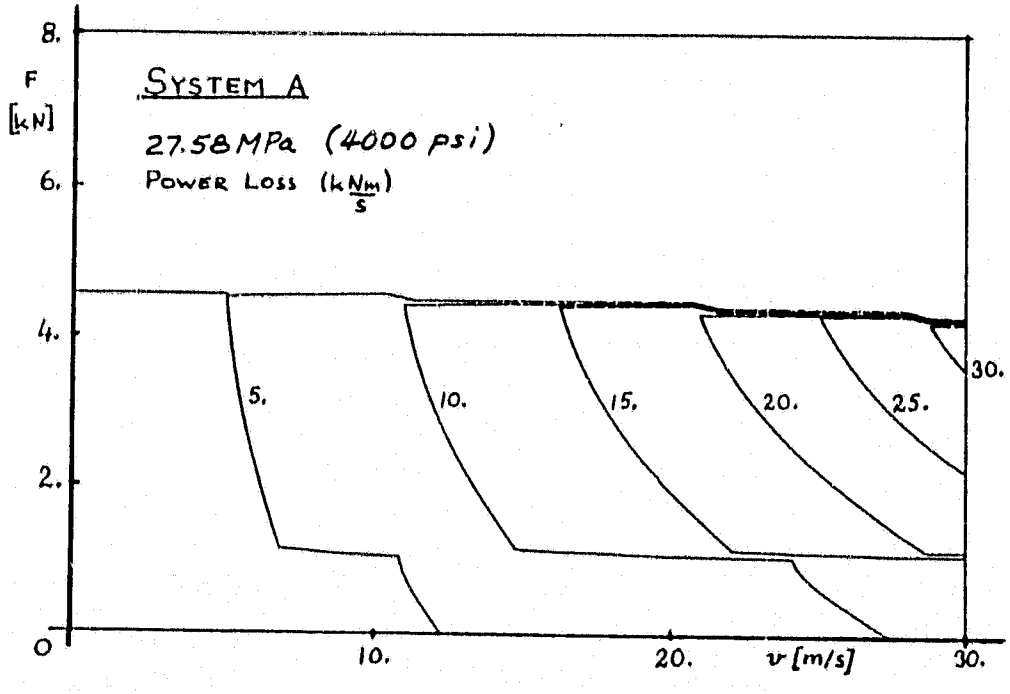
8.
F
[kN]
6.
4.
2.
0
SYSTEM A
27.58 MPa (4000 psi)
POWER LOSS (kNm/s)
5.
10.
15.
20.
25.
30.
10.
20.
v [m/s]
30.

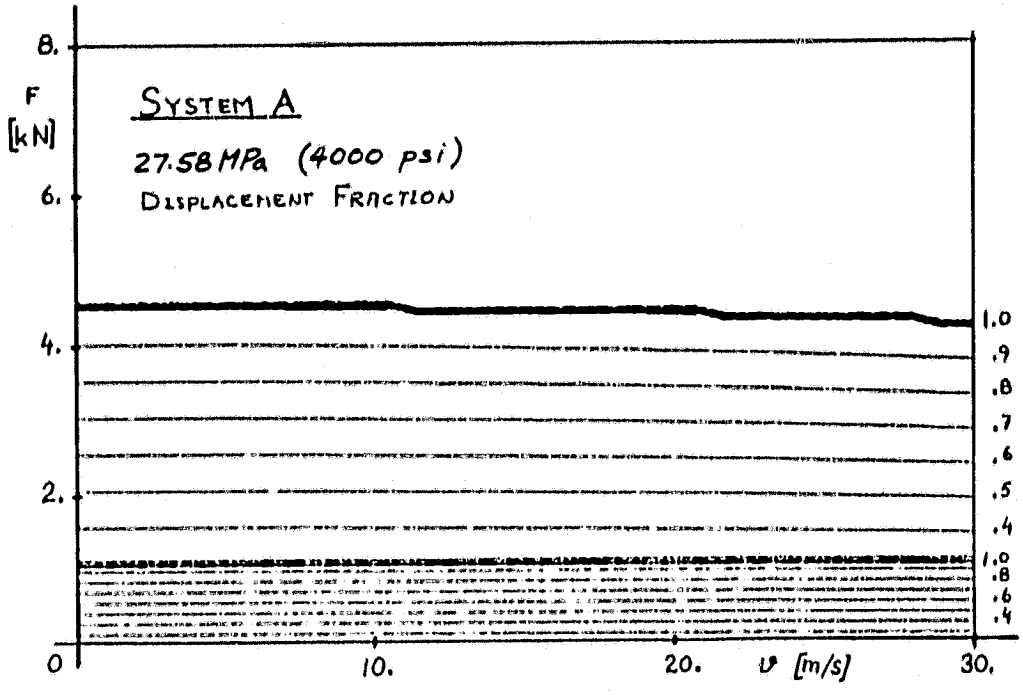
8.
F
[kN]
6.
4.
2.
0
SYSTEM A
27.58 MPa (4000 psi)
DISPLACEMENT FRACTION
1.0
.9
.8
.7
.6
.5
.4
1.0
.8
.6
.4
10.
20.
v [m/s]
30.

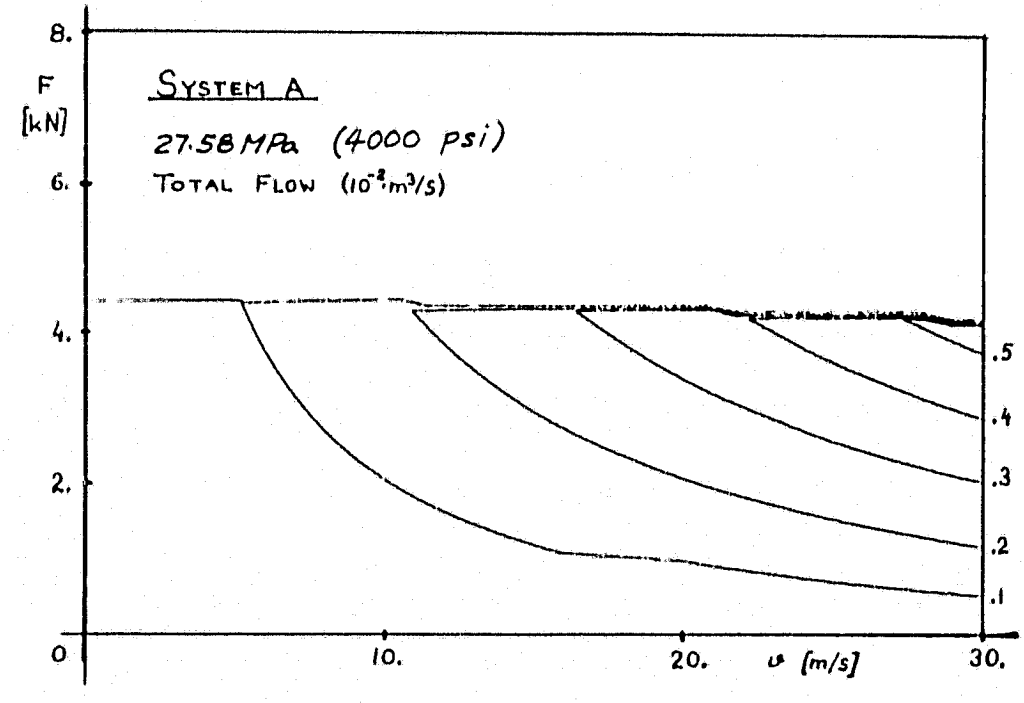
8.
F
[kN]
6.
4.
2.
0
SYSTEM A
27.58 MPa (4000 psi)
TOTAL FLOW (10^{-2} m³/s)
.5
.4
.3
.2
.1
10.
20.
v [m/s]
30.

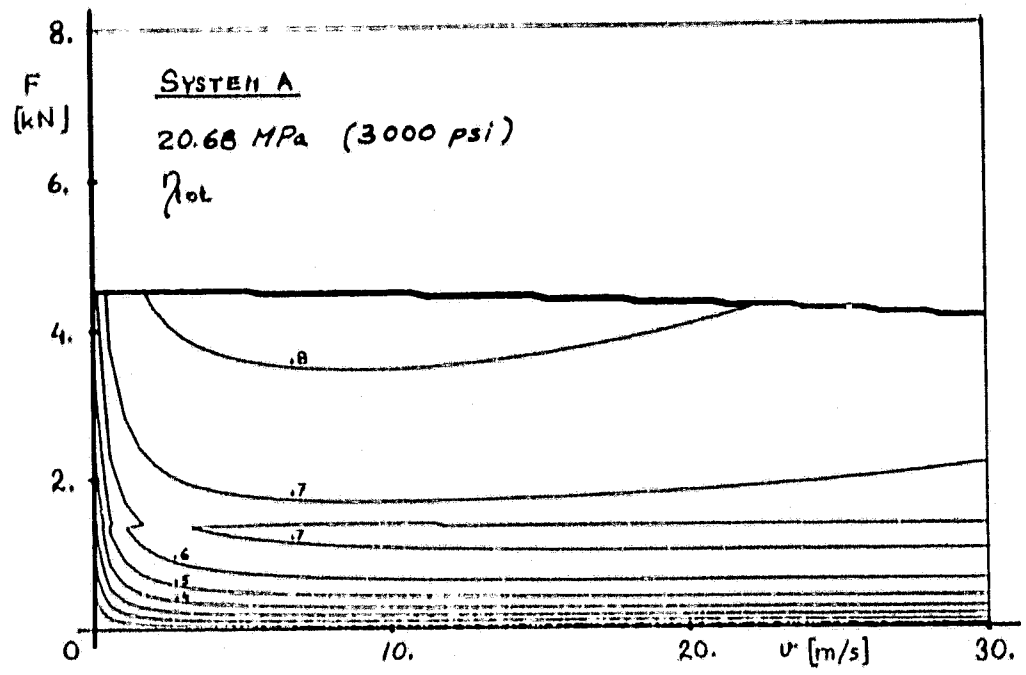
8.
F
[kN]
6.
4.
2.
0
SYSTEM A
20.68 MPa (3000 psi)
η_{vol}
.8
.7
.7
.6
.5
.4
10.
20.
v [m/s]
30.

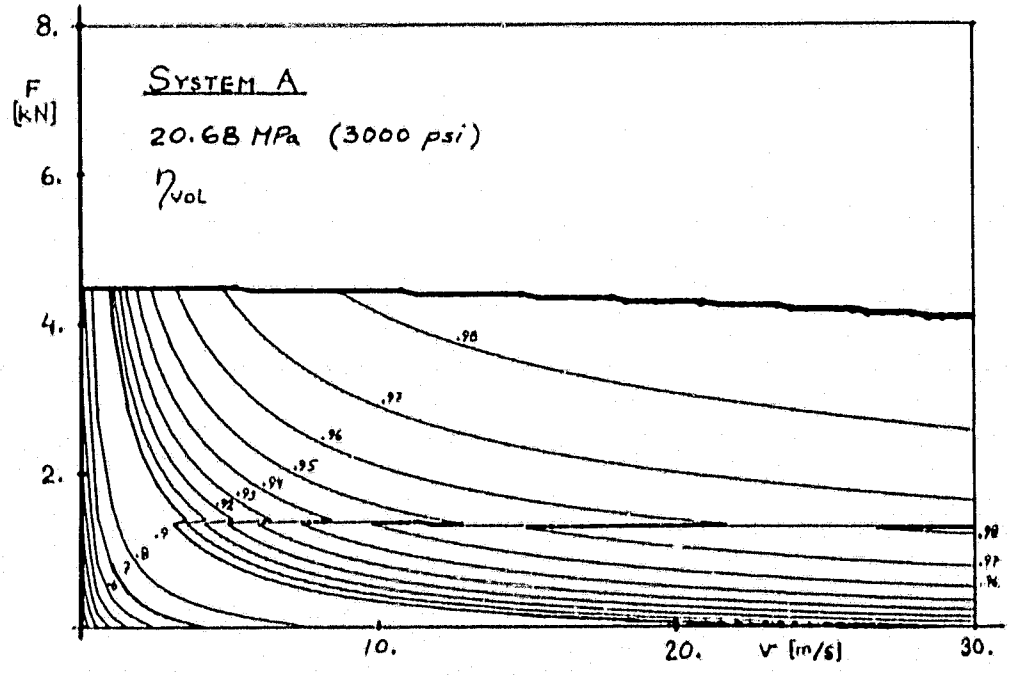
8.
F
[kN]
6.
4.
2.
SYSTEM A
20.68 MPa (3000 psi)
η_{vol}
.98
.97
.96
.95
.94
.93
.92
.9
.8
.7
.98
.97
.96
10.
20.
v [m/s]
30.

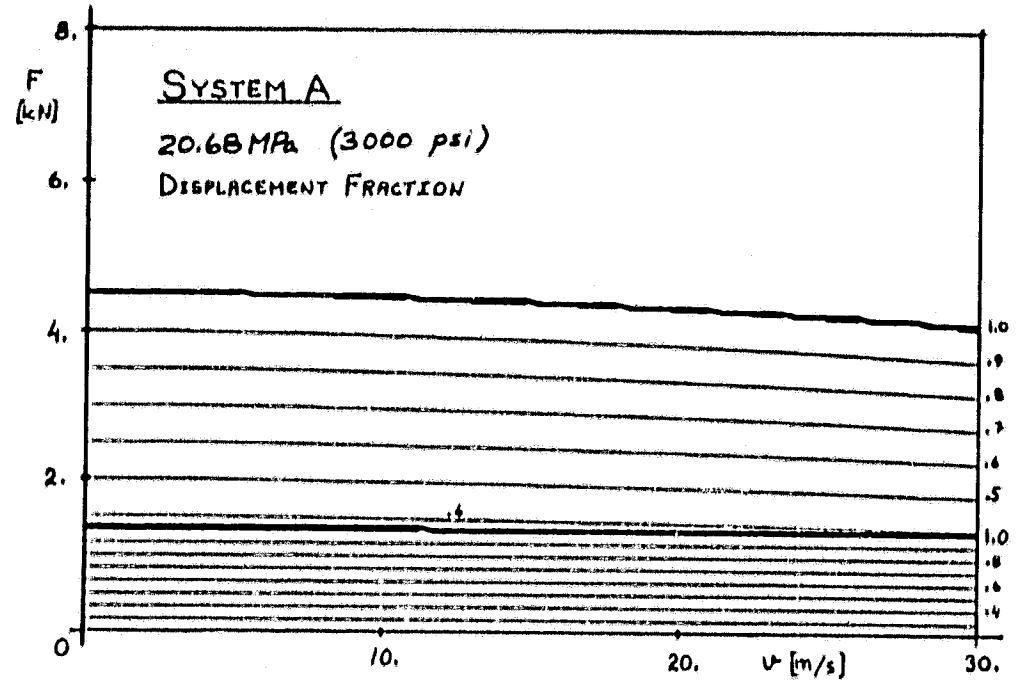
8.
F
[kN]
6.
4.
2.
0
SYSTEM A
20.68 MPa (3000 psi)
DISPLACEMENT FRACTION
1.0
.9
.8
.7
.6
.5
.4
1.0
.8
.6
.4
10.
20.
v [m/s]
30.

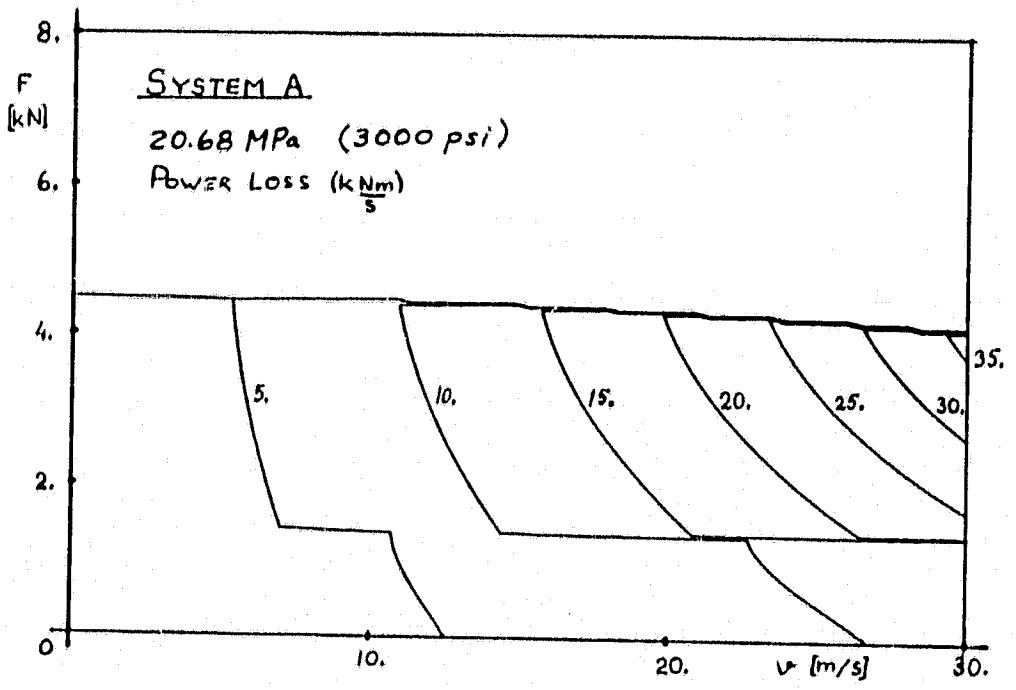
8.
F
[kN]
6.
4.
2.
0
SYSTEM A
20.68 MPa (3000 psi)
POWER LOSS (kNm/s)
5.
10.
15.
20.
25.
30.
35.
10.
20.
v [m/s]
30.

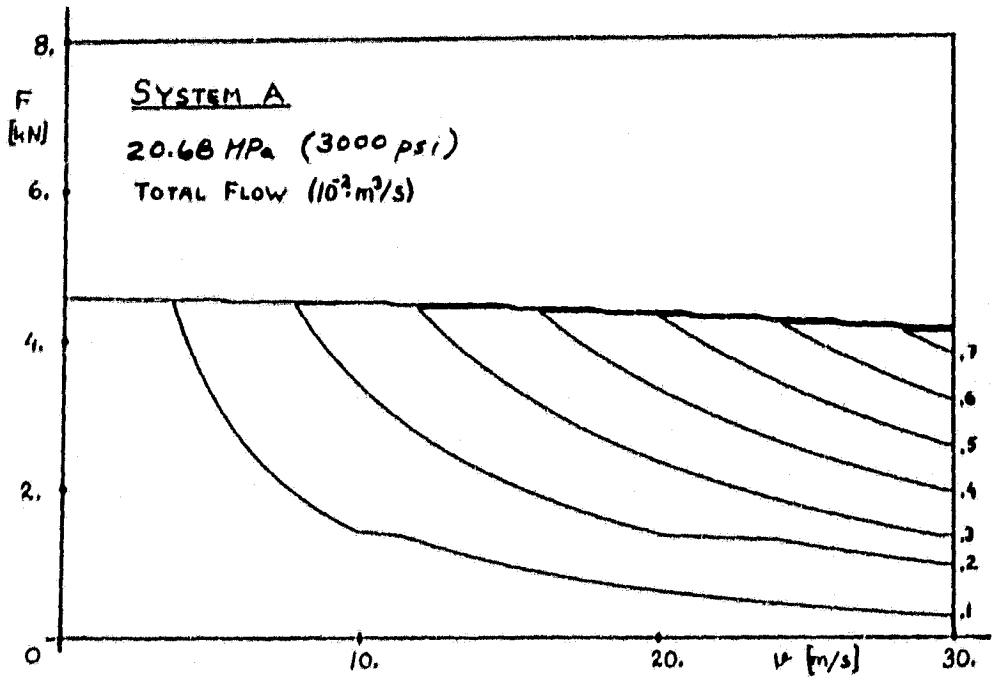
8.
F
[kN]
6.
4.
2.
0
SYSTEM A
20.68 MPa (3000 psi)
TOTAL FLOW (10^{-3} m^3/s)
.7
.6
.5
.4
.3
.2
.1
10.
20.
v [m/s]
30.

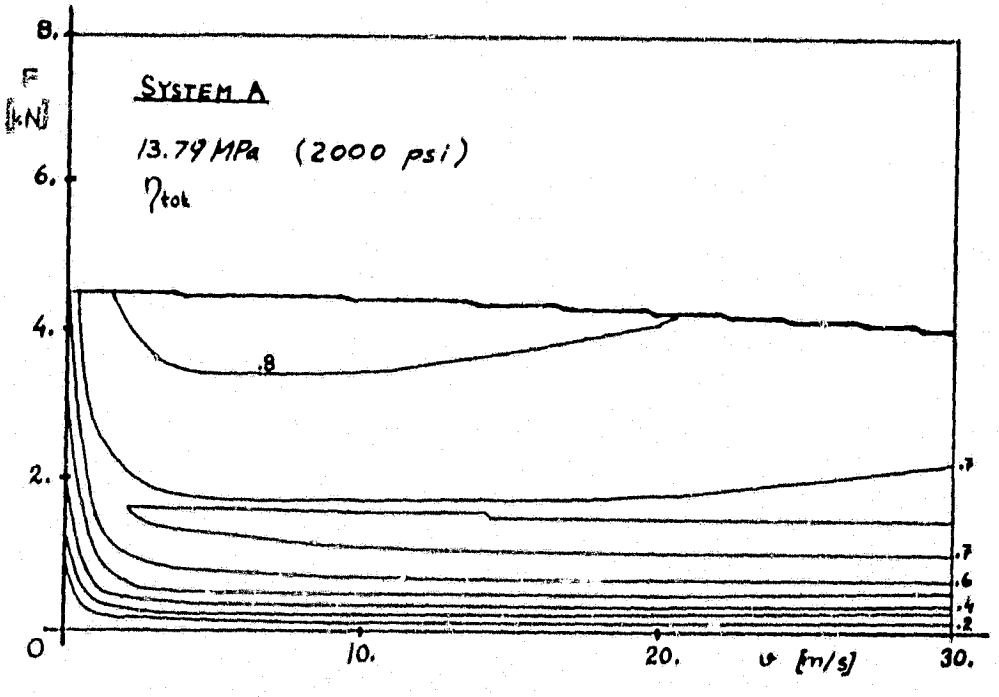
8.
F
[kN]
6.
4.
2.
0
SYSTEM A
13.79 MPa (2000 psi)
η_{tot}
.8
.7
.7
.6
.4
.2
10.
20.
v [m/s]
30.

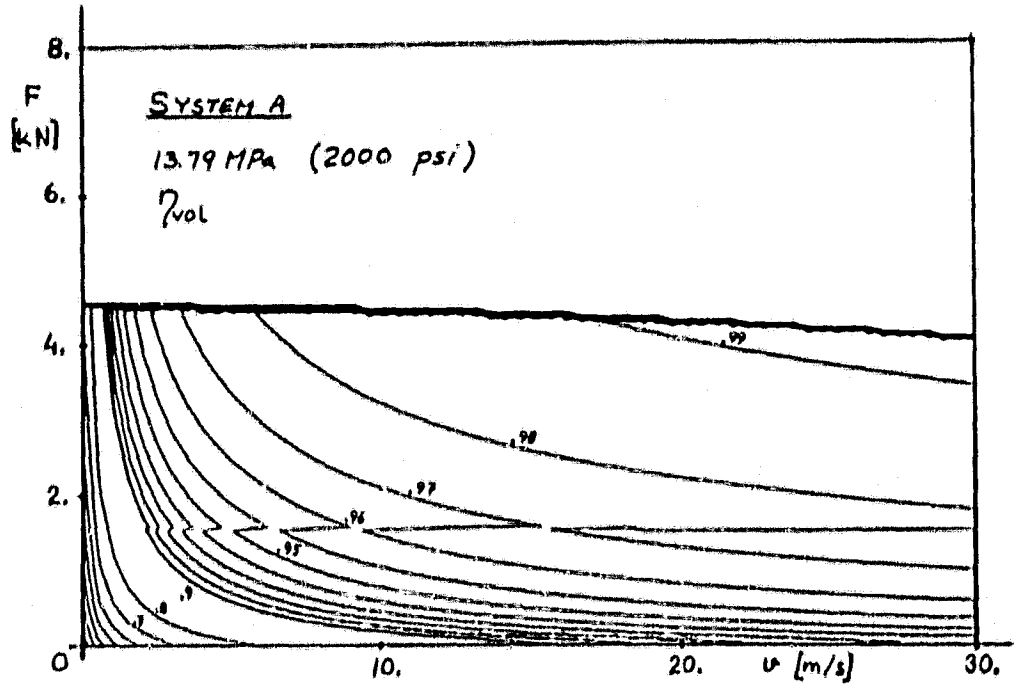
8.
F
[kN]
6.
4.
2.
0
SYSTEM A
13.79 MPa (2000 psi)
η_{vol}
.99
.98
.97
.96
.95
.9
.8
.7
10.
20.
v [m/s]
30.

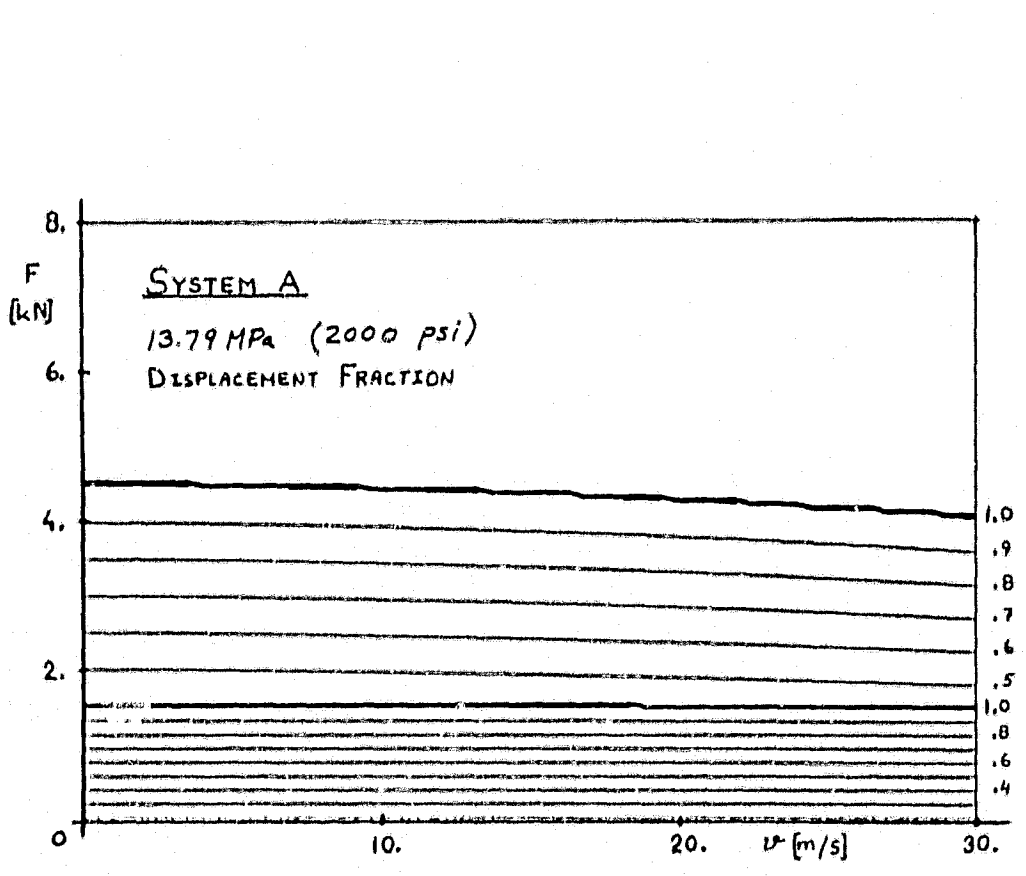
8.
F
[kN]
6.
4.
2.
0
SYSTEM A
13.79 MPa (2000 psi)
DISPLACEMENT FRACTION
1.0
.9
.8
.7
.6
.5
1.0
.8
.6
.4
10.
20.
v [m/s]
30.

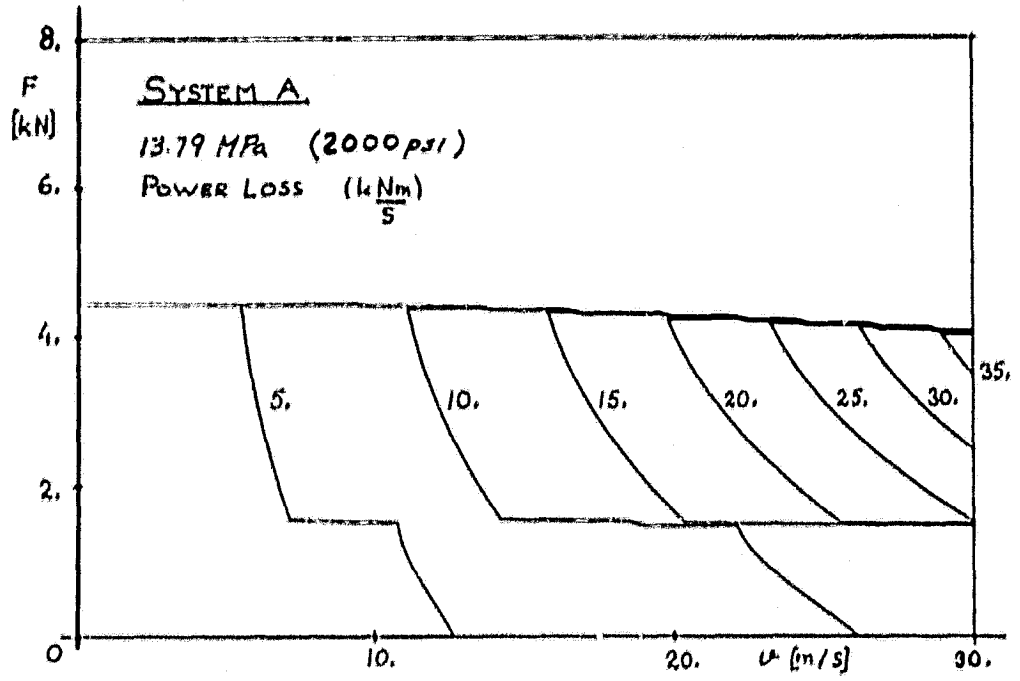
8.
F
[kN]
6.
4.
2.
0
SYSTEM A
13.79 MPa (2000 psi)
POWER LOSS (kNm/s)
5.
10.
15.
20.
25.
30.
35.
10.
20.
v [m/s]
30.

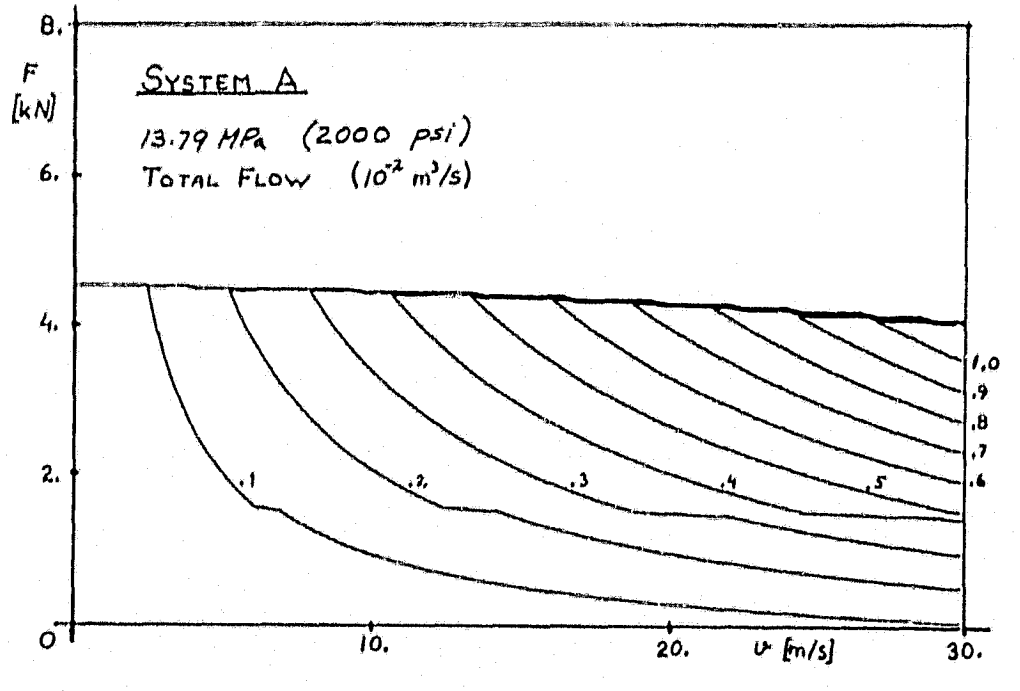
8.
F
[kN]
6.
4.
2.
0
SYSTEM A
13.79 MPa (2000 psi)
TOTAL FLOW (10^{-2} m³/s)
.1
.2
.3
.4
.5
.6
.7
.8
.9
1.0
10.
20.
v [m/s]
30.

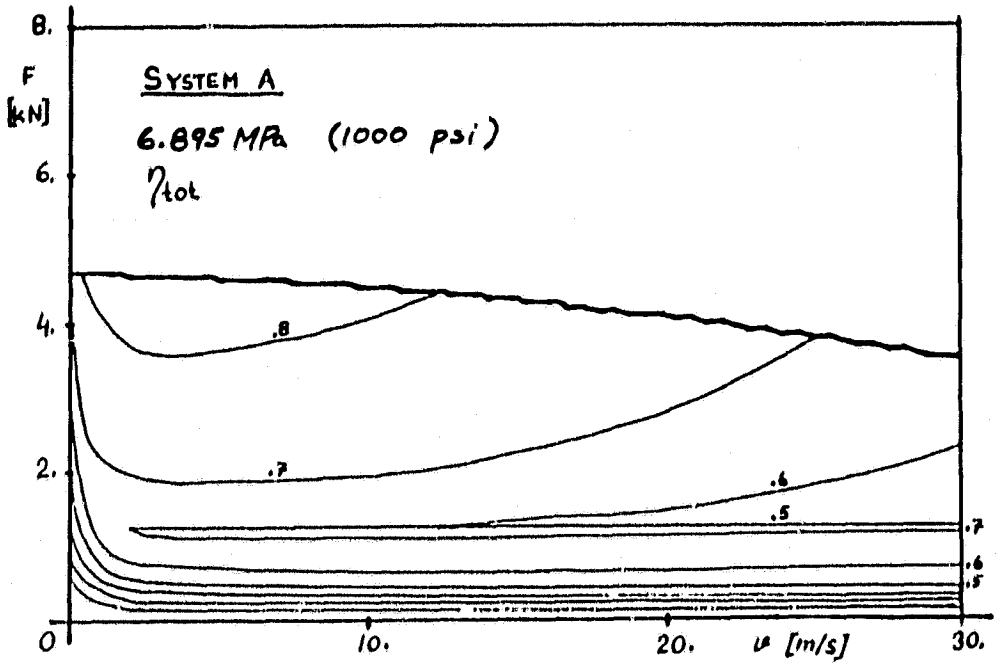
8.
F
[kN]
6.
4.
2.
0
SYSTEM A
6.895 MPa (1000 psi)
η_{tot}
.8
.7
.6
.5
.7
.6
.5
10.
20.
v [m/s]
30.

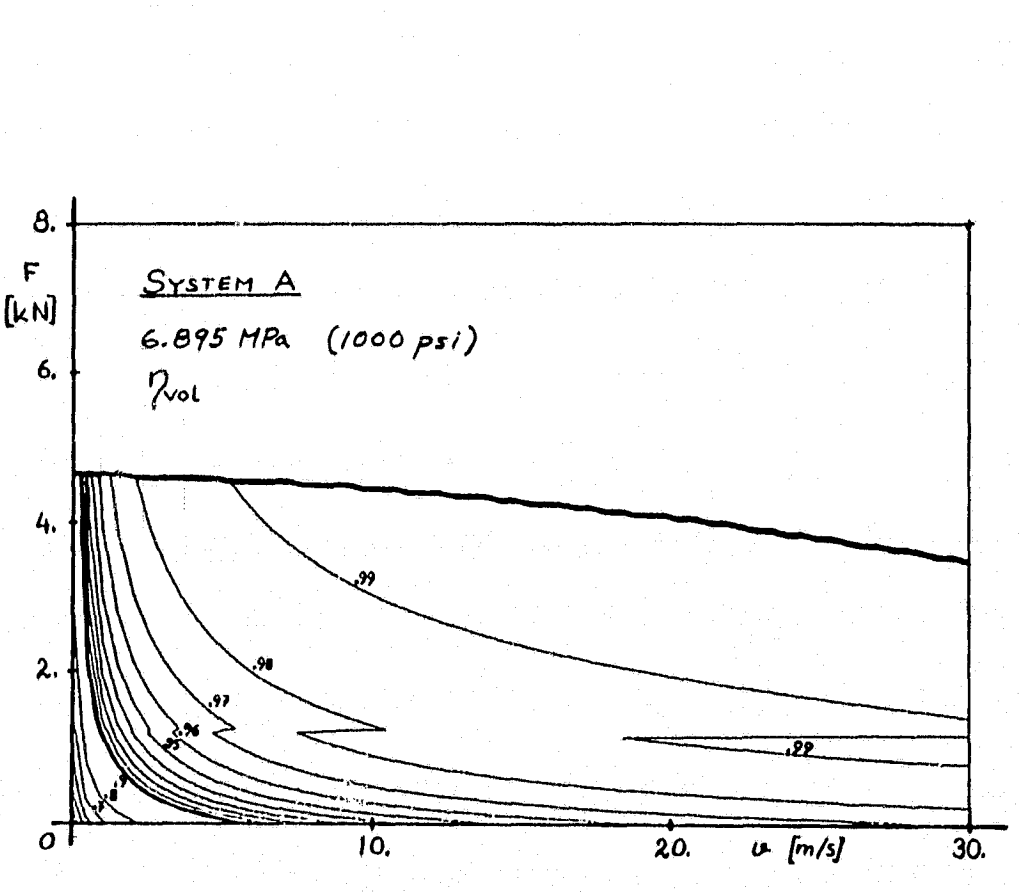
8.
F
[kN]
6.
4.
2.
0
SYSTEM A
6.895 MPa (1000 psi)
η_{vol}
.99
.98
.97
.96
.95
.9
.8
.99
10.
20.
v [m/s]
30.

C-2

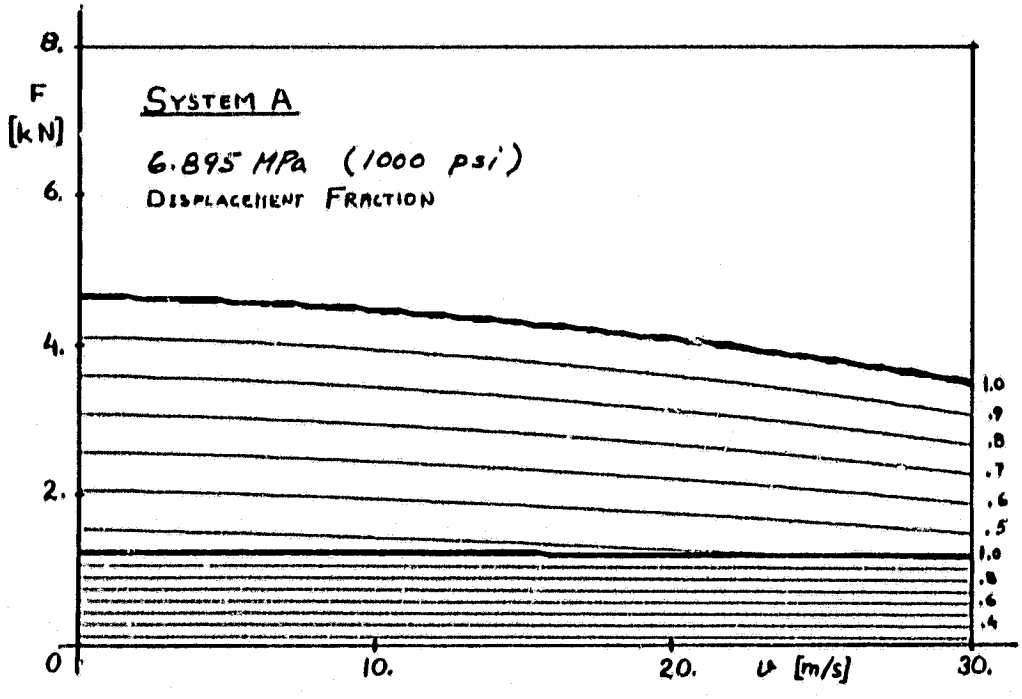
8.
F
[kN]
6.
4.
2.
0
SYSTEM A
6.895 MPa (1000 psi)
DISPLACEMENT FRACTION
1.0
.9
.8
.7
.6
.5
1.0
.8
.6
.4
10.
20.
v [m/s]
30.

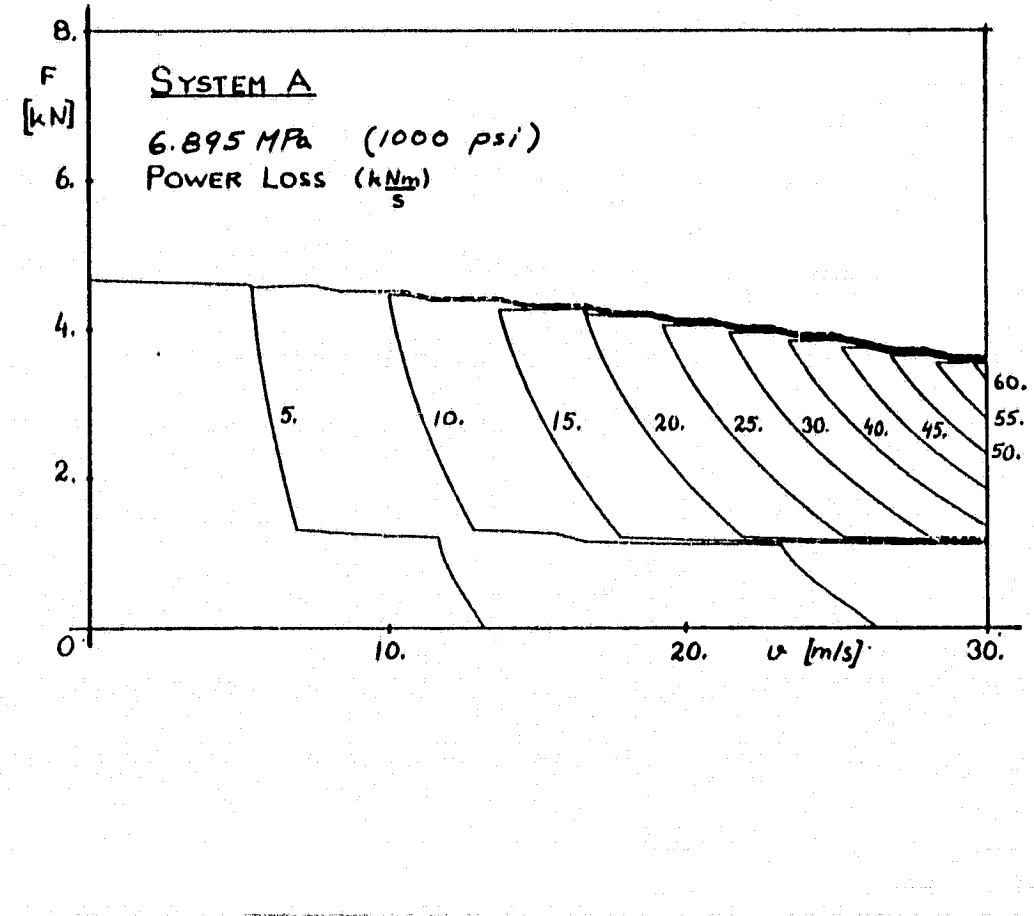
8.
F
[kN]
6.
4.
2.
0
SYSTEM A
6.895 MPa (1000 psi)
POWER LOSS (kNm/s)
5.
10.
15.
20.
25.
30.
40.
45.
60.
55.
50.
10.
20.
v [m/s]
30.

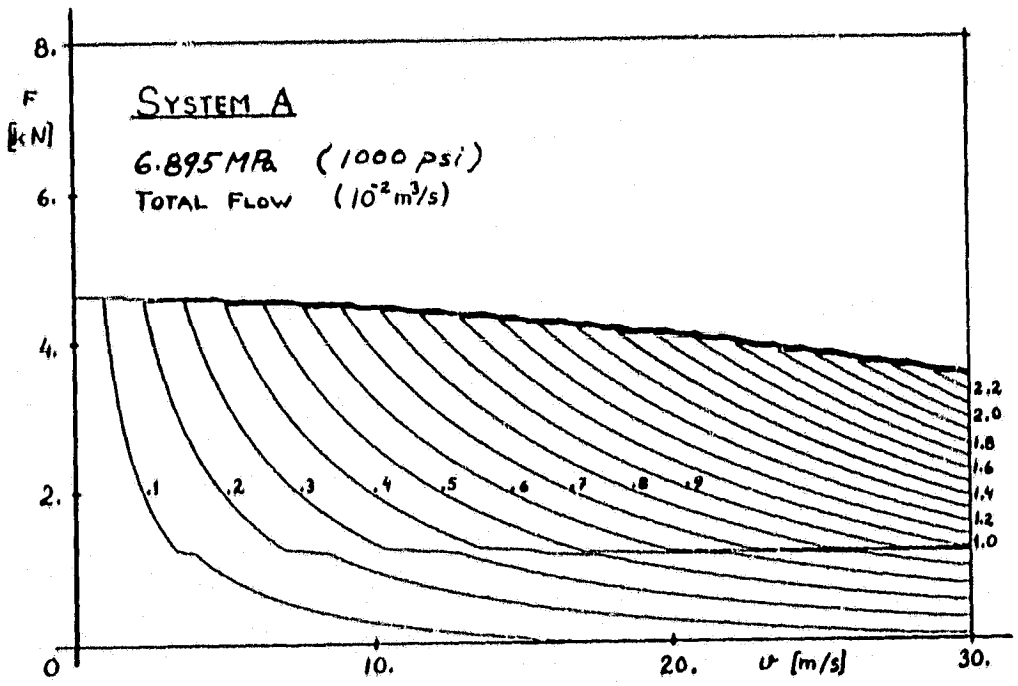
SYSTEM A
6.895 MPa (1000 psi)
TOTAL FLOW (10^{-2} m³/s)
F [kN]
8.
6.
4.
2.
0
10.
20.
30.
v [m/s]
.1
.2
.3
.4
.5
.6
.7
.8
.9
2.2
2.0
1.8
1.6
1.4
1.2
1.0

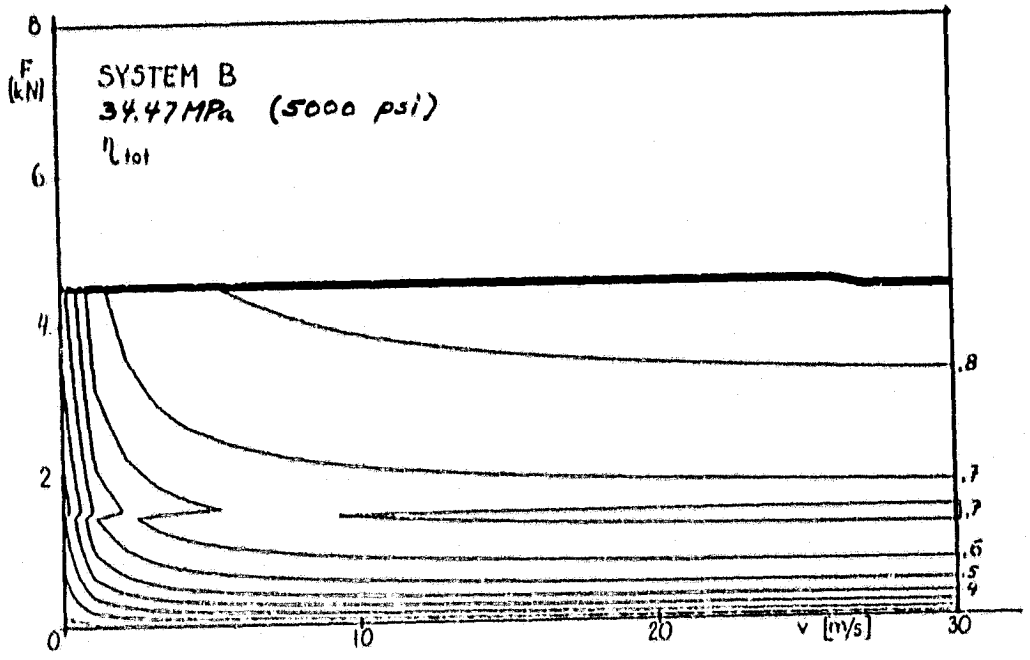
SYSTEM B
34.47 MPa (5000 psi)
η_{tot}
F [kN]
8
6
4
2
0
10
20
30
v [m/s]
.8
.7
.7
.6
.5
.4

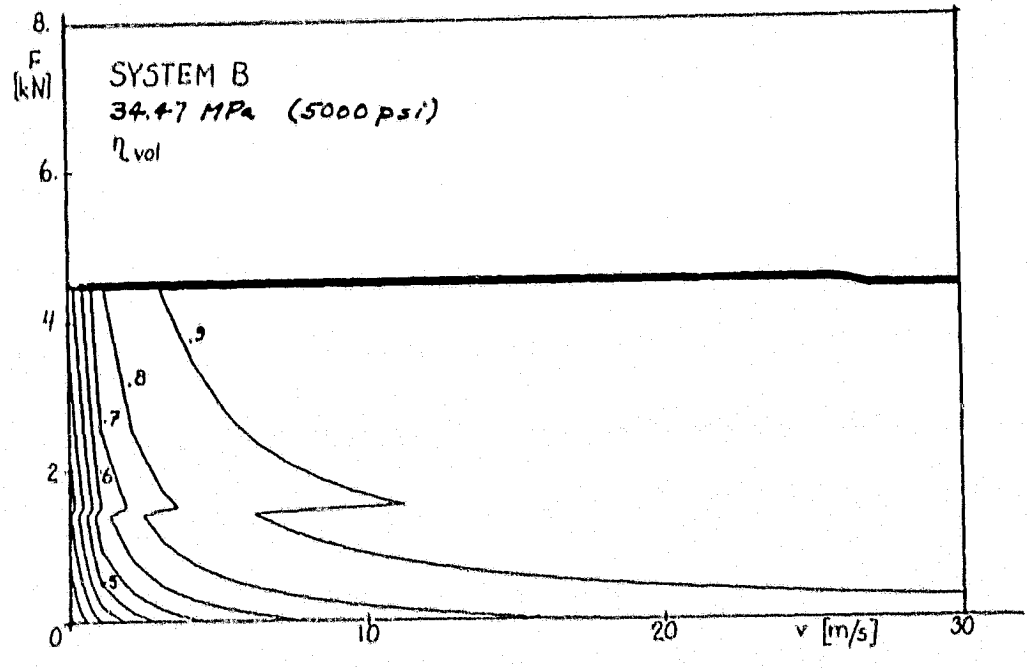
SYSTEM B
34.47 MPa (5000 psi)
η_{vol}
F [kN]
8.
6.
4
2
0
10
20
30
v [m/s]
.9
.8
.7
.6
.5

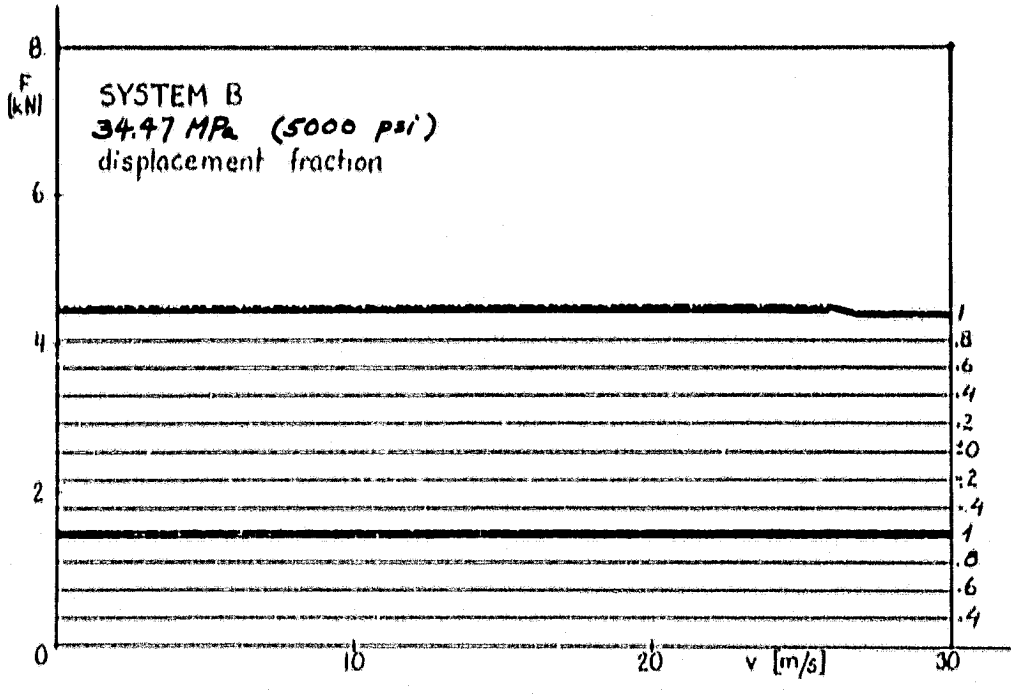
8.
F [kN]
6
4
2
0
SYSTEM B
34.47 MPa (5000 psi)
displacement fraction
1
.8
.6
.4
.2
0
.2
.4
1
.8
.6
.4
10
20
v [m/s]
30

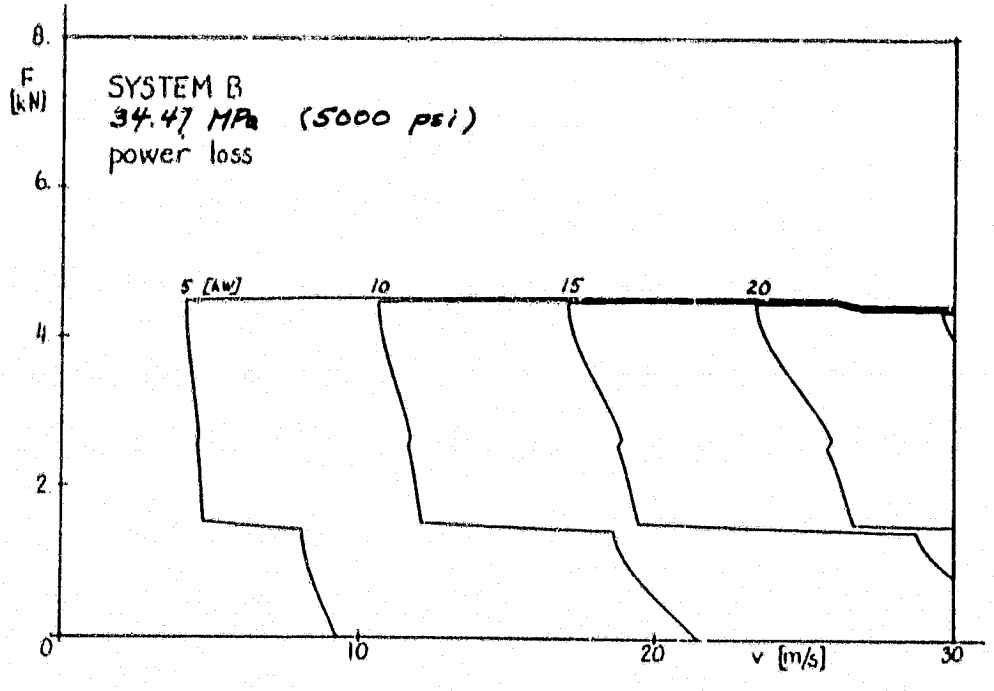
8.
F [kN]
6.
4
2
0
SYSTEM B
34.47 MPa (5000 psi)
power loss
5 [kW]
10
15
20
10
20
v [m/s]
30

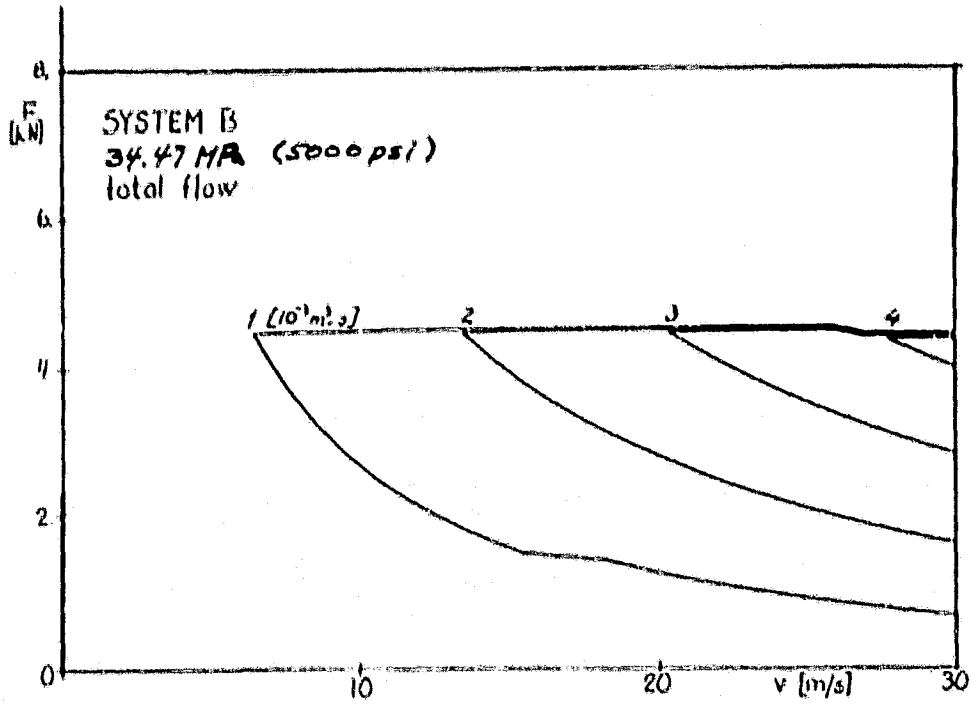
F [kN]
SYSTEM B
34.47 MPa (5000 psi)
total flow
1 [10⁻³m³/s]
2
3
4
8
6
4
2
0
10
20
v [m/s]
30

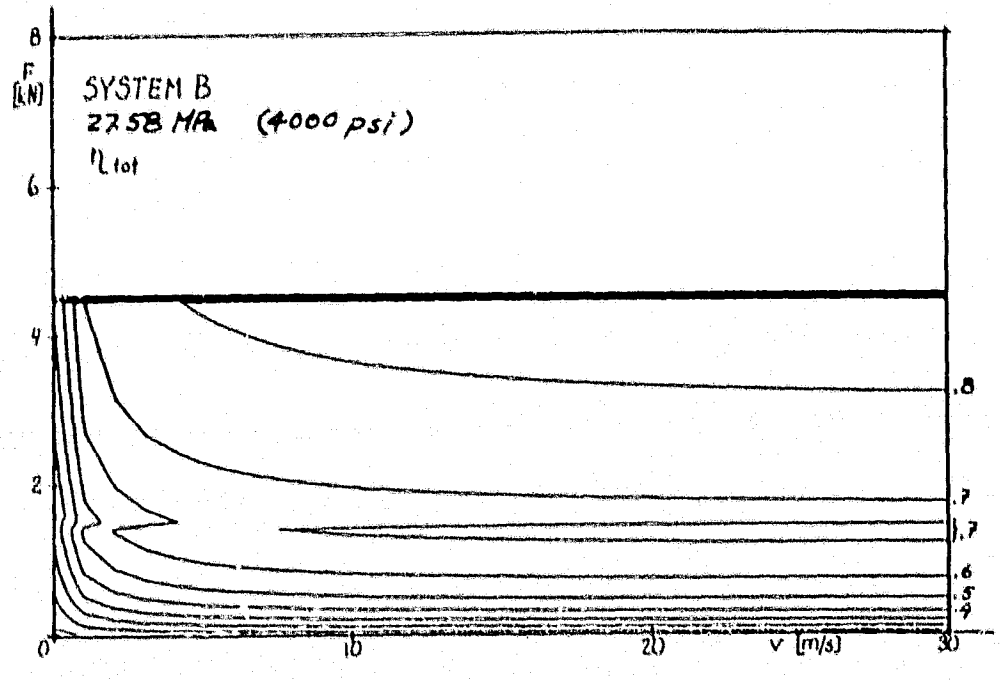
F [kN]
SYSTEM B
27.58 MPa (4000 psi)
η tot
8
6
4
2
0
10
20
v [m/s]
30
.8
.7
.7
.6
.5
.9

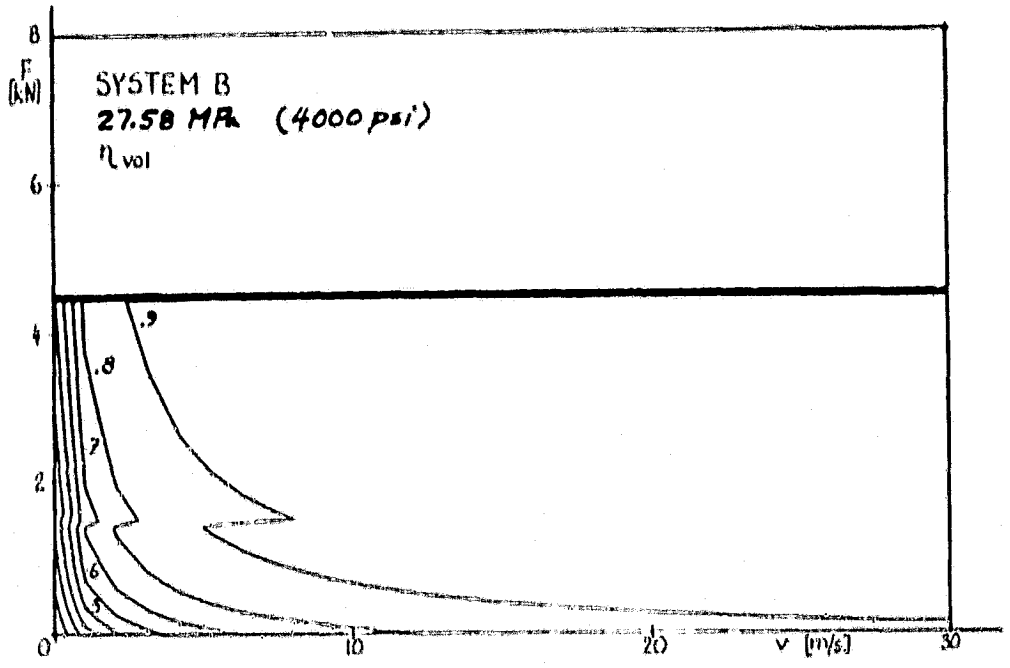
F [kN]
8
6
4
2
0
SYSTEM B
27.58 MPa (4000 psi)
η_{vol}
.9
.8
.7
.6
.5
10
20
V [m/s]
30

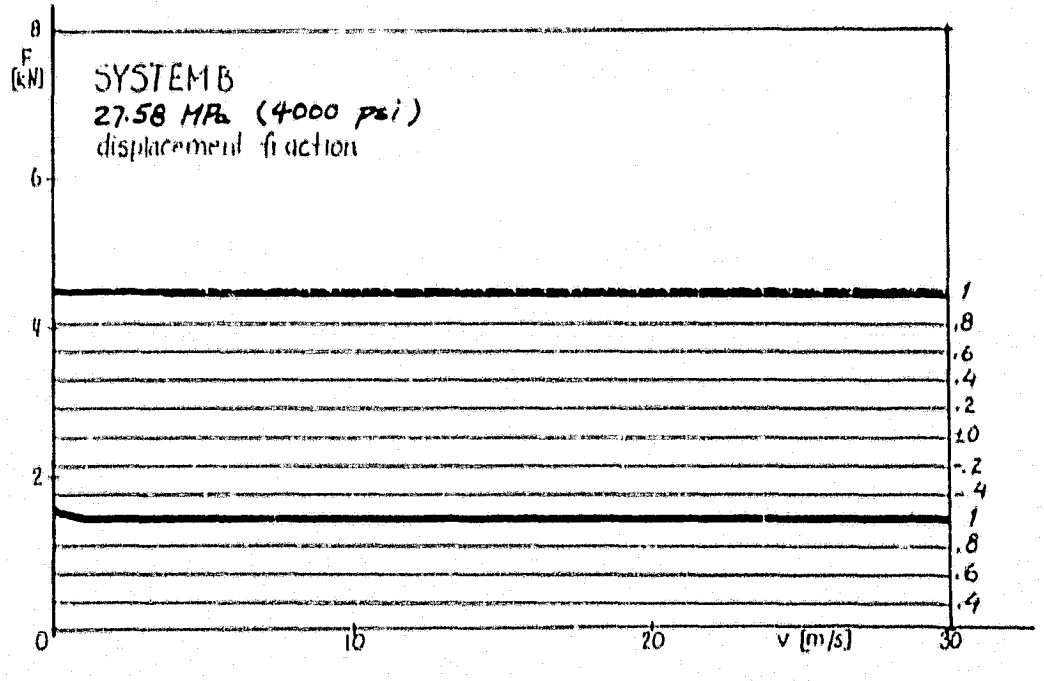
F [kN]
8
6
4
2
0
SYSTEM B
27.58 MPa (4000 psi)
displacement fraction
1
.8
.6
.4
.2
±0
-.2
-.4
1
.8
.6
.4
10
20
V [m/s]
30

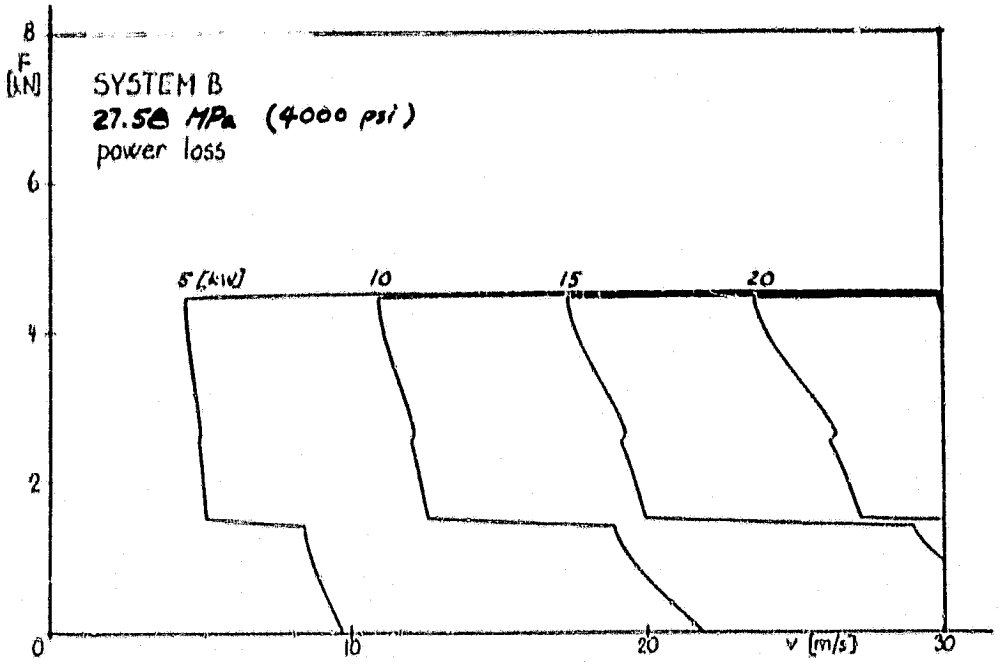
F [kN]
SYSTEM B
27.58 MPa (4000 psi)
power loss
5 [kW]
10
15
20
8
6
4
2
0
10
20
v [m/s]
30

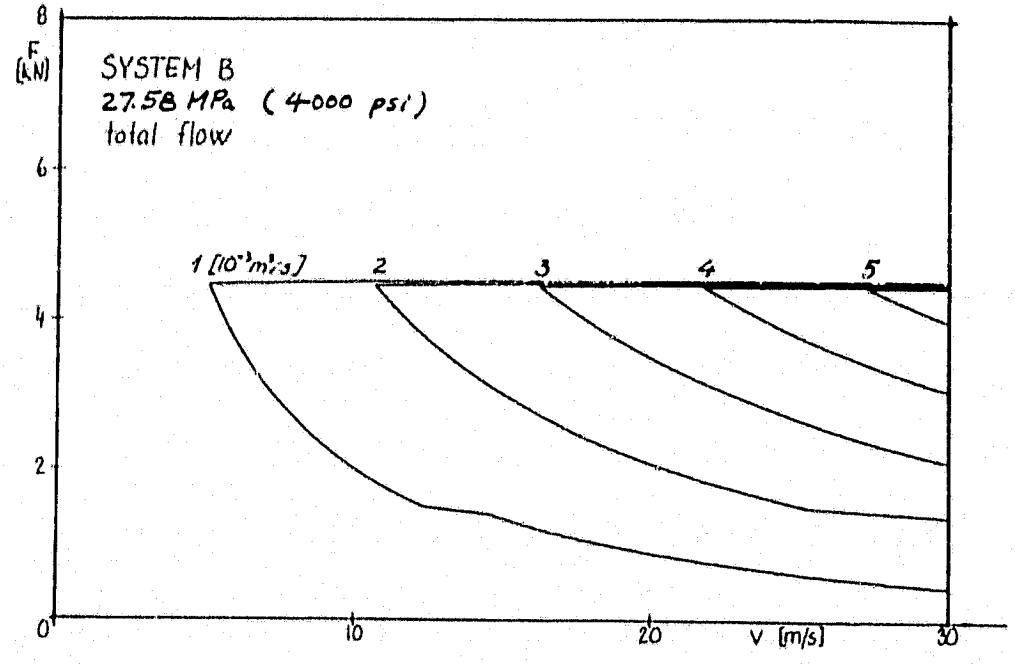
F [kN]
SYSTEM B
27.58 MPa (4000 psi)
total flow
1 [10⁻³m³/s]
2
3
4
5
8
6
4
2
0
10
20
v [m/s]
30

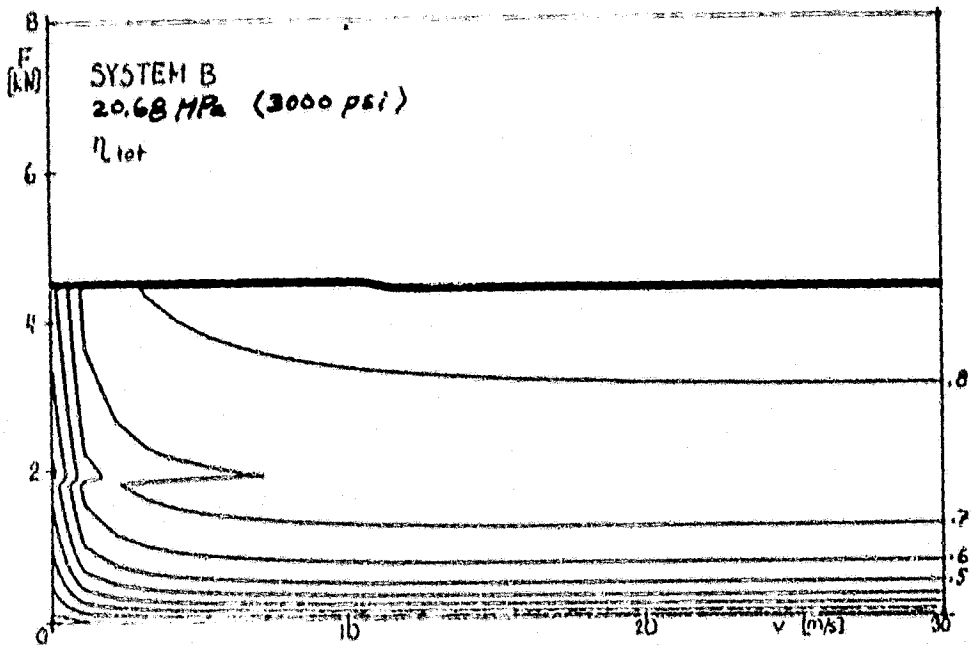
SYSTEM B
20.68 MPa (3000 psi)
η tot
F [kN]
8
6
4
2
0
10
20
V [m/s]
30
.8
.7
.6
.5

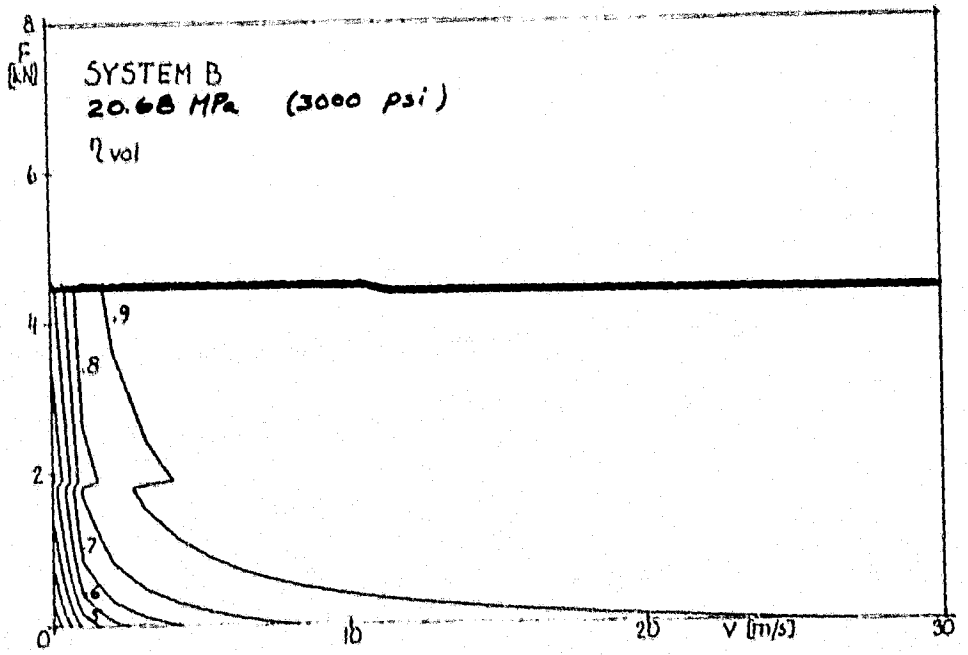
SYSTEM B
20.68 MPa (3000 psi)
η vol
F [kN]
8
6
4
2
0
10
20
V [m/s]
30
.9
.8
.7
.6

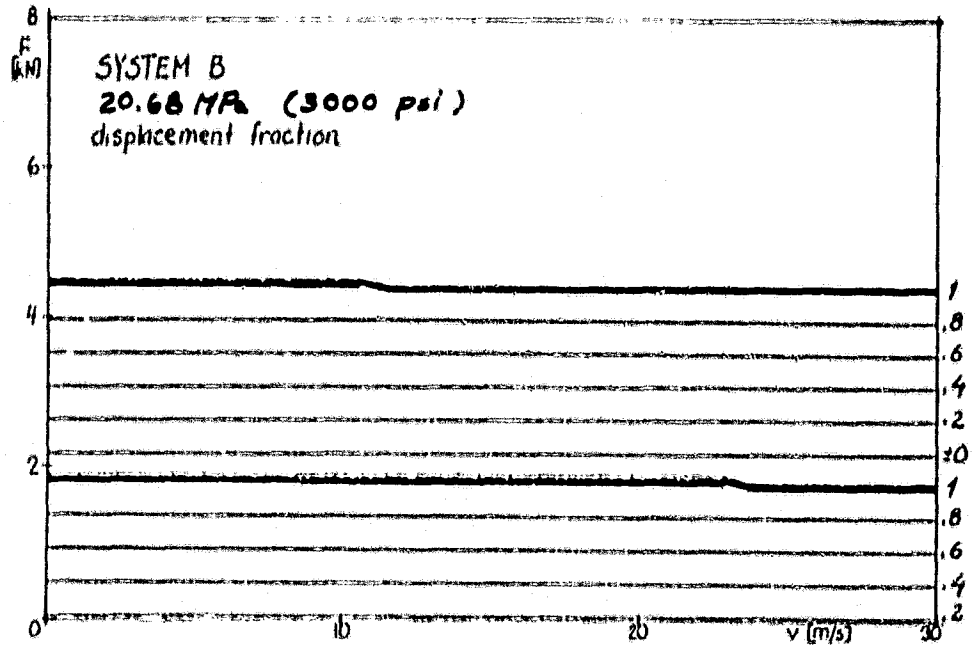
8
F
[kN]
SYSTEM B
20.68 MPa (3000 psi)
displacement fraction
6
4
2
0
1
.8
.6
.4
.2
.0
1
.8
.6
.4
.2
10
20
v [m/s]
30

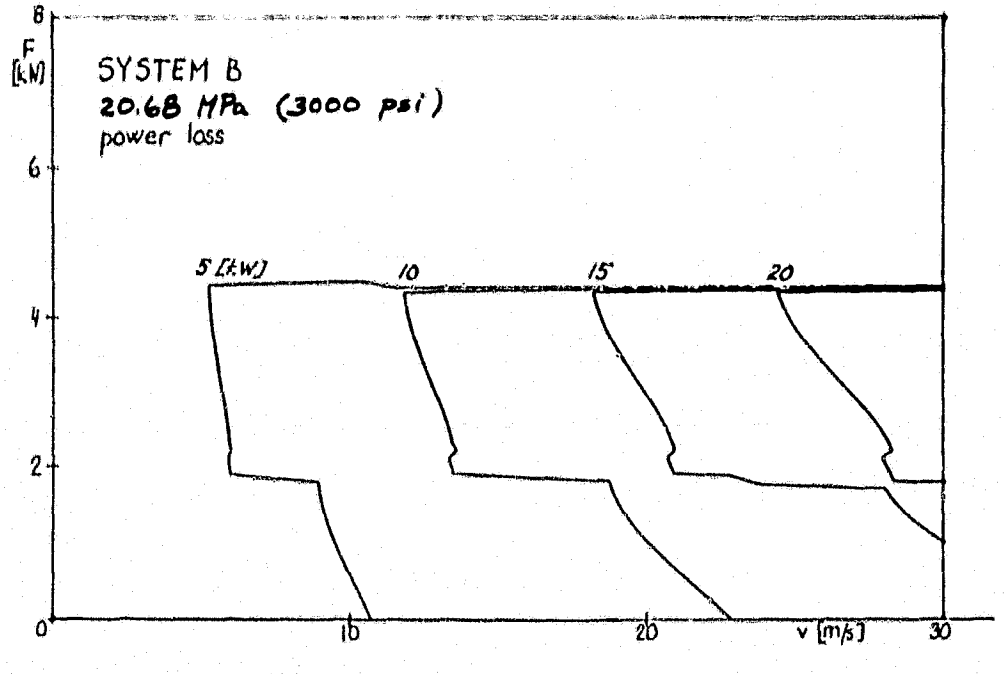
8
F
[kN]
SYSTEM B
20.68 MPa (3000 psi)
power loss
6
4
2
0
5 [kW]
10
15
20
10
20
v [m/s]
30

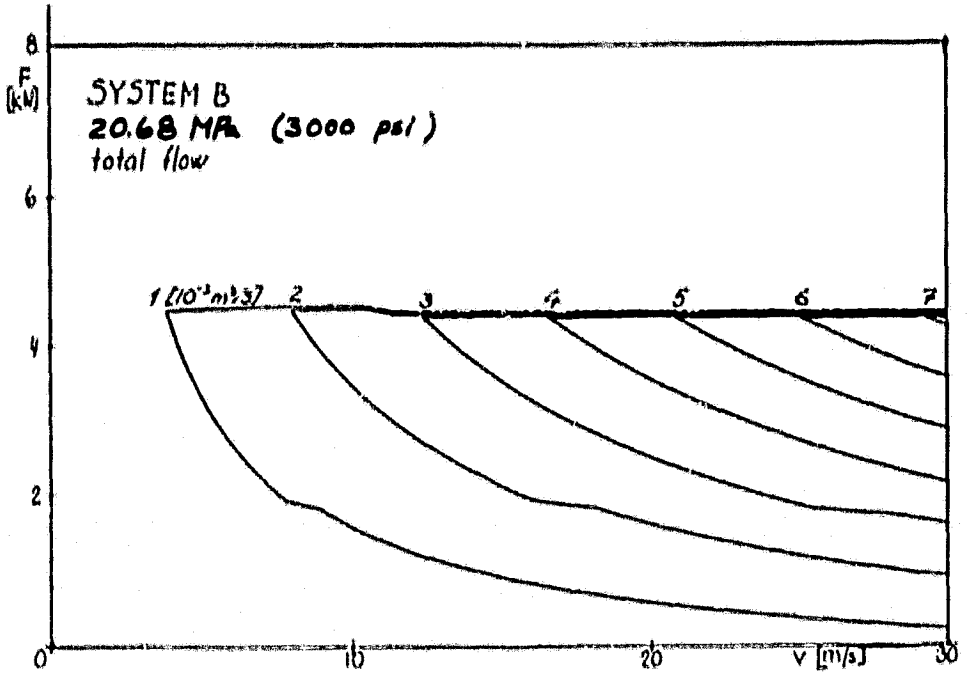
F [kN]
SYSTEM B
20.68 MPa (3000 psi)
total flow
1 [10⁻³m³/s]
2
3
4
5
6
7
8
6
4
2
0
10
20
V [m/s]
30

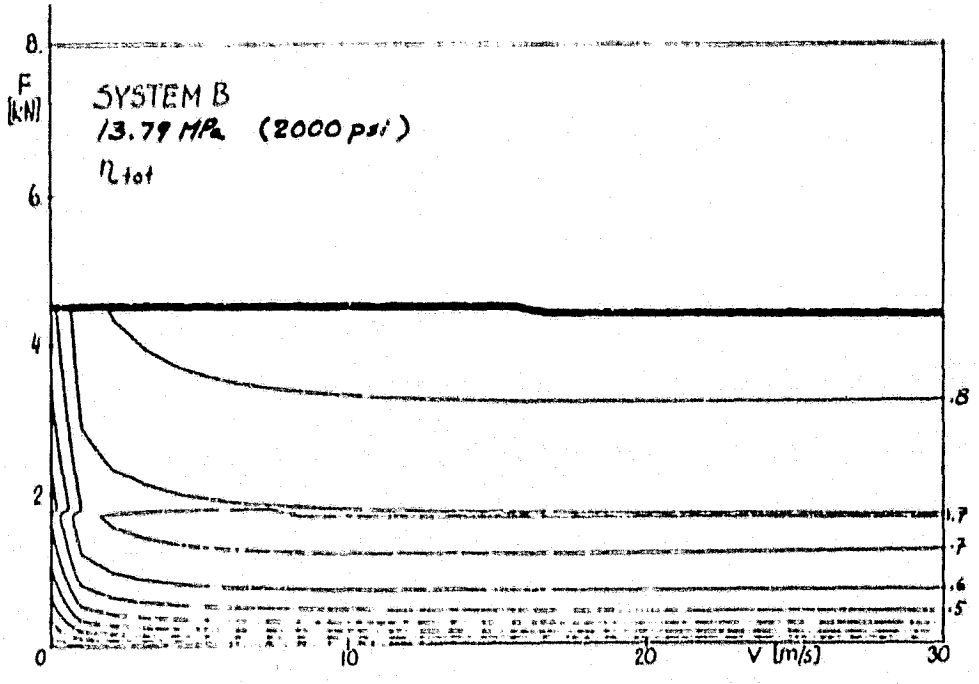
F [kN]
SYSTEM B
13.79 MPa (2000 psi)
η tot
8.
6
4
2
0
10
20
V [m/s]
30
.8
.7
.6
.5

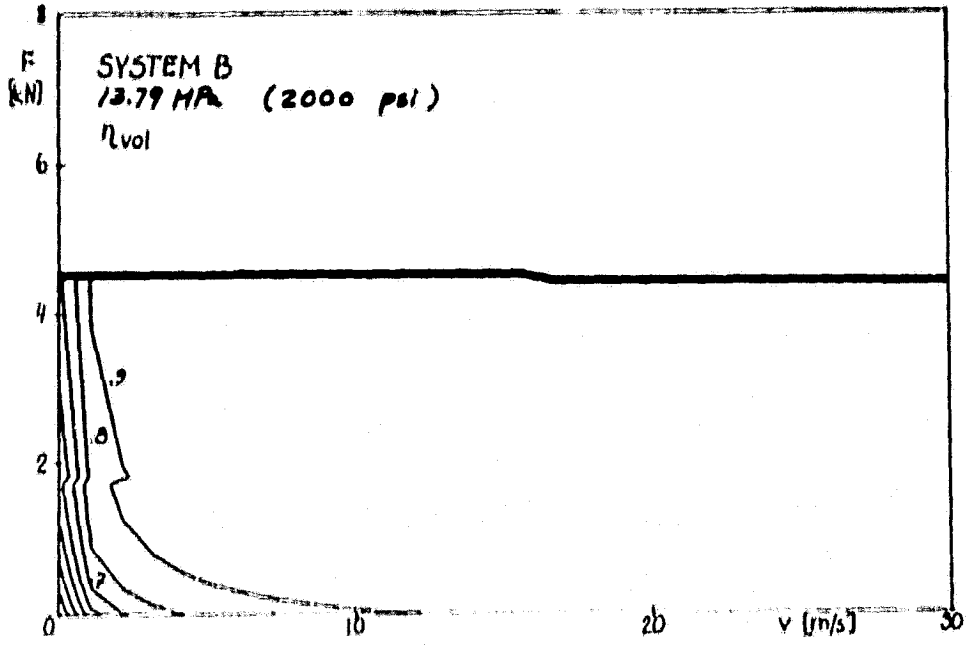
F
[kN]
SYSTEM B
13.79 MPa (2000 psi)
η_{vol}
8
6
4
2
0
.9
.8
.7
10
20
v [m/s]
30

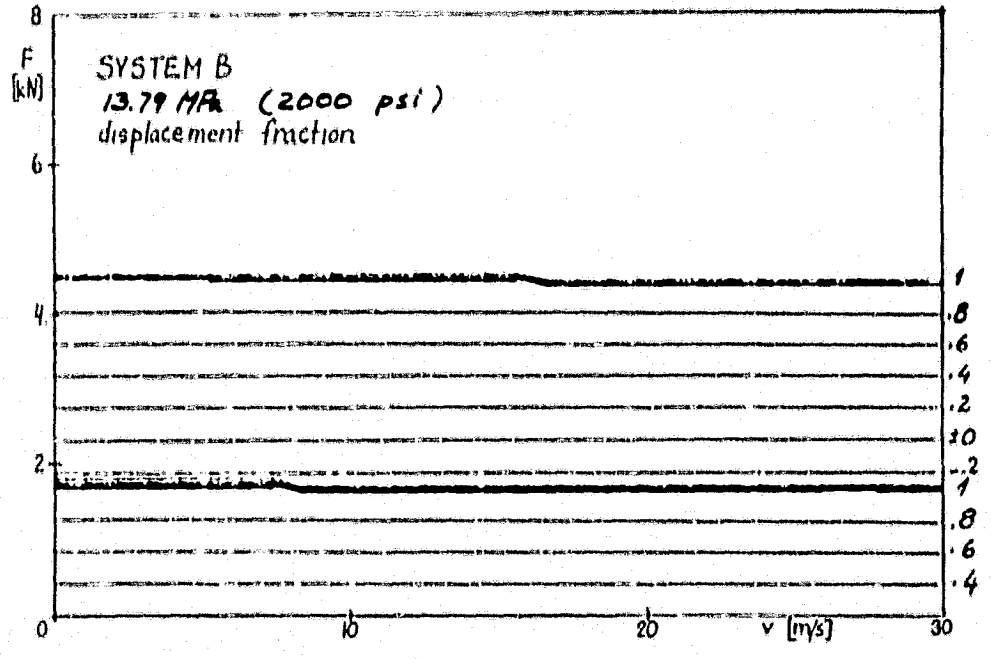
F
[kN]
SYSTEM B
13.79 MPa (2000 psi)
displacement fraction
8
6
4
2
0
1
.8
.6
.4
.2
.0
.2
1
.8
.6
.4
10
20
v [m/s]
30

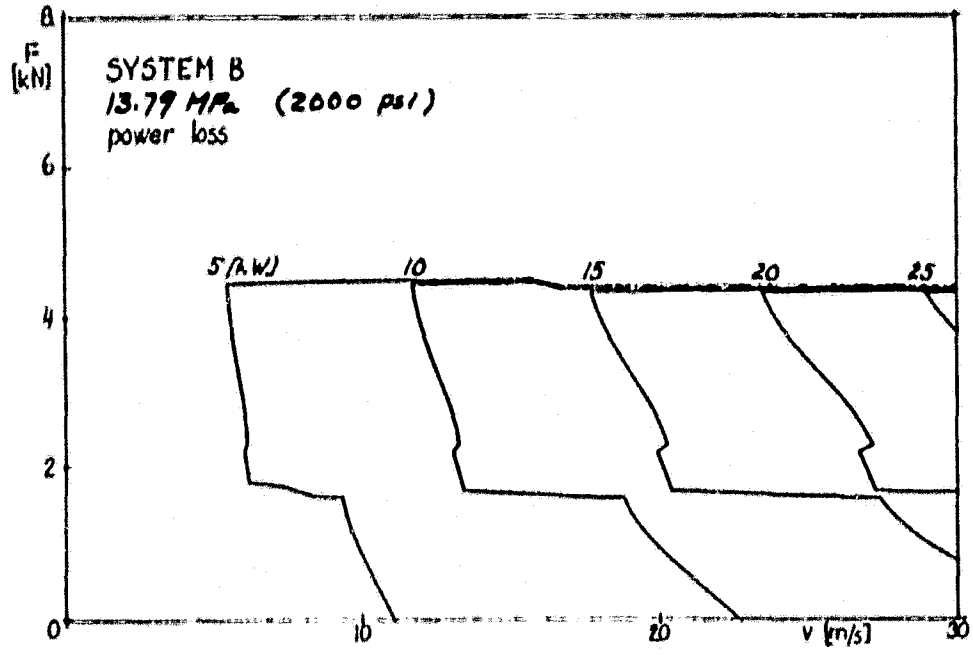
F [kN]
SYSTEM B
13.79 MPa (2000 psi)
power loss
5 [kW]
10
15
20
25
0
2
4
6
8
10
20
30
v [m/s]

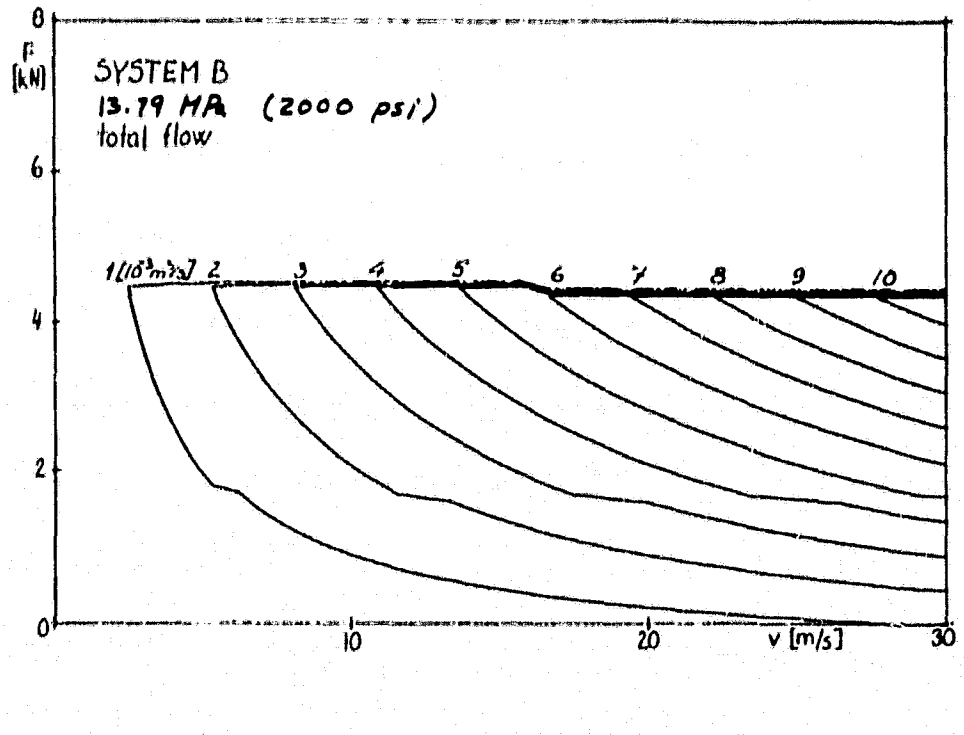
F [kN]
SYSTEM B
13.79 MPa (2000 psi)
total flow
1 [10⁻³m³/s]
2
3
4
5
6
7
8
9
10
0
2
4
6
8
10
20
30
v [m/s]

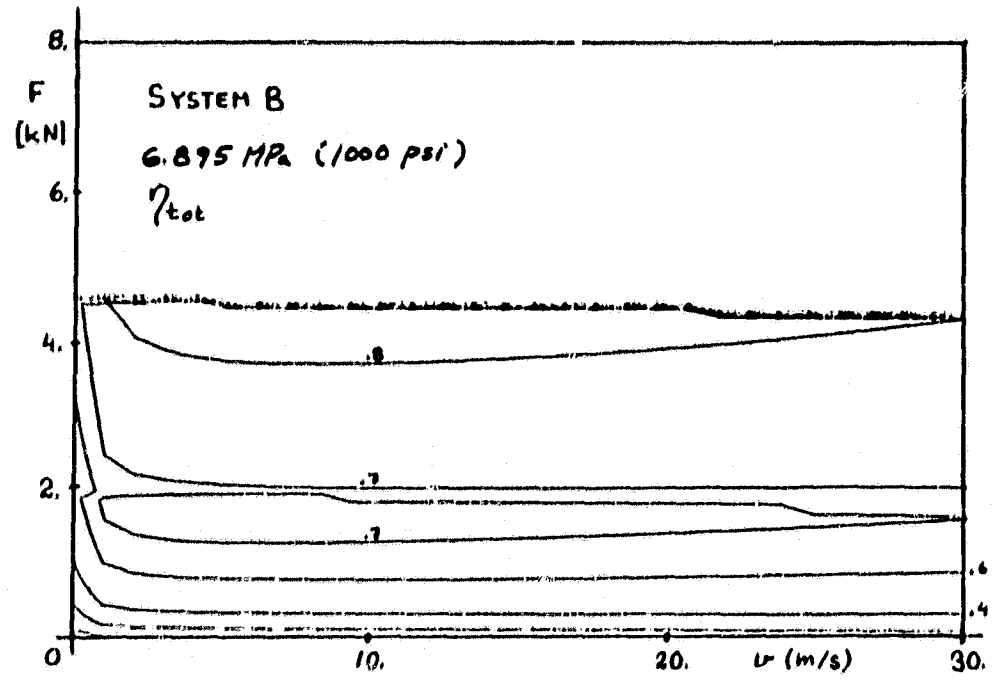
8.
F
[kN]
6.
4.
2.
0
SYSTEM B
6.895 MPa (1000 psi)
η_{tot}
.8
.7
.7
.6
.4
10.
20.
v (m/s)
30.

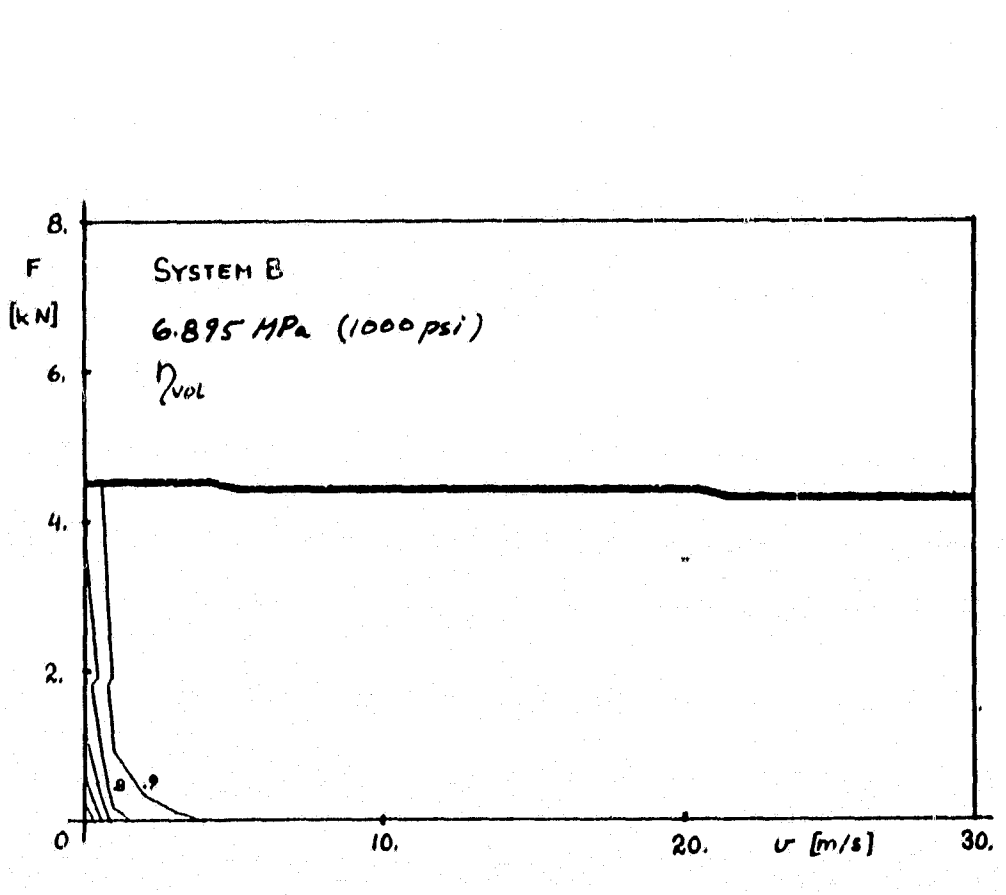
8.
F
[kN]
6.
4.
2.
0
SYSTEM B
6.895 MPa (1000 psi)
η_{vol}
.8
.9
10.
20.
v [m/s]
30.

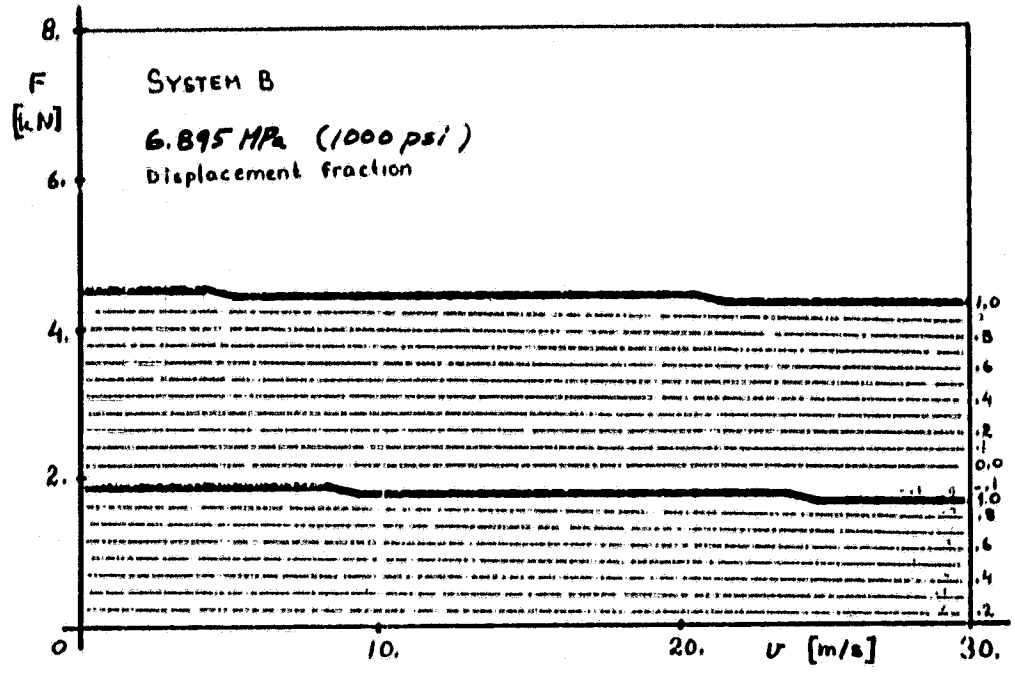
8.
F
[kN]
6.
4.
2.
0
SYSTEM B
6.895 MPa (1000 psi)
Displacement fraction
10.
20.
v [m/s]
30.
1.0
.8
.6
.4
.2
0.0
-.1

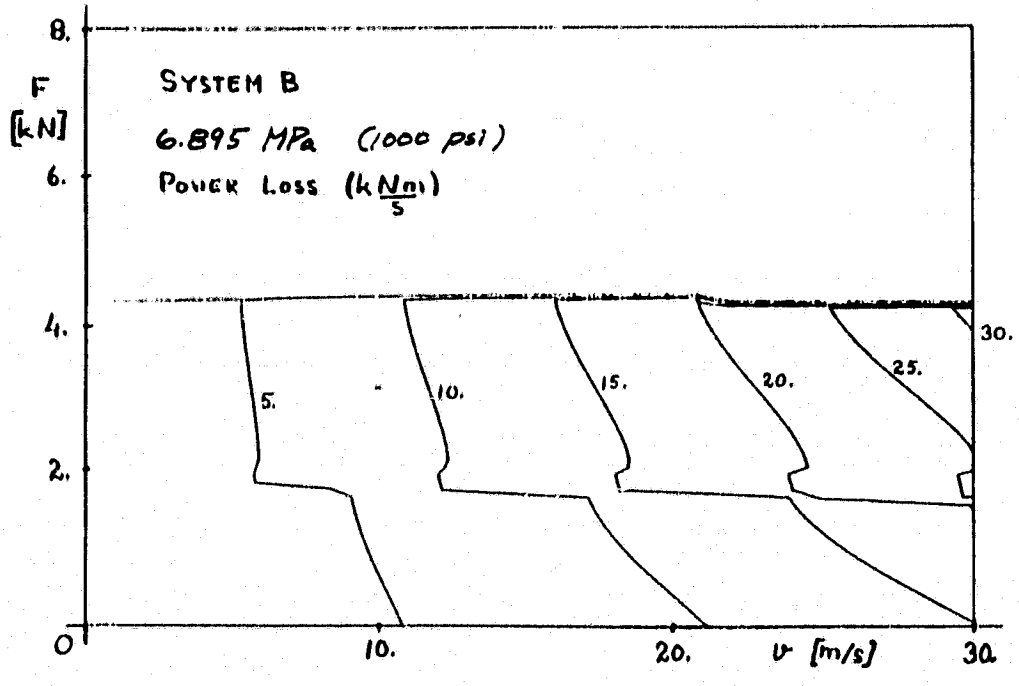
8.
F
[kN]
6.
4.
2.
0
SYSTEM B
6.895 MPa (1000 psi)
POWER LOSS (kNm/s)
5.
10.
15.
20.
25.
30.
10.
20.
v [m/s]
30.

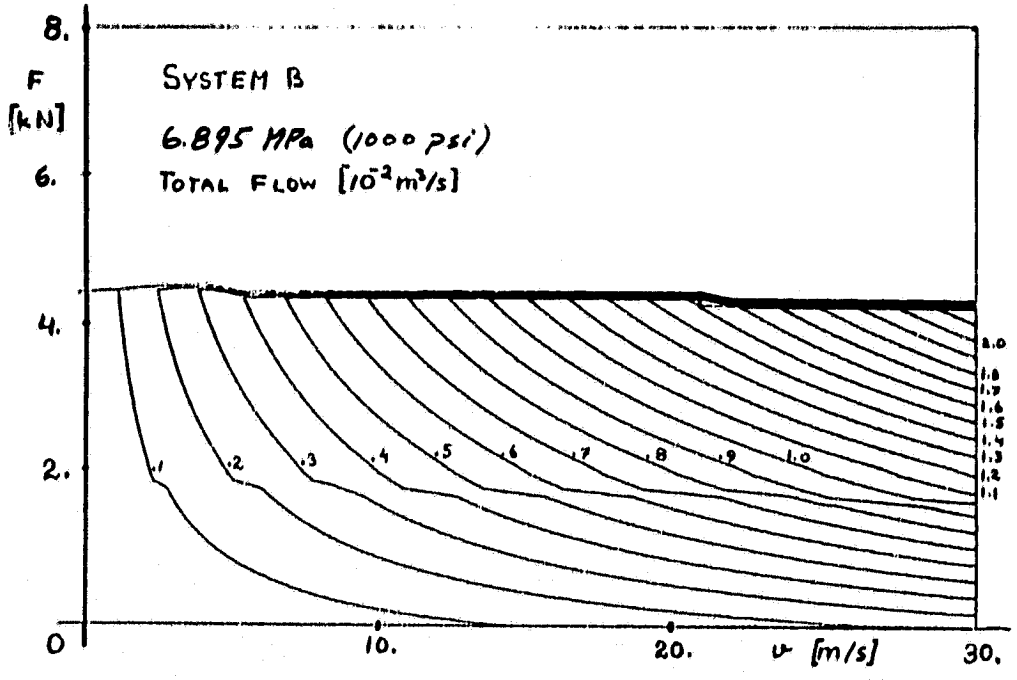

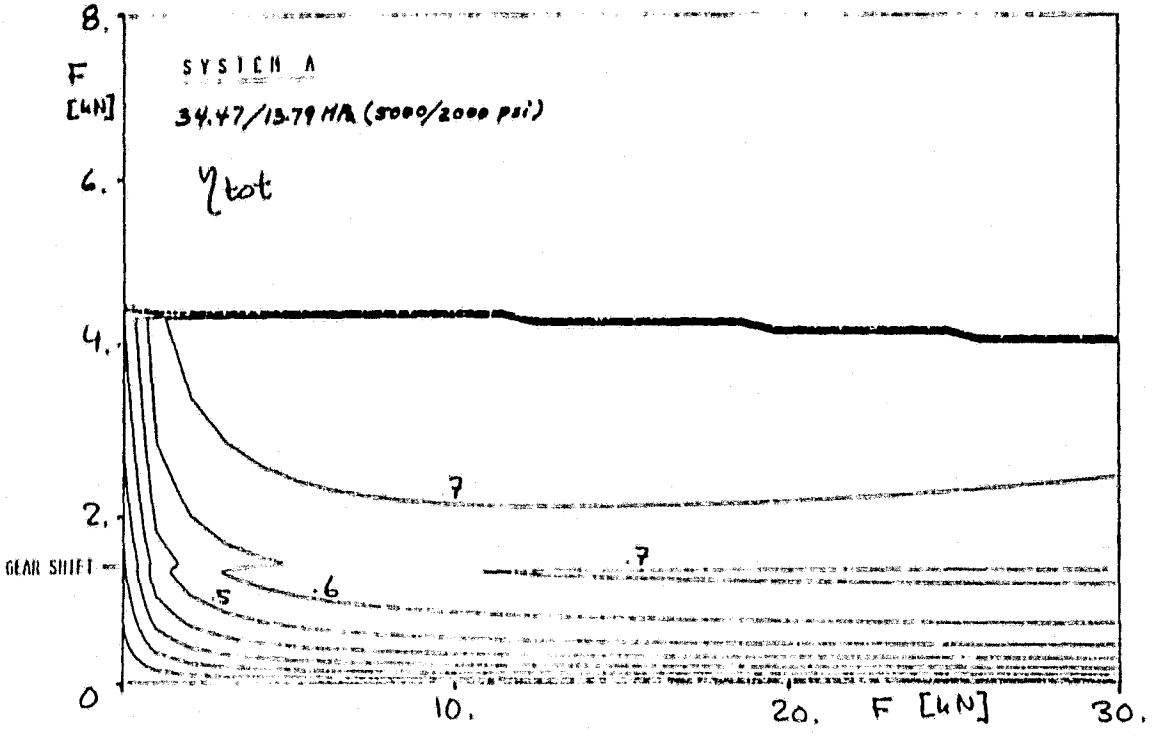
8.
F
[kN]
SYSTEM A
34.47/13.79 MPa (5000/2000 psi)
ηtot
6.
4.
2.
GEAR SHIFT
0
.7
.7
.6
.5
10.
20.
F [kN]
30.

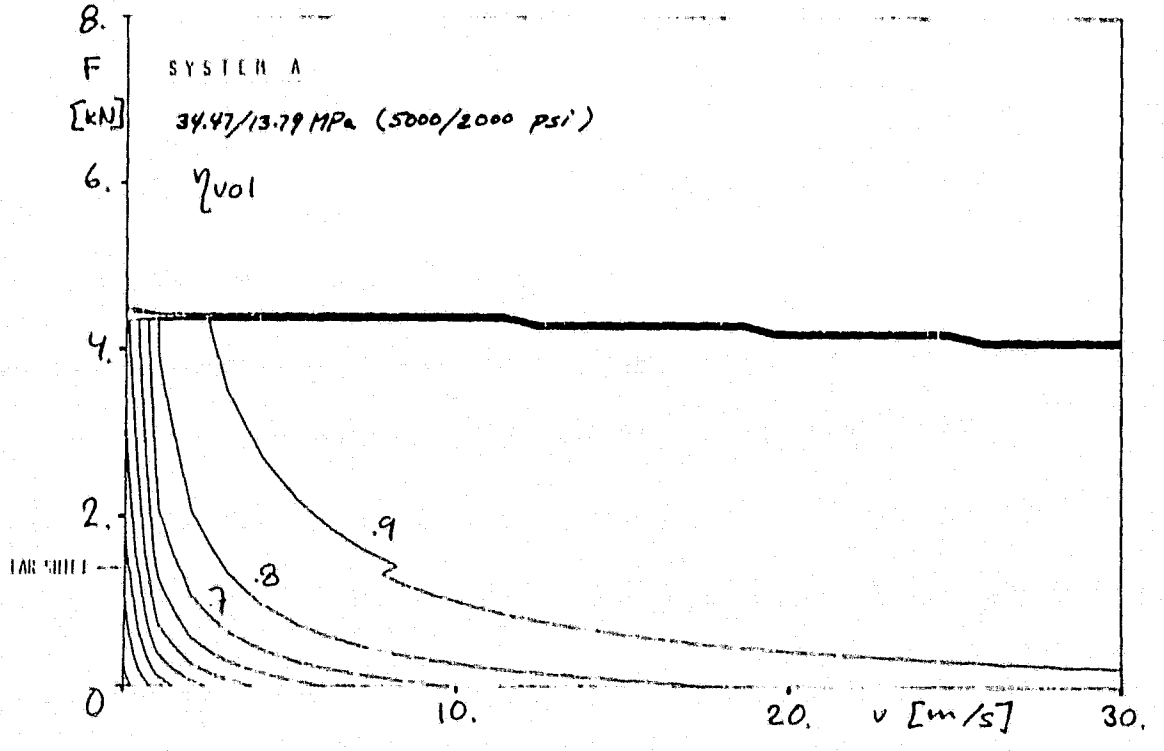
8.
F
[kN]
SYSTEM A
34.47/13.79 MPa (5000/2000 psi)
ηvol
6.
4.
2.
GEAR SHIFT
0
.9
.8
.7
10.
20.
v [m/s]
30.

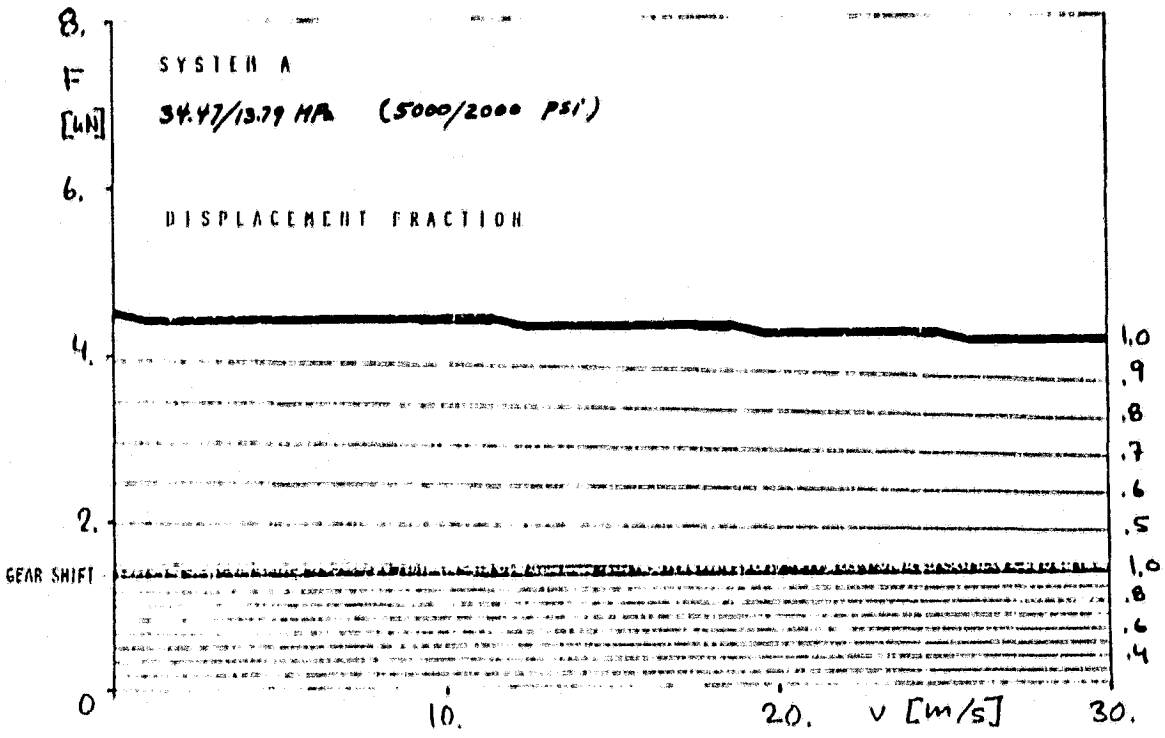
8.
F
[kN]
6.
4.
2.
GEAR SHIFT
0
SYSTEM A
34.47/13.79 MPa (5000/2000 PSI)
DISPLACEMENT FRACTION
1.0
.9
.8
.7
.6
.5
1.0
.8
.6
.4
10.
20.
v [m/s]
30.

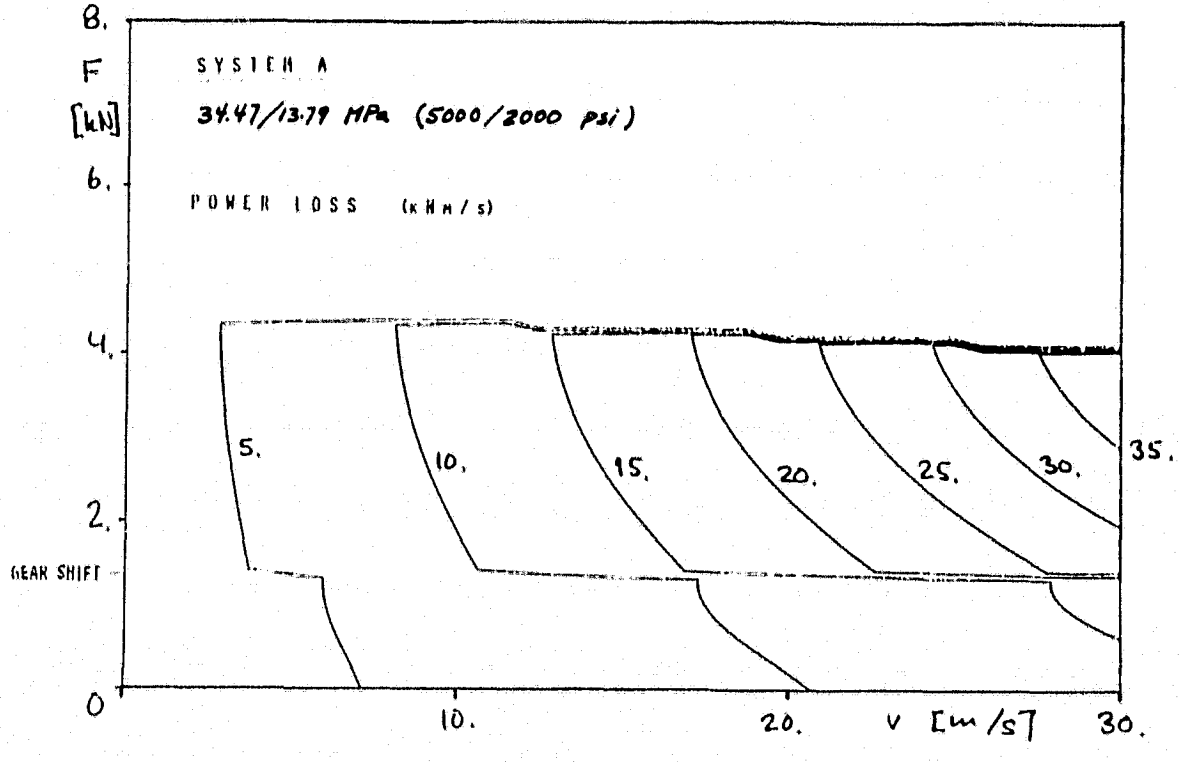
8.
F
[kN]
6.
4.
2.
GEAR SHIFT
0
SYSTEM A
34.47/13.79 MPa (5000/2000 psi)
POWER LOSS (kW/s)
5.
10.
15.
20.
25.
30.
35.
10.
20.
v [m/s]
30.

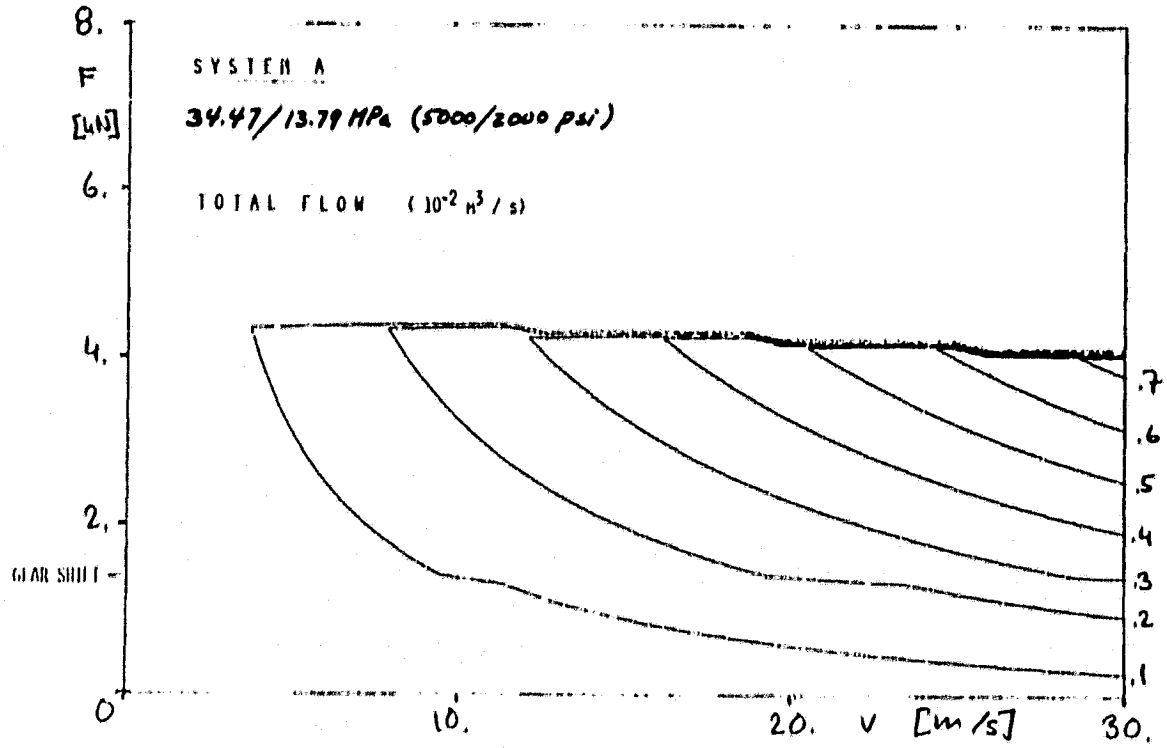

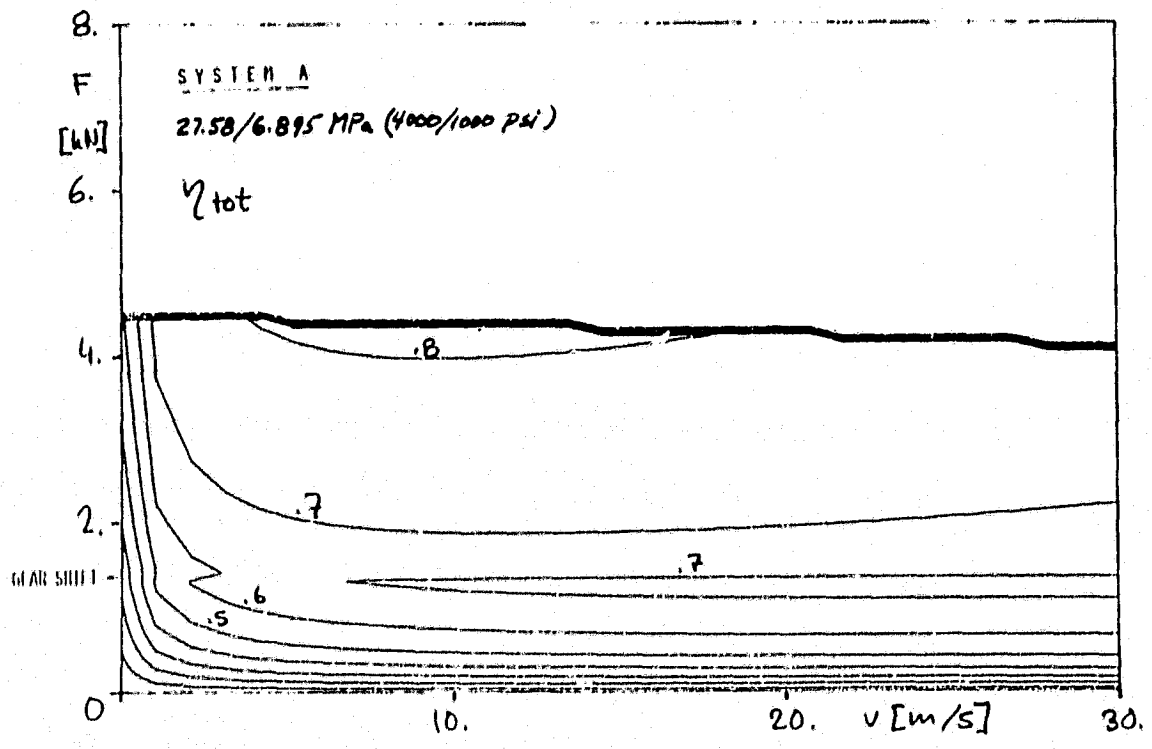

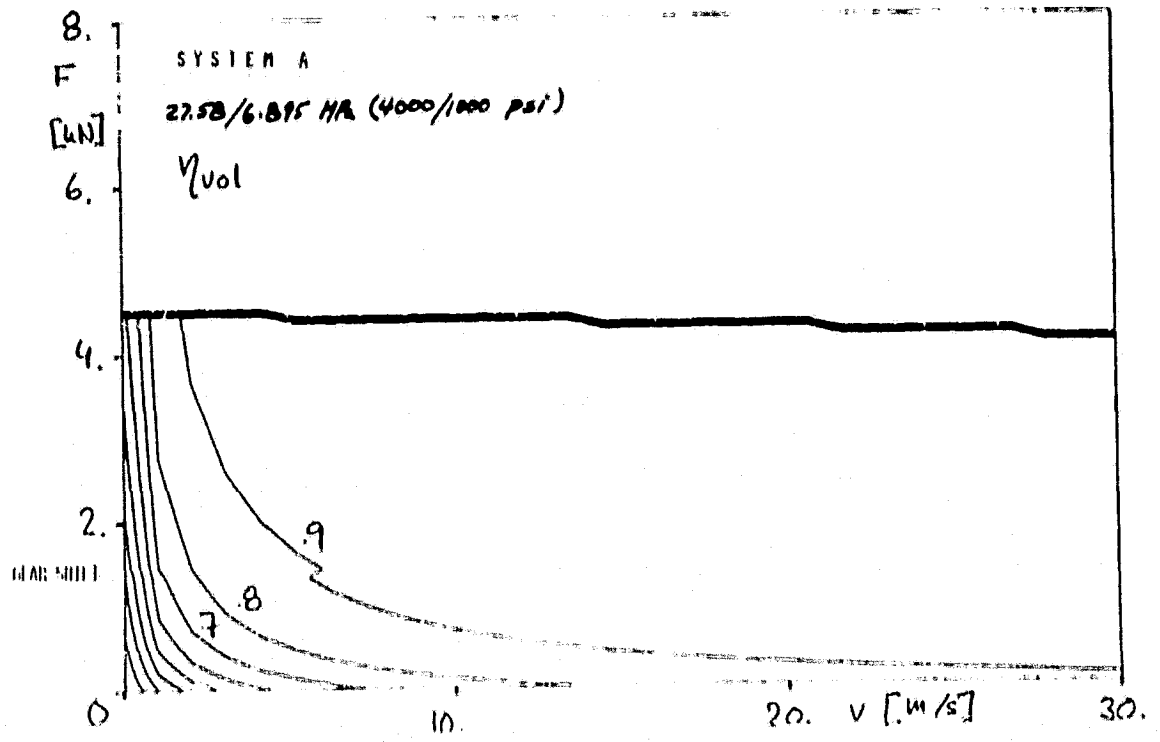
8.
F
[kN]
6.
SYSTEM A
27.58/6.895 MPa (4000/1000 psi)
ηvol
4.
2.
GEAR SHIFT
.9
.8
.7
0
10.
20.
v [m/s]
30.

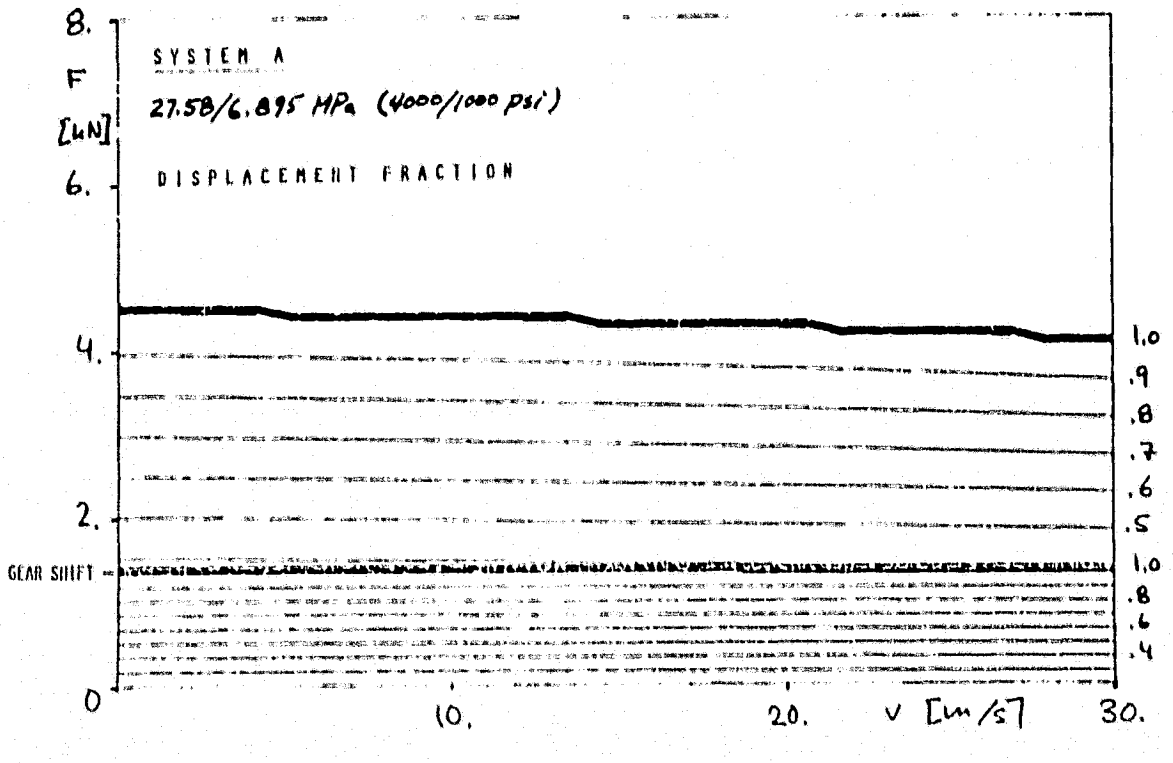
8.
F
[kN]
6.
SYSTEM A
27.58/6.895 MPa (4000/1000 psi)
DISPLACEMENT FRACTION
4.
2.
GEAR SHIFT
1.0
.9
.8
.7
.6
.5
1.0
.8
.6
.4
0
10.
20.
v [m/s]
30.

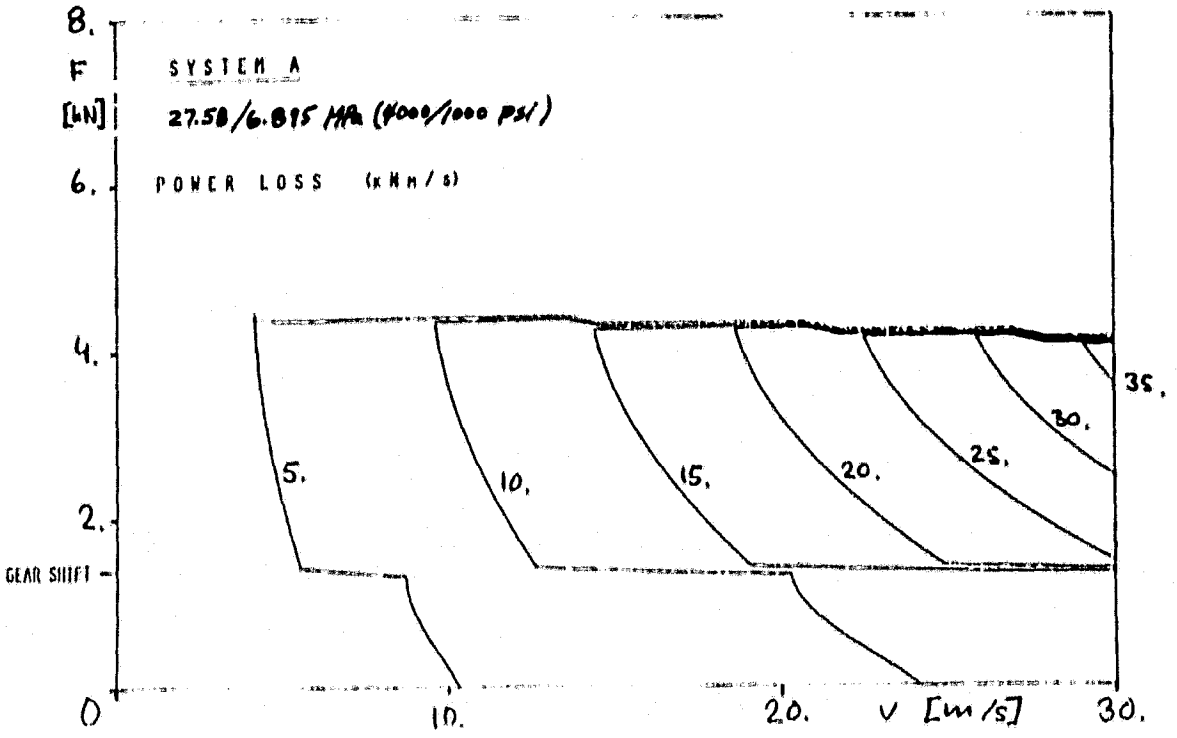

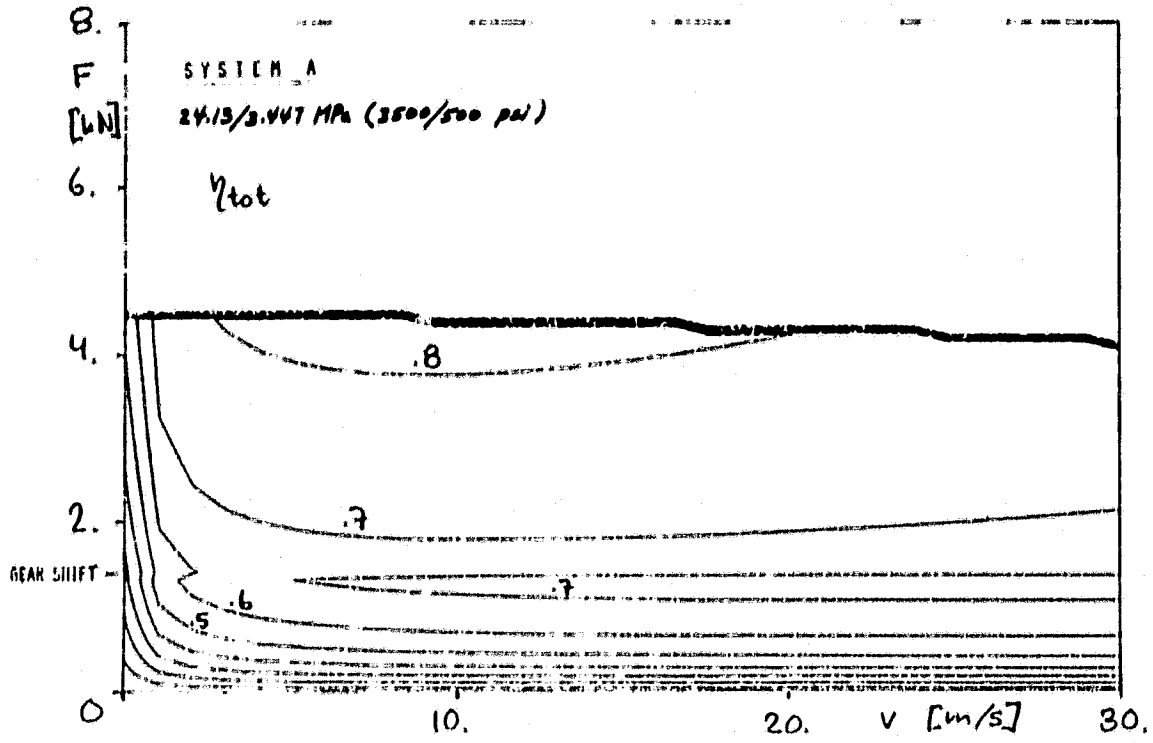

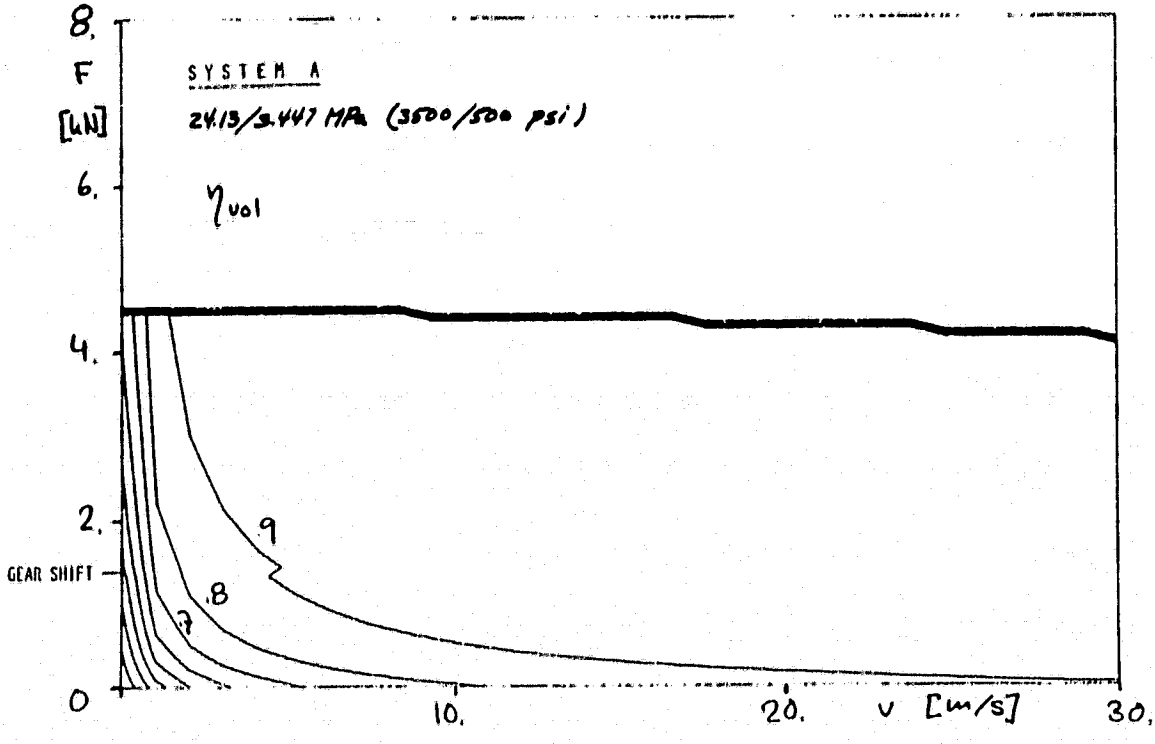

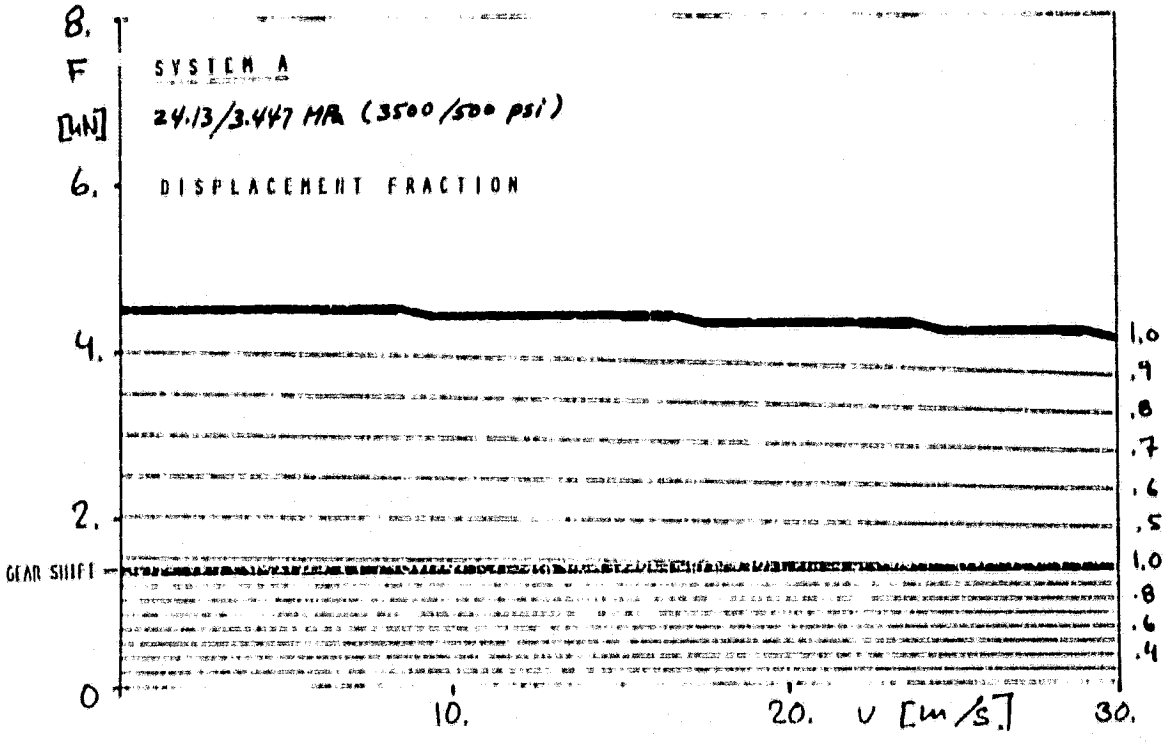

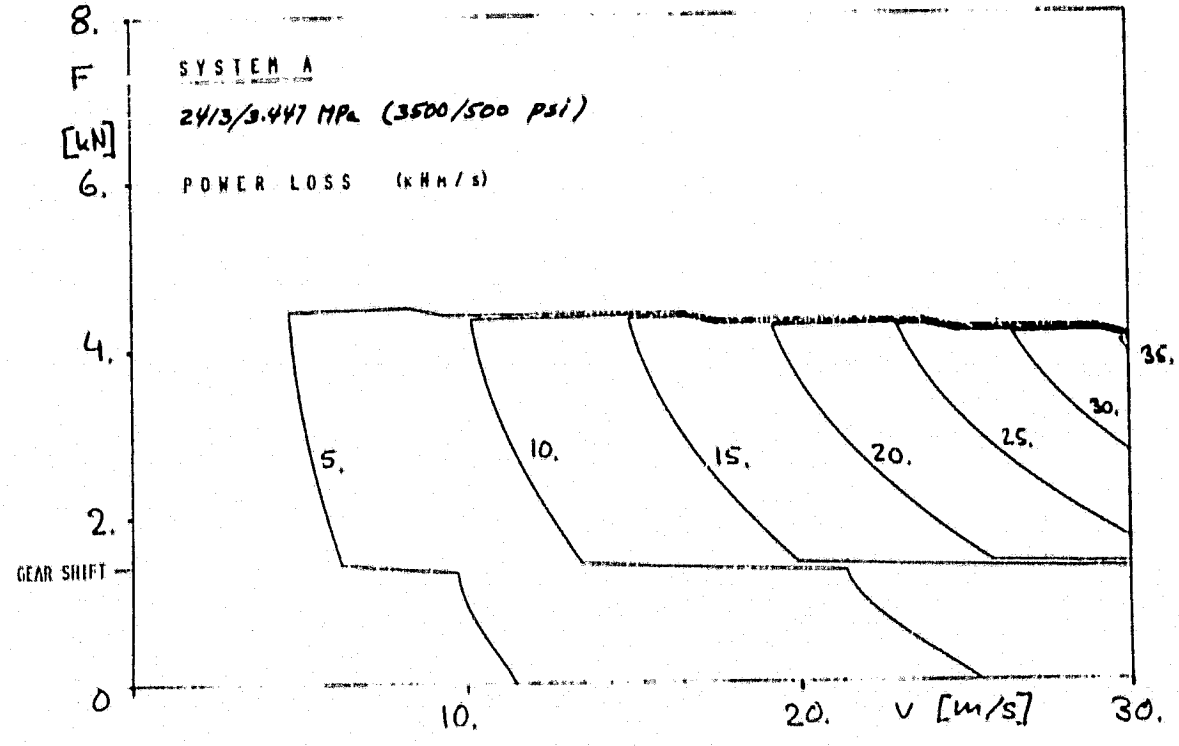

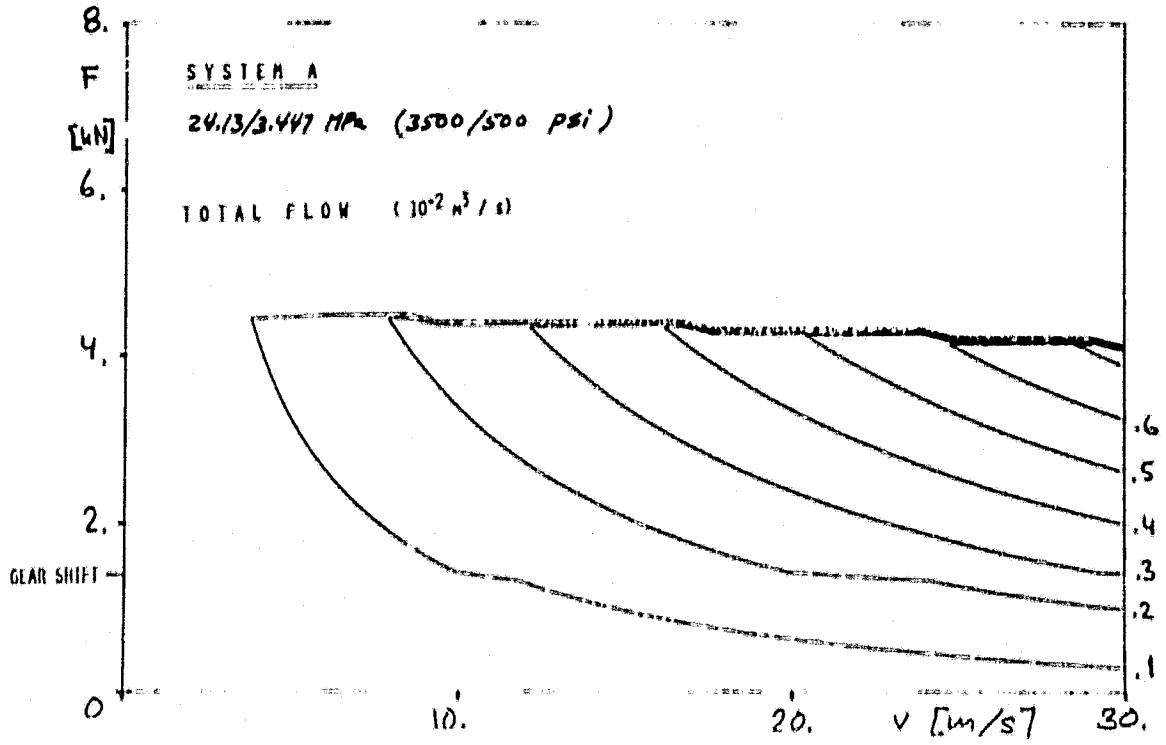
8.
F
[kN]
6.
4.
2.
GEAR SHIFT
0
SYSTEM A
24.13/3.447 MPa (3500/500 psi)
TOTAL FLOW (10^{-2} m³/s)
.6
.5
.4
.3
.2
.1
10.
20.
v [m/s]
30.